


Spring 2019

Study of the Effects of Silver Ions and Silver Nanoparticles on Embryonic Development

Martha Sharisha Johnson
Old Dominion University, mjohn175@odu.edu

Follow this and additional works at: https://digitalcommons.odu.edu/gradschool_biomedicalsciences_etds

 Part of the [Analytical Chemistry Commons](#), [Biochemistry Commons](#), and the [Developmental Biology Commons](#)

Recommended Citation

Johnson, Martha S.. "Study of the Effects of Silver Ions and Silver Nanoparticles on Embryonic Development" (2019). Doctor of Philosophy (PhD), Dissertation, Chemistry & Biochemistry, Old Dominion University, DOI: 10.25777/x8gj-n522
https://digitalcommons.odu.edu/gradschool_biomedicalsciences_etds/1

This Dissertation is brought to you for free and open access by the Graduate School Interdisciplinary Programs at ODU Digital Commons. It has been accepted for inclusion in Biomedical Sciences Theses & Dissertations by an authorized administrator of ODU Digital Commons. For more information, please contact digitalcommons@odu.edu.

**STUDY OF THE EFFECTS OF SILVER IONS AND SILVER NANOPARTICLES ON
EMBRYONIC DEVELOPMENT**

by

Martha Sharisha Johnson
B.S. Chemistry May 2010, Jackson State University
M.S. Chemistry May 2013, Jackson State University

A Dissertation Submitted to the Faculty of
Old Dominion University in Partial Fulfillment of the
Requirements for the Degree of

DOCTOR OF PHILOSOPHY

BIOMEDICAL SCIENCES

OLD DOMINION UNIVERSITY
May 2019

Approved by:

Xiao-Hong Nancy Xu (Director)

John Cooper (Member)

Chris Osgood (Member)

James Lee (Member)

ABSTRACT

STUDY OF THE EFFECTS OF SILVER IONS AND SILVER NANOPARTICLES ON EMBRYONIC DEVELOPMENT

Martha Sharisha Johnson
Old Dominion University, 2019
Director: Dr. Xiao-Hong Nancy Xu

This dissertation focuses on the study of the toxicity of metal nanoparticles (NPs) and their ions on the development of zebrafish embryos, aiming to understand unique biological effects of NPs and ions, and design new *in vivo* assays to characterize the toxicity of these metal NPs and metal ions. Currently, the underlying molecular mechanisms of biological effects of nanomaterials are partially understood. Some studies assume that the toxic effects of NPs can be attributed to the release of their ions. We investigate the effects of silver NPs (Ag NPs) and silver ions (Ag⁺ ions) on the embryonic development of zebrafish and compare both of their biocompatibility and toxicity. By statistically comparing the distributions of normal, deformed, and dead embryos, we conclude that the Ag⁺ ions cause deformities and death of developing embryos in a concentration dependent manner, where the critical concentration of the Ag⁺ ion is 0.20 μM for chronic exposure and varies in a stage-dependent manner in acute exposures during specific developmental stages. Exposure to Ag⁺ ions influences specific types of defects in development, which are far less drastic than those caused by the purified Ag NPs with the same amount of Ag atom. Thus, we can conclude that toxicity of Ag NPs on embryonic development is not due to the release of Ag⁺ ions, but rather their own unique physicochemical properties. We also synthesized and purified spherical Ag NPs (42 nm in diameter) that are stable (non-aggregated) in egg water media. We examined

the biocompatibility and toxicity of single Ag NPs *in vivo* at specific stages of development and the defects associated with treatment at those specific developmental stages. We then developed new imaging approaches to characterize single Ag NPs as they interact with key brain biomarkers that are significant for neurological development in zebrafish embryos. More specifically, we exposed Tg(*pax2a*:GFP) zebrafish embryos to various concentrations of the Ag NPs, and studied the effects of Ag NPs on the expression of the *pax2a* gene during treatment using fluorescent microscopy. Sublethal concentrations of the Ag NPs (0.00, 0.50, 1.00, 2.00, and 5.00 pM) resulted in a phenotypical dependent effect on embryonic development. However, we did not observe a significant decrease in expression of *pax2a*:GFP when exposing developing embryos to the Ag NPs. We did, however, observe that a higher dose of the Ag NPs led to severe deformities. We have further demonstrated the effects of Ag NPs on cardiac response. We found a decrease in heart-rate of both normal and deformed zebrafish, as the developing embryos were exposed to the Ag NPs. Our study also shows the dose-dependent effects of Ag NPs on eye development, where higher concentrations of Ag NPs leads to microphthalmia in developing embryos. We further studied the accumulation of Ag NPs in treated embryos. We found that each embryo accumulated a significant amount of Ag NPs in a dose dependent manner, which explains why some embryos developed normally, abnormally or resulted in embryonic death during treatment. In summary, this study demonstrates that developing zebrafish embryos can serve as effective *in vivo* model organism to study biocompatibility and toxicity of nanomaterials and metal ions, and can potentially lead to better design of applications to study developmental biology.

Copyright © 2019, by Martha Sharisha Johnson and Xiao-Hong Nancy Xu,
All Rights Reserved.

This dissertation is dedicated to my parents, Mr. Linzie Johnson and Mrs. Patricia Johnson for their unrelenting love, support, and financial assistance, which made all of this possible.

ACKNOWLEDGEMENTS

There are far too many individuals to name who have assisted me in getting to where I desire to be. First and Foremost, I thank God for granting me the opportunity to achieve my goals and desires to do something that I absolutely love. Through His strength, I am able to achieve all things. I would like to, also, thank my advisor and mentor, Dr. Xiao-Hong Nancy Xu for her continuous aid and support throughout my Ph.D. study at Old Dominion University. Without her dedication to me and my studies, this dissertation would not be possible. I appreciate her for allowing me to learn a variety of scientific techniques and multiple disciplines of the sciences. I am thankful for her ambition for success in everything I have sought out to achieve throughout my research career. I have learned from her to love scientific research. I am grateful for her inspiration and perseverance for me to present our work at national meetings and conferences. For this, I have gained so much confidence in presenting my research to those who I aspire to be like in the future. I also thank her for showing me how to mentor and guide young minds in this field of biomedical research.

I would like to extend thanks to the members of my dissertation committee, Drs. Christopher Osgood, John Cooper, and James Lee for their accommodating knowledge and support. I thank my fellow lab group members, for their valuable assistance and support. I am extremely grateful to Dr. Preeyaporn Songkiatisak, who worked beside me in all of these studies. Thanks also to Dr. Pavan Cherukuri for the synthesis of the nanoparticles we used during these studies. Without either of their collaboration, I would not be able to accomplish such an immense volume of work. Our lab group is one of the most supportive group of colleagues who I am happy to call my research family.

I would also like to thank my family, friends, mentors, and fellow blerds for their support and love. They have always kept me on my toes and continuously help me to excel in my “*black girl magic*”. Their support and encouraging words pushed me to continue with my goals and dreams. Never giving up was always their encouraging motto and I have taken that to my heart. And I will always remember the motto from a hometown legend: “*Good, Better, Best. Never let it rest, until Good is better and Better is Best*” - *W.S. Mims*.

I thank National Science Foundation (NIRT: CBET 0507036 and CBET 1450936) and NIH (R21 HL127580 and R15 NIGMS119116), especially NSF Graduate Research Diversity Supplement (GRDS) for their financial support of this work and my graduate education.

The work was carried out at the Department of Chemistry and Biochemistry, Old Dominion University, Norfolk, VA.

NOMENCLATURE

ε	Extinction coefficient
$\mu\text{g/mL}$	Microgram per milliliter
μm	Micrometer
η	Viscosity
ζ	Zeta potential in mV
Ag	Silver
AgClO_4	Silver perchlorate
AgNO_3	Silver nitrate
cm	centimeter
C	Concentration
CCD	Charge coupled device used for imaging nanoparticles with high sensitivity, temporal resolution and spatial resolution
CS	Chorion space
DFOM	Dark field optical microscopy
DFOMS	Dark field optical microscopy and spectroscopy
DI	De-ionized
DLS	Dynamic light scattering
DNA	Deoxyribonucleic acid
EM	Electron microscopy
FWHM	Full width at half maxima
h	Hour
H_2O_2	Hydrogen peroxide

hpf	Hours post fertilization
HRTEM	High resolution transmission electron microscopy
LSPR	Localized surface plasmon resonance
mm	Millimeter
MSI	Multi-spectral imaging
mV	Millivolt
nM	Nanomolar
nm	Nanometer
NaBH ₄	Sodium tetrahydroBoride
NaCl	Sodium chloride
NPs	Nanoparticles
Pax2a	Paired box 2a gene name
pM	Picomolar
QDs	Quantum dots
QY	Quantum yield
SEM	Scanning electron microscopy
SMD	Single molecule detection
SPR	Surface plasmon resonance
T	Temperature in kelvin
TCDD	2, 3, 7, 8 – tetrachlorodibenzo-p-dioxin
TEM	Transmission electron microscopy
Tg	Transgenic Mutant
UV-vis	Ultraviolet- visible
W	Watt

WT	Wild type
YS	Yolk sac

TABLE OF CONTENTS

	Page
LIST OF TABLES.....	xiii
LIST OF FIGURES.....	xiv
CHAPTER	
I. OVERVIEW	1
II. <i>IN VIVO</i> STUDY OF CHRONIC TREATMENT OF SILVER CATIONS ON EMBRYONIC DEVELOPMENT	10
INTRODUCTION.....	10
RESULTS AND DISCUSSION.....	12
SUMMARY	22
MATERIALS AND METHODS	29
III. <i>IN VIVO</i> STUDY OF THE ACUTE TOXICITY OF SILVER IONS ON EARLY DEVELOPMENT OF ZEBRAFISH EMBRYOS	32
INTRODUCTION.....	32
RESULTS AND DISCUSSION.....	34
SUMMARY	50
MATERIAL AND METHODS.....	51
IV. STUDY OF STAGE DEPENDENT BIOCOMPATIBILITY AND TOXICITY OF SINGLE 42 NM SILVER NANOPARTICLES USING EARLY DEVELOPMENT OF ZEBRAFISH EMBRYOS	54
INTRODUCTION.....	54
RESULTS AND DISCUSSION.....	57
SUMMARY	77
MATERIALS AND METHODS	78
V. STUDY OF EFFECTS OF SILVER NANOPARTICLES ON EARLY NEUROLOGICAL DEVELOPMENT OF ZEBRAFISH EMBRYOS	82
INTRODUCTION.....	82
RESULTS AND DISCUSSION.....	86
SUMMARY	106
METHODS	107

	Page
VI. CONCLUSION.....	112
REFERENCES.....	117
VITA	132

LIST OF TABLES

Table	Page
1. Summary of Dependence of Number of Normal and Deformed Zebrafish upon concentration of AgNO_3	20
2. Critical Ag^+ ion Concentration for Specific Developmental Stages of Zebrafish.....	40

LIST OF FIGURES

Figure	Page
1. Schematic illustration of in vivo study of chronic treatment of silver cations on embryonic development.	6
2. Illustration of probing of stage-dependent toxicity of AgNO ₃ using zebrafish embryos.	7
3. Illustration of using 43 nm, Ag NPs to study the biocompatibility and toxicity in living zebrafish embryos in real-time at specific developmental stages.	8
4. Illustration of using 43 nm single Ag NPs to study the toxicological effects on neurological development in zebrafish embryos in real-time.	9
5. Optical images of zebrafish embryos.	14
6. Biocompatibility and toxicity of Ag ⁺ Ions show dependency on its concentration....	16
7. Deformities of Zebrafish resulted from being treated chronically by AgNO ₃	18
8. Study of hatching rate of zebrafish treated chronically by AgNO ₃	24
9. Study of heart rates of zebrafish treated chronically by AgNO ₃	25
10. Study of Ag ⁺ ion uptake in zebrafish treated chronically by AgNO ₃ since their cleavage stage shows concentration dependency.	27
11. Normally developed zebrafish at stages I – V at the time of acute treatment and observations after acute treatment.	37
12. Study of concentration and stage dependent toxic effects of AgNO ₃ on embryonic developments.	39

Figure	Page
13. Representative optical images of deformities observed in stages I – V after acute treatment with AgNO ₃	42
14. Quantitative Heartbeat Analysis for specific developmental stages of embryos.	46
15. Rate of Hatched Zebrafish Exposed to Ag ⁺ ions at specific developmental stages.	49
16. Characterization of sizes, shapes, and plasmonic optical properties of single Ag NPs.....	59
17. Characterization of stability of Ag NPs in egg water (C _{NPs} = 0.5 nM) for 120 h.	60
18. Normally developed zebrafish at stages I – V at the time of acute treatment and observations after acute treatment.....	64
19. Histograms displaying the distribution of effects resulting from treatment with Ag NPs and the supernatant on zebrafish.	65
20. Representative optical images of deformities observed at 120 hpf in stages I – V after acute treatment with Ag NPs.	70
21. Histograms of the types of deformities concentration of Ag NPs treatment in zebrafish.	73
22. Quantitative Study of Heart Rates of Treated embryos per stage of development	76
23. Characterization of sizes, shapes, and plasmonic optical properties of single Ag NPs.....	88
24. Characterization of stability of Ag NPs in egg water (C _{NPs} = 0.5 nM) for 120 h.	89

Figure	Page
25. Study of dose-dependent effects of Ag NPs on embryonic development using embryos as ultrasensitive <i>in vivo</i> assays.	91
26. Dependence of types of deformed zebrafish on NP concentration.	93
27. Representative images of Expression of Tg(<i>pax2a</i> :GFP) in developing embryos exposed to Ag NPs	95
28. Development of Tg(<i>pax2a</i> :GFP) embryos at 1 key developmental stages of brain development	96
29. Expression of <i>pax2a</i> :GFP protein in zebrafish embryos at 24 hpf	97
30. Quantitative analysis of heartbeat of normally developed and heart deformed zebrafish.	100
31. Zebrafish embryos exposed to Ag NPs result in microphthalmia after 120 h incubation.	102
32. Quantitative study of accumulation of Ag NPs in normally developed and deformed zebrafish after treatment.	105

CHAPTER I

OVERVIEW

Nanomaterials pose unique physicochemical and optical properties that allow real-time observation of cellular uptake and functions in single living cells and other animal models, like zebrafish embryos.¹⁻³ These unique properties allow for their use in many interdisciplinary fields, and medical, industrial and commercial applications. However, there is still limited knowledge about the biocompatibility of these nanomaterials. A better understanding of their effects on living organisms will enable us to rationally design more biocompatible nanomaterials for a wide variety of applications. The challenges with conventional studies and methods currently available are that they are not able to characterize both dose and physiochemical properties of nanomaterials *in vivo* and *in situ* in real time at the single cellular resolution. Many of these studies use methods that are used for common chemical techniques to analyze toxicity and biocompatibility. However, as shown in other studies,¹⁻⁷ nanomaterials are unlike conventional chemicals because they are highly heterogeneous and yet single NPs have distinct physiochemical properties as well as highly dynamic systems that can alter over time. Bioanalytical tools that strive to analyze these properties further at single cellular resolution is vastly needed and can tell more prominent information about their capabilities.

Noble metal nanoparticles possess physicochemical properties that are exceedingly compatible in a wide range of applications, including biomedical engineering and design. Silver nanoparticles (Ag NPs) possess a broad range of potential applications including serving as therapeutic agents and ultrasensitive optical imaging probes.^{5, 6, 8, 9} As Ag NPs have also been used in consumer products, the potential

release of Ag NPs to aquatic environments could lead to adverse health impacts on humans.

Ag NPs possess distinct plasmonic optical properties and very high Rayleigh scattering. Because Ag NPs resist photobleaching and photoblinking, the optical properties allow our lab to design Single Nanoparticle Optical Biosensors (SMNOBS) that distinctively overcomes the optical drawbacks of other fluorescent super-resolution imaging methods. We have demonstrated that single Ag NPs can serve as superior photostable optical molecular probes and sensors for imaging of single biomarker molecules, probing ligand-receptor interactions in real time, and imaging single live cells and embryos in real time, using dark-field optical microscopy and spectroscopy (DFOMS).

5

Previous studies from our group have explored in depth how nanotoxicity can contribute to malformations and abnormalities in embryonic development. We have designed ultrasensitive *in vivo* bioanalytical imaging tools to address the questions of toxicity and biocompatibility of nanoparticles in living systems by using zebrafish embryos as our *in vivo* animal model. Zebrafish (*Danio rerio*) serves as an excellent model organism to study human development and physiology, human diseases, and toxicity screening for many potential drugs. They have many distinct advantages over other *in vivo* models like mice and rats. Zebrafish embryos have a rapid developmental process where they will complete embryogenesis within 120 hours post fertilization (hpf). This is faster than most animal models used in other studies. During their development, zebrafish embryos are transparent. This enables real-time monitoring and studying the effects and transport of single NPs. This also allows for direct imaging of molecular

changes and abnormalities during embryogenesis. Because zebrafish has a genetic makeup that is similar to humans, zebrafish have been used in many screenings for therapeutic agents and toxicity studies of many conventional chemicals and drugs.¹⁰⁻¹⁶ Transgenic zebrafish are highly used as the go-to *in vivo* animal model for the exploration of the molecular development and for the design of newer imaging tools used in many labs.¹⁷⁻¹⁹ Using these transgenic models has allowed many researchers to essentially study biomarkers that were otherwise impossible to research *in vivo*.

In developmental biology, embryonic development is still not fully understood, but with the help of transgenic zebrafish *in vivo* models, much has been accomplished within the last decade, which has contributed to improving the design of transgenic models to study mechanisms regulated by embryogenesis. The biological functions that are enabled during embryogenesis are highly regulated and complex processes that involve many different macromolecules that are still being identified. Our lab is particularly interested in neurological development because this is the central control center of living systems. Neurological development has many dynamic processes that still puzzle the neuroscience and developmental biology community. Understanding how the developing brain and all of its components are regulated and function will aid in establishing better molecular assays to further explore these and similar questions, leading to the increase of knowledge in the field of neuroscience.

For this dissertation, we explored *in vivo* assays and applications to study silver nanoparticles (Ag NPs) and silver ions (Ag⁺ ions) upon their effect on embryonic development, and also the molecular mechanism of embryonic neurological development and how nanomaterials can influence and alter this development over time. Each study

discussed will highlight a significant bioanalytical design that will allow further exploration into key developmental stages that can contribute to the understanding of biomedical applications using nanomaterials. This dissertation includes six chapters. In Chapter I, we provide a brief overview of the research background, the significance of this dissertation research, and outline the contents of each chapter.

In Chapter II, we describe the design of standard *in vivo* toxicological assays that are efficient, easy to use, and affordable to screen the toxicity of silver cations during embryogenesis, as illustrated in Figure 1. To this end, we have demonstrated an ultrasensitive method to study the toxicity of Ag^+ ions on zebrafish embryos aiming to assess nanotoxicity on embryonic development, heart functions, and hatched time. Dose-dependent toxic effects of the Ag^+ ions on embryonic development were observed, showing that the number of zebrafish developed normally decreased while the number of dead zebrafish increased as Ag^+ ion concentrations increased. The Ag^+ ions not only interfere with embryonic development but also heart development and functions. We observed heart deformities and lower heart rates in zebrafish exposed to Ag^+ ions. Studies are needed for a more in-depth mechanistic understanding of Ag^+ ion induced heart deformities. Moreover, delays in hatching mechanisms of treated zebrafish were observed in a dose-dependent manner. Zebrafish embryos exposed to high concentrations of Ag^+ ions hatched later.

In Chapter III, we investigated the effects of silver cations to determine their effects on various developmental stages and their related mechanisms as illustrated in Figure 2. To this end, we incubated the embryos with Ag^+ ions for two hours and characterized their effects upon embryonic development over time using a wide variety of bioanalytical tools.

We found that the effects of silver cations on embryonic development highly depended upon embryonic developmental stage and incubation time. We also saw concentration and stage dependent effects of Ag^+ ions on hatching rate and cardiac response. The results demonstrated the need for future investigation of heavy metal toxicity exploring key developmental stages.

In Chapter IV, we continued our *in vivo* assay design to explore the biocompatibility and toxicity of 41.5 nm Ag NPs in zebrafish embryos at key developmental stages, as illustrated in Figure 3. To determine the specific effects of Ag NPs on various developmental stages and their related mechanisms, we incubated the embryos with Ag NPs for two hours and characterized their effects upon embryonic development over time using similar bioanalytical tools described in **chapter II** and **chapter III**. We found that the effects of NPs on embryonic development highly depended upon the embryonic developmental stage, incubation time, the size and dose of NPs.

In Chapter V, we used our *in vivo* model to investigate the mechanisms of effects of purified and well-characterized nanoparticles (NPs) on embryonic developments, specifically neurological development. To that end, we selected a vital protein biomarker that plays an important role in neurological development, used transgenic embryos that express the protein biomarker fused with fluorescence proteins as model organisms, and studied the effects of NPs on their functions using fluorescence microscopy and plasmonic spectroscopy.

In Chapter VI, we summarized our research findings described in the preceding chapters, pointed out the primary contributions of these original research activities, and emphasized the possible future research directions.

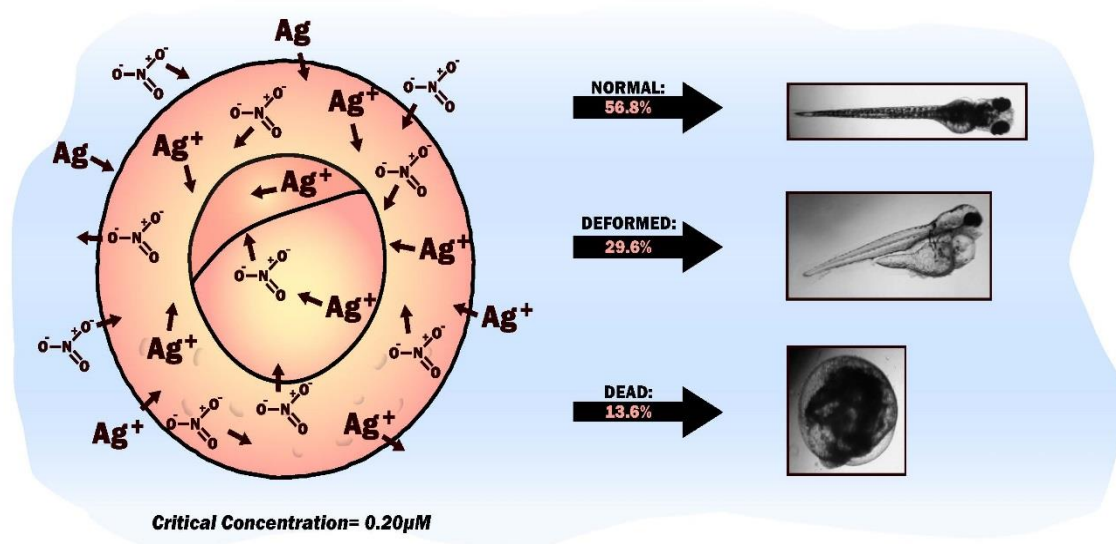


Figure 1: Schematic illustration of in vivo study of chronic treatment of silver cations on embryonic development.

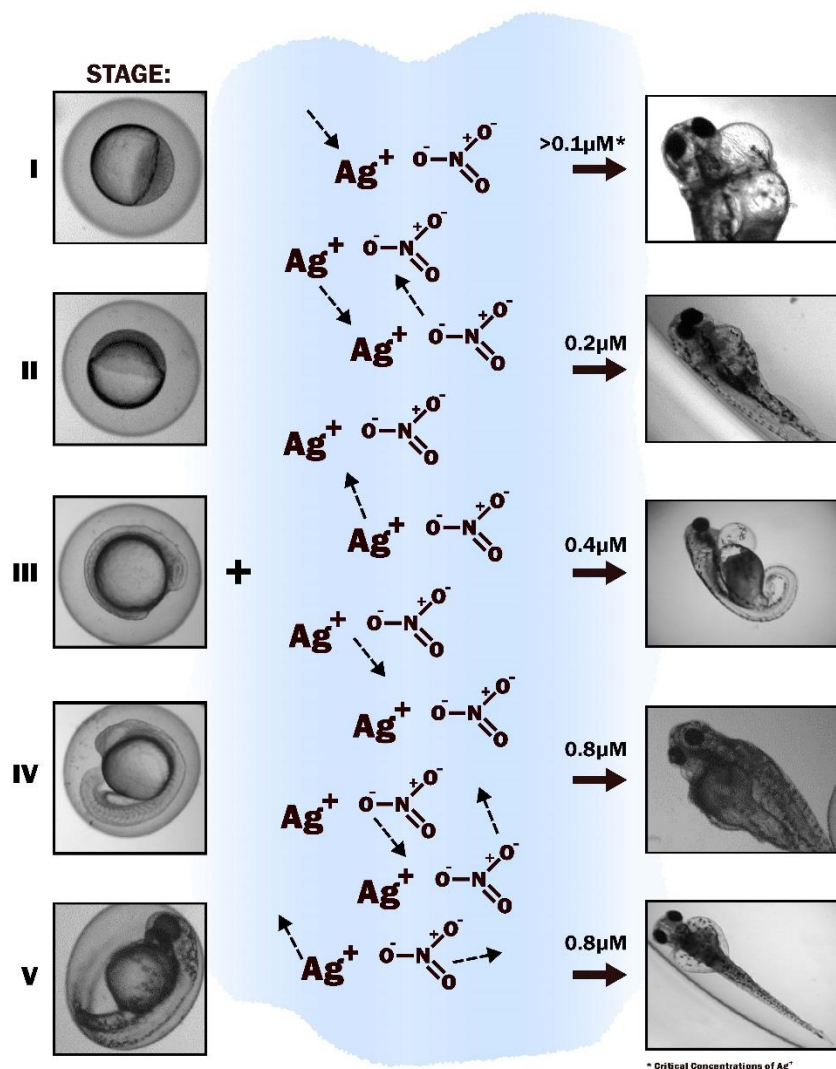


Figure 2: Illustration of probing of stage-dependent toxicity of AgNO_3 using zebrafish embryos.

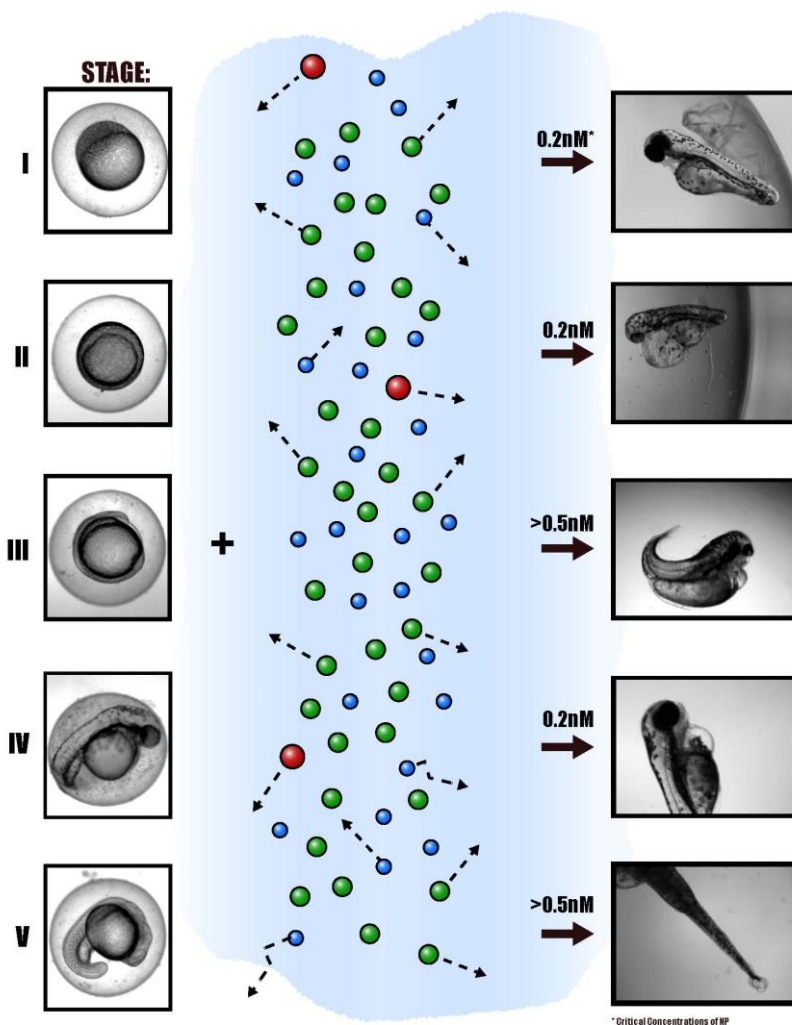


Figure 3: Illustration of using 43 nm, Ag NPs to study the biocompatibility and toxicity in living zebrafish embryos in real-time at specific developmental stages.

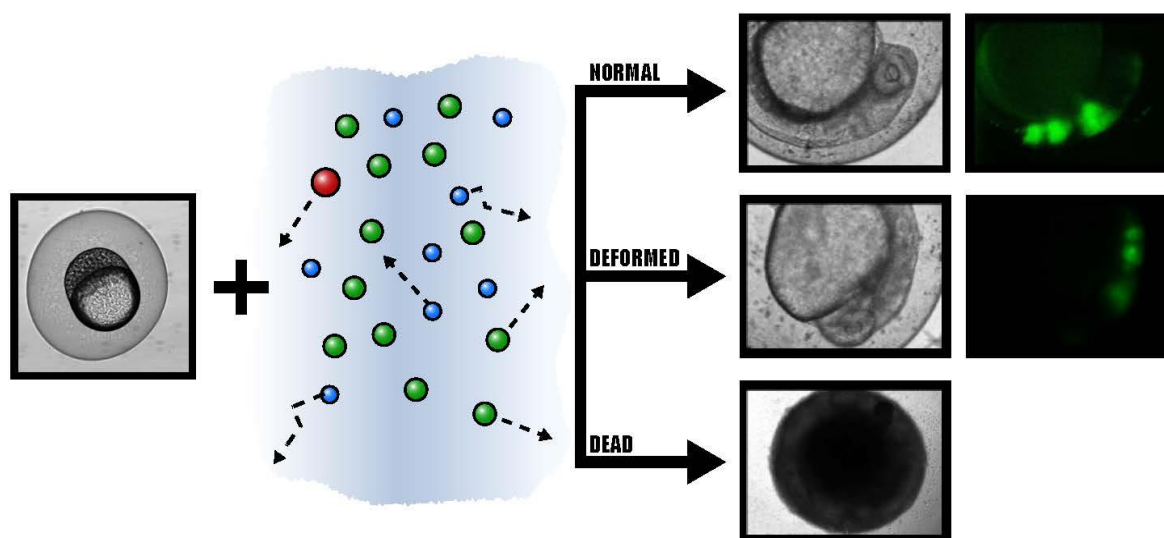


Figure 4: Illustration of using 43 nm single Ag NPs to study the toxicological effects on neurological development in zebrafish embryos in real-time.

CHAPTER II

***IN VIVO* STUDY OF CHRONIC TREATMENT OF SILVER CATIONS ON EMBRYONIC DEVELOPMENT**

INTRODUCTION

Heavy metals have been widely used in multiple fields from domestic and industrial, to medical and technological applications. With this wide distribution of use across many fields, their potential impact on both environmental and biological health has been well studied over the years. Understanding the impact requires studies to understand the mechanisms of exposure and toxicity. Some toxicological studies of some heavy metals, such as cadmium and mercury have shown that heavy metals and their ions can lead to genetic mutations and functional decrease in biological systems.²⁰⁻²³ Other studies have shown a loss of enzyme stability and an increase of apoptotic biomarkers in vitro when exposed to heavy metals such as titanium and zinc.^{24, 25} These studies have allowed for modifications to be made when utilizing heavy metals in research and applications. Although many strides have been made to understand the toxicity of heavy metals, a better approach and application is needed to address early developmental adversities from heavy metal exposure.

Silver metal has been used throughout the decades for its unique properties. Silver ions (Ag^+ ions) and their toxicological exposure have been of great concern with a very significant increase of silver being used in nanotechnology.²⁶⁻³¹ This increase is in response to silver's antimicrobial and antibacterial properties. Silver nanomaterial has shown increasing use in consumer products (such as clothing and home appliances) as well as in biomedical applications (such as biosensors and imaging probes). Although

increasingly used in biomedical applications, understanding the biocompatibility of silver nanomaterial is essential for their success in clinical applications. Our studies have shown a toxicology concentration and stage dependent effect of Ag nanoparticles on embryonic development.

Many suggest that the toxicity of Ag NPs is reflected in the ionic properties of silver. Some attribute the toxicity of Ag NPs to the dissolution of Ag ion, without a direct link of the ionic relationship with NP toxicity. In order for us to understand nanoparticle toxicity to rationally design more biocompatible nanoparticles, we must understand the mechanism of toxicity of the nanomaterial, thus we can rationally design more biocompatible applications.

Zebrafish (*Danio rerio*) have been extensively used as an in vivo model for embryological development because of its small size, its short breeding cycle, and the wealth of information available for manipulation. The zebrafish is transparent throughout development, allowing for surveillance of development from outside the chorion without disturbing its developmental process. Zebrafish can spawn in large numbers from week to week, producing large masses of fertilized eggs, which are ideal for observing different developmental stages. The embryonic development is so fast and efficient that primary organ development is completed within the first 48 hours post fertilization (hpf), and the normal embryo will hatch and swim by 72 hpf. Since zebrafish are so genetically similar to other organisms and even humans, zebrafish have been widely used for chemical and drug analysis and screening. Our group was the first to use the zebrafish to study the toxicity of nanomaterials. Therefore, zebrafish embryos offer a unique opportunity to

investigate developmental processes upon treatment with heavy metals to determine the adverse effects during development.

Here, we investigate the roles of Ag^+ ions on embryonic development in comparison to our previous studied silver nanoparticles. Here, zebrafish embryos were chronically exposed to silver nitrate in corresponding concentrations that corresponded to the published toxicological concentrations of our Ag NPs studies. Phenotypic and survivability observations can be compared to other toxicological studies. Heartbeat analysis was also studied to show the effects of ionic concentrations on cardiac function. Analysis was also carried out on embryo hatching mechanisms from treatment with Ag^+ ions.

RESULTS AND DISCUSSION

Early-developing embryos as *in vivo* model organisms and assays

Zebrafish embryos have recently gained interest as being an optimal animal model for toxicity and genetic studies. Zebrafish has several unique properties that allow them to be a well-defined animal model. Optical images in Figure 5 A-B show normal developmental zebrafish embryos at cleavage (0.75-2.25 hours-post-fertilization, hpf), germ ring stage (8-10 hpf), late segmentation (24 hpf), hatching (48 hpf), hatched embryo (72 hpf), and fully developed larvae (120 hpf). Fast embryogenesis allows rapid multiple studies to be performed in a shorter amount of time than using other animal models that take longer to develop. Because zebrafish are optically transparent during embryogenesis, which is a characteristic of using zebrafish embryos, monitoring of cellular division and migration as well as the development of primary and secondary organs can be observed and characterized. This allows for real-time monitoring and

analysis of the effects of toxins on development can be observed during the experiment. Furthermore, a large number of embryos can be generated rapidly (overnight) at very low cost, serving as high-throughput *in vivo* assays to screen biocompatibility and toxicity of many toxins and materials. Zebrafish have gained a lot of focus from genetic and developmental biologists because of the similarity with humans in genetic makeup. Behavioral studies using Zebrafish have led to many breakthroughs in neurological development allowing scientists to explore mutated genes and disarrayed pathways that have been found to occur in early stages of neurological abnormalities.

Using embryos *in vivo* in studies have numerous advantages over *in vitro* cultured cells for the study of biocompatibility and toxicity of metal ions. For instance, *in vivo* assay enables one to investigate the effects of heavy metals upon different development stages of cells while studying multiple others all in one organism. Thus, the selection of zebrafish embryos as our animal model to study the toxicity of silver ions was our preference.

Study of concentration-dependent toxicity of Ag⁺ on embryonic development

To study the concentration dependent toxicity of our silver ions, we incubated cleavage-stage embryos (2-4 hpf) with a series of concentrations of AgNO₃ (0-1.20 μM) that was suspended in egg water for 120 hours (h). Representative embryonic developmental stages were imaged and assayed every 24 h over 120 hpf until the embryos fully developed (Figure 6A). We determined and characterized the number of embryos that developed to normal zebrafish (Figure 5A), died (Figure 6B), or developed into deformed zebrafish (Figure 5A). The results in Figure 6 show various degrees of dependence on embryonic development upon the concentrations of AgNO₃. As the ion concentration increased from 0 to 1.20 μM, the number of embryos that developed to

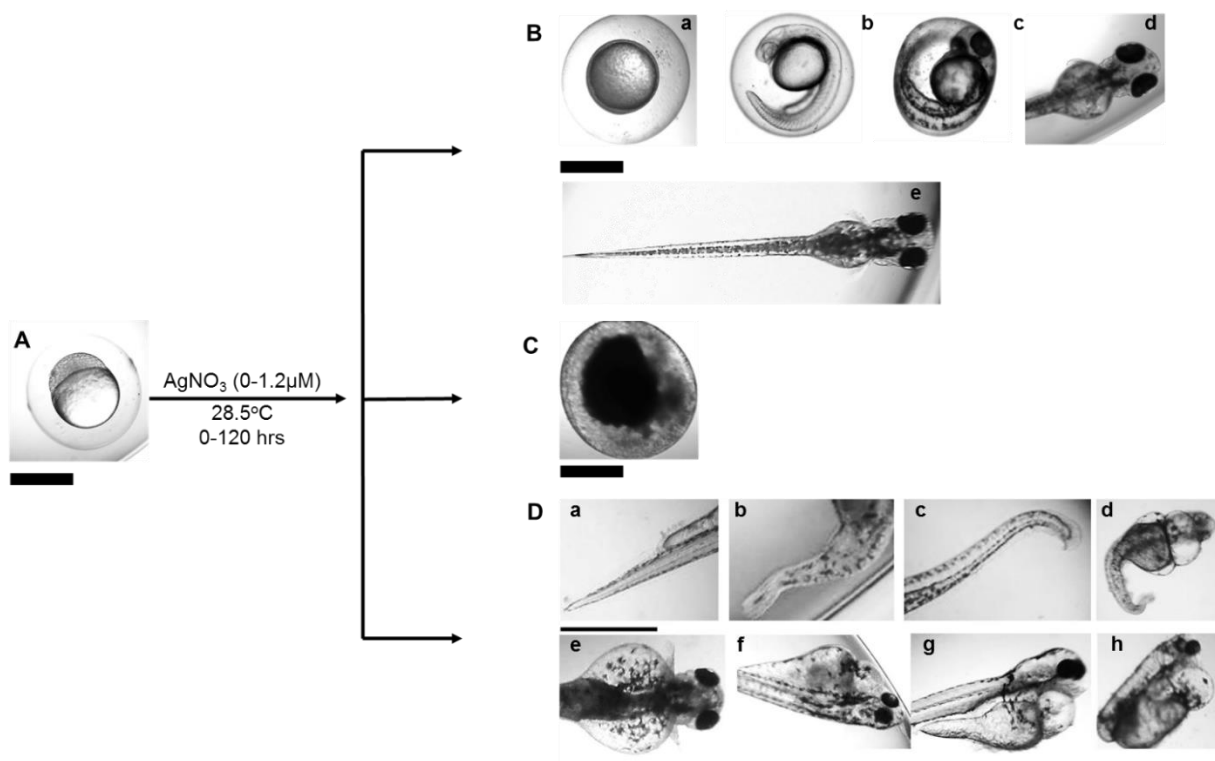


Figure 5. Optical images of zebrafish embryos.

(A) Cleavage stage embryo (0.75-2.25 hpf) incubated with AgNO_3 (0.00-1.20 μM) over 120 h at 28.5°C. (B) Normally developing embryos: (a) germ-ring stage (8-10 hpf); (c) late segmentation stage (24 hpf); (d) hatching stage (48 hpf); (d) protruding mouth pharyngula stage (72 hpf); and (e) fully developed larvae (120 hpf) lateral view. (C) Dead embryos. (D) Abnormally developed embryos at 120 hpf showing (a-b) finfold abnormality; (c-d) tail/spinal cord flexure and truncation; (e-g) pericardial sac edema and yolk sac edema; and (h) eye and head abnormalities. Many of the deformed zebrafish had multiply types of deformities. Scale bar for (A -C) = 200 μM ; Scale bar for (D) = 250 μm .

normal zebrafish decreased, while the number of embryos that became dead or developed to the deformed zebrafish increased, given way to a concentration dependency of AgNO_3 .

High concentrations of the silver ion generated several common and severe deformed zebrafish (Figure 5D) observed starting at 48 hpf in the embryos exposed to 0.2-0.8 μM AgNO_3 , which included: (a-b) finfold abnormality; (c-d) tail/spinal cord flexure and truncation; (e-g) pericardial sac edema and yolk sac edema; and (h) eye and head abnormalities. The distributions of types of deformities versus the Ag ion concentrations in Figure 7 show that more embryos develop to severely deformed zebrafish (e.g., cardiac malformations and head abnormalities) in the 0.3 and 0.4 μM AgNO_3 .

Interestingly enough, the most severe deformities that showed multiple abnormalities were observed in the 0.4 and 0.8 μM concentrations. Taken altogether, these interesting findings show definite concentration dependent toxic effects of Ag ion upon embryonic development. This is interesting, considering EPA guidelines for Silver Acute toxicity falls within the toxicity range of 2-3 $\mu\text{g/L}$ silver ion.³² Table 1 shows representative images of deformities for each concentration treatment group. These deformities were scored from 1 being the least severe in abnormality and 4 being the most severe in abnormality. As we can see, the more severe deformed zebrafish were captured in the 0.3 – 1.2 μM , where head abnormalities and eye abnormalities were prevalent. We did observe that the more severe zebrafish with these abnormalities also had multiple other deformities like pericardial sac edema and yolk sac edema.

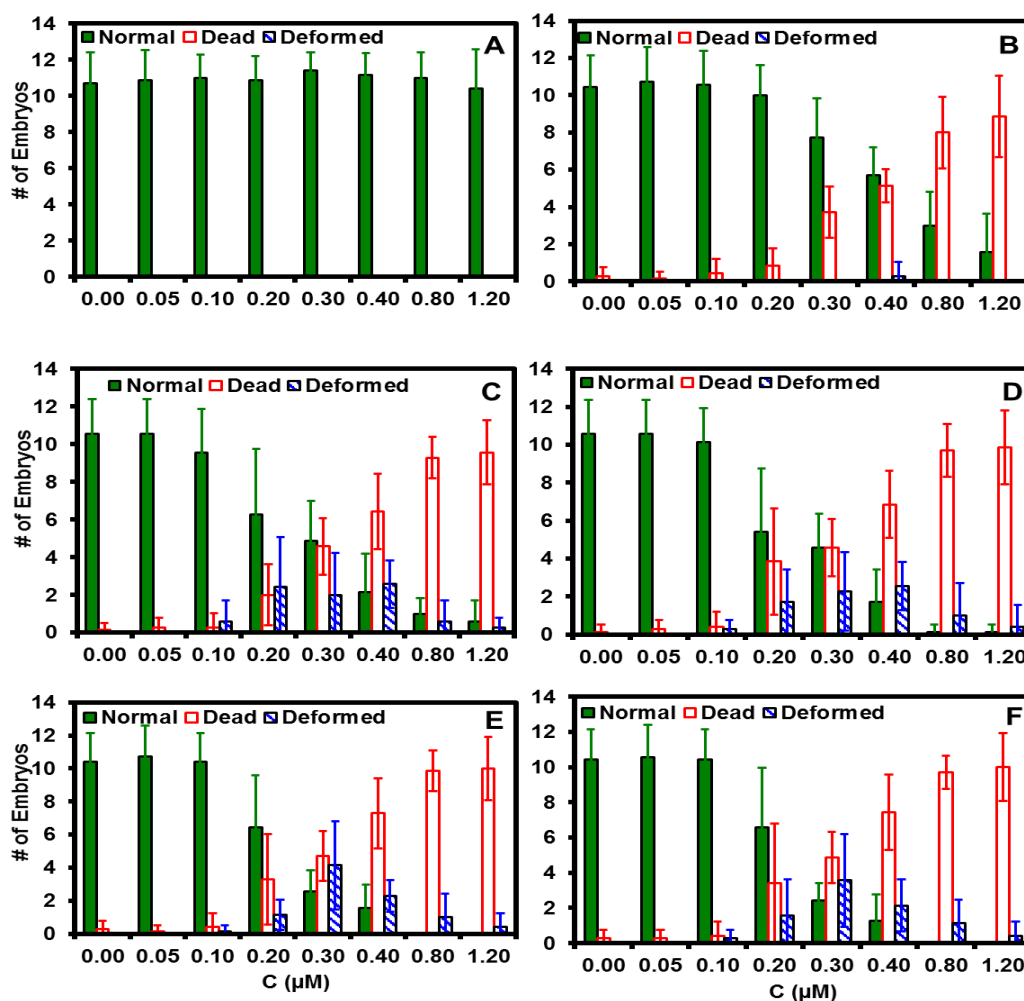


Figure 6: Biocompatibility and toxicity of Ag^+ ions show dependency on its concentration.

Histogram of distribution of normally developed (green), dead (red), and deformed (blue) zebrafish versus concentration of the Ag^+ ion for (A) 4 hpf; (B) 24 hpf; (C) 48 hpf; (D) 72 hpf; (E) 96 hpf; and (F) 120 hpf. The means and standard deviations (error bars) of the total number of embryos that developed normal and deformed, or became dead shown for each given concentration are from triplicate measurements.

Since toxicity of metal ion nanomaterials has been cited to be caused by the leaching or exposure to the metal ion, we decided to evaluate the overall toxicity Silver Nanoparticles to our toxicity levels in this study.³³⁻³⁸ We found that the abnormalities observed from the exposure of the Ag⁺ ions (finfold abnormality, tail flexure, yolk sac edema, pericardial sac edema, and eye and head abnormalities) were all similar to those exposed to Ag NPs.^{33, 35, 37, 38} This suggests that the toxicity biological mechanisms that are involved in the formation of these abnormal developments (i.e. molecular biomarkers and genetic pathways) are similar between Ag⁺ and Ag NPs, which are still not well understood. However, the lethal level of toxicity in Ag NPs was found to be much lower when converted to Ag⁺ molarity concentrations for comparisons, where concentrations were in the nanomolar range. Thus, challenging the theory that the toxicity of metal and metal oxide nanoparticles, or in this case Ag NPs, is related to the release of the Ag⁺ ion.

Study of effects of Ag⁺ on hatching of embryos

Zebrafish embryos will hatch out of their chorions after organogenesis for survivability. The longer the embryo stays inside the chorion may lead to the embryo being more susceptible to predators or abnormal growth.³⁹ During natural hatching, the chorion is digested from the inner surface, and tail movements of the embryo help to break the remaining chorion. This hatching usually happens between 48-72 hpf. Many studies have reported the delay in hatching after exposure to different toxins.^{28, 30, 36, 40} Mechanisms of this delay, although not widely understood, has been theorized to be because of the hardening of the outer layer of the chorion, making it difficult for the embryo to break free. Effects of Ag⁺ ions on this hatching process has not been widely studied in zebrafish.

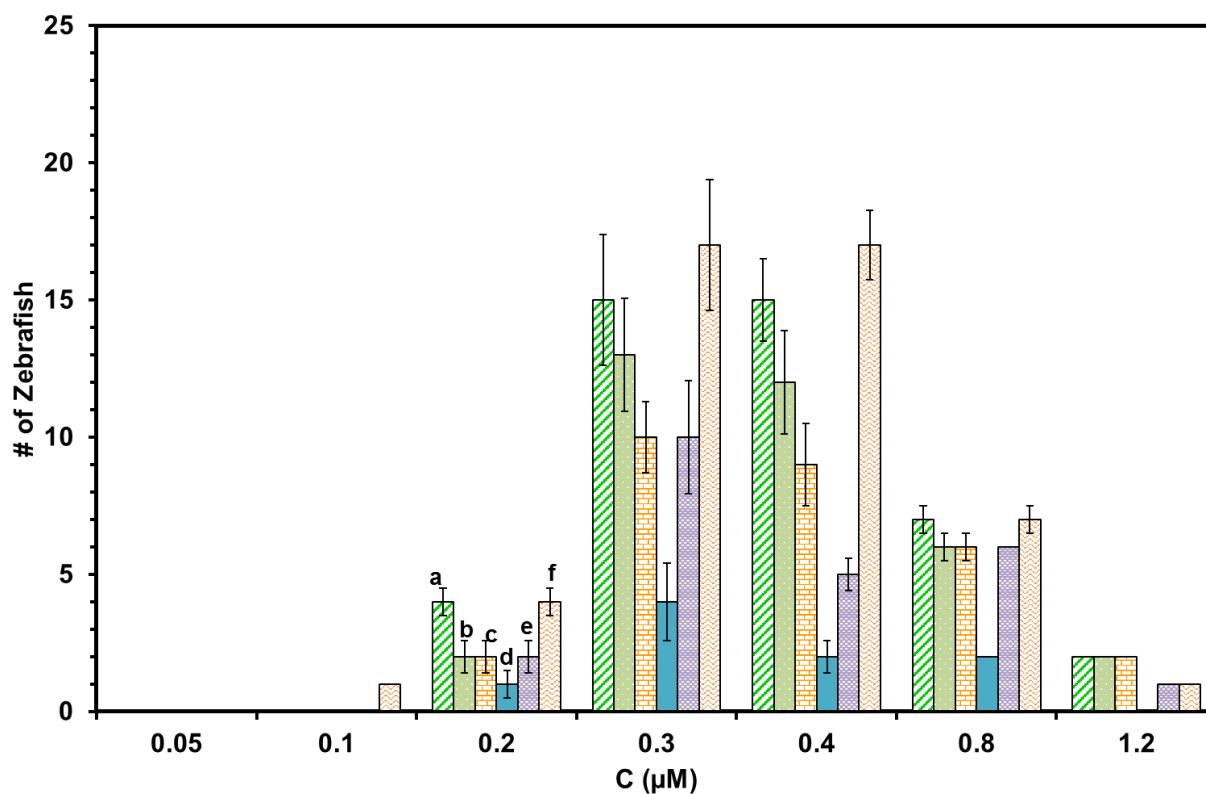
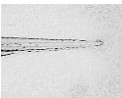



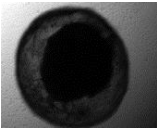
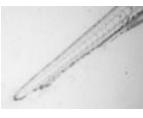
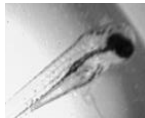






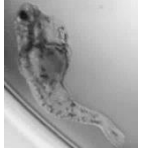

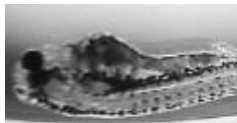





Figure 7: Deformities of Zebrafish resulted from being treated chronically by AgNO_3 .

Histograms of the percentages of Zebrafish with five representative types of deformities *versus* concentration of Ag^+ ions; (a) finfold; (b) tail flexure; (c) yolk sac edema; (d) eye abnormality; (e) head abnormality; and (f) pericardial sac edema. The means and standard deviations (error bars) of the total number of embryos that developed each type of deform shown for each given concentration are from triplicate measurements.

		Number of Zfish with Severity Scale					
C (μM)	Images of Zebrafish	0	1	2	3	4	Number of Dead Embryos
0	Normal Development	74 ±1.8					2 ±0.5
	   						
0.05	Normal Development	74±1.8					2±0.5
0.1	Pericardia Sac Edema, Finfold Abnormities	73±1.8		1			3±0.8
	   						
0.2	Pericardia Sac Edema, Finfold Abnormities	46±3.4		1	1	2	24±3.4
	  						
0.3	Head and Eye Abnormities, Yolk Sac Edema, Pericardial Sac Edema, Tail Flexures	17±1.0	4	3	4	9	34±1.5
	  						
	 						
0.4	Head and Eye Abnormities, Yolk Sac Edema, Pericardial Sac Edema	9±1.5	3	6	2	9	52±2.1
	 						


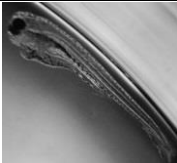

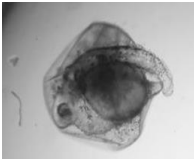


								
	Head and Eye Abnormities, Yolk Sac Edema, Pericardial Sac Edema		0±0				7	68±1.0
0.8								
	Head and Eye Abnormities, Yolk Sac Edema, Pericardial Sac Edema		0±0				2	70±2.0
1.2								

Table 1: Summary of Dependence of Number of Normal and Deformed Zebrafish upon concentration of AgNO₃.

To study hatching, observations were made every 2 hours to identify what hpf the embryo hatched from the chorion. Figure 8 shows that as the concentration of Silver nitrate increase, embryo hatching time was decreased. The controls hatched out of chorions around 50-60 hpf. Lower concentrations, 0.05-0.1 μM , also showed a normal rate in hatching time. However, the higher concentrations, 0.20-0.80 μM , μM showed a hatching rate up until 96 hpf. This delay in hatching does show a concentration dependency. We also noticed that deformed zebrafish hatched out at a later rate than those zebrafish that developed normally. These deformed zebrafish could potentially be delayed in hatching because of a lack of physical abilities to move, as well as a delay in chemical release of hatching enzymes. Further genetically studies could be used to reflect these enzyme levels during hatching.

Quantitative study of effects of Ag^+ on heart rate of developing embryos

Heartbeat analysis was taken at 24, 48, and 120 hpf by visually counting of the beats per minute and compared between concentrations, as well as normal or abnormal development. Figure 9A shows the quantitative results of those zebrafish that were normally developed at each time point. Heart rates show a decreasing effect as the treatment concentration increases, with a significant decrease at 48 and 120 hpf for the 0.4 μM treated zebrafish. Figure 9B shows the quantitative results of those zebrafish that were abnormally developed at each time point. There is a significant decrease, again, with the higher concentration (0.8 μM) compared to the other two concentrations. These results do, in fact, reflect that higher silver ion concentrations have an effect on cardiac function.

We observed a significant difference in heart rate between normal development and deformed zebrafish at those treated ion concentrations that had both normal and deformed zebrafish. This demonstrated an adverse effect on cardiac development in embryos treated with silver nitrate.

Study of accumulation of Ag⁺ ions in developing embryos

Treatment solution from each individual zebrafish larvae was analyzed before and after the treatment of the ion using GF-AAS. Figure 10 shows the amount of Ag⁺ that was accumulated in the individual normal larvae (a), deformed larvae (c), and those embryos that were dead (e) by the end of the 120 hr treatment plotted over at the different concentrations. The averages of those normal (b), deformed (d), and dead (f) embryos are also shown in the plots. From the results, we show that the amount of Ag⁺ found in the 0.4-1.2 μM abnormally developed larvae was not significantly different from those that were dead by the end of the treatment in the same concentrations. However, we do see a significant difference in the 0.4 and 0.8 μM treated larvae that developed normally compared to the deformed and dead larvae. The accumulation rate is much longer at the end of exposure for those larvae that developed normally. This could suggest that the zebrafish that developed normally were able to extrude the Ag⁺ from its system, allowing it to function normally under heavy metal exposure, compared to those who either died during exposure or developed abnormally.

SUMMARY

In conclusion, we have demonstrated an ultrasensitive method to study the toxicity of Ag⁺ ions on zebrafish embryos aiming to assess nanotoxicity on embryonic development, heart functions, and hatched time. Dose-dependent toxicity effects of the

Ag^+ ions on embryonic development were observed, showing that the numbers of zebrafish developed normally decreased while the numbers of dead zebrafish increased as Ag^+ ion concentrations increased. The Ag^+ ions not only interfere with embryonic development but also heart development and functions. We observed heart deformities and lower heart rates in zebrafish exposed to Ag^+ ions. Further studies are needed for a deeper understanding of how Ag^+ ions cause heart deformities from a mechanistic perspective. Moreover, delays hatching in zebrafish were observed in a dose-dependent manner. Zebrafish embryos exposed to high concentrations of Ag^+ ions hatched later.

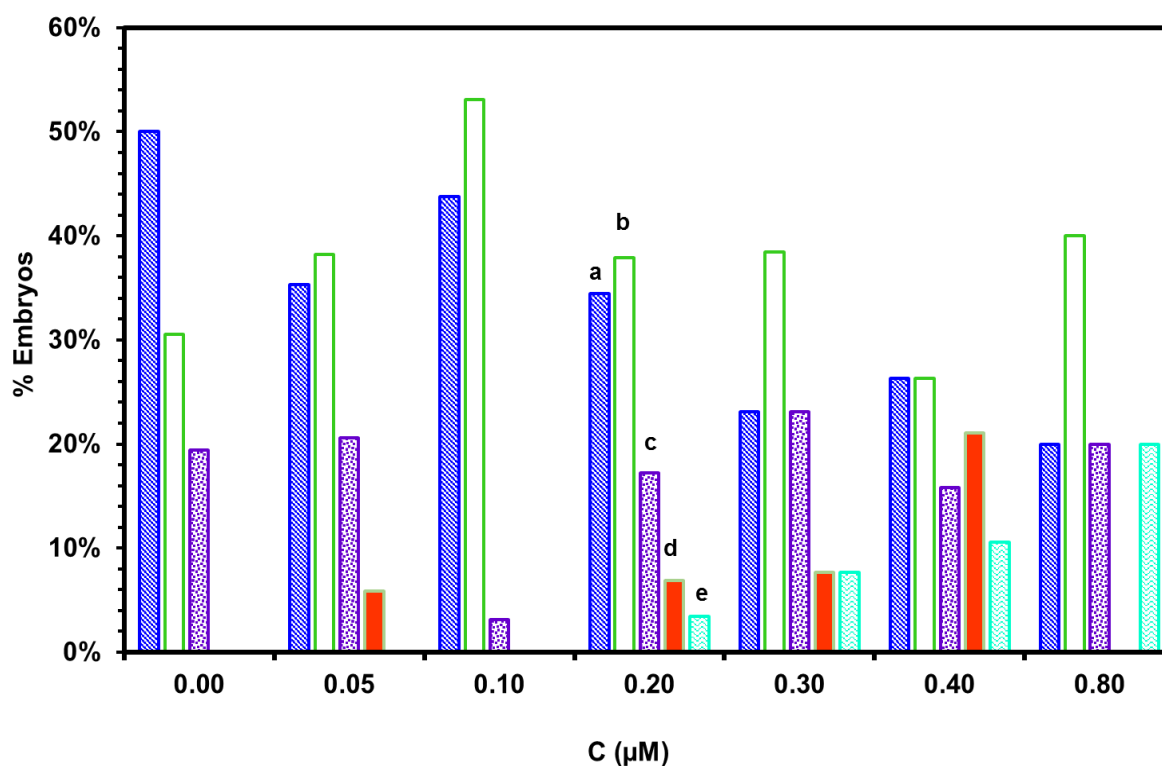


Figure 8: Study of hatching rate of zebrafish treated chronically by AgNO_3 .

Histogram of the percentages of Zebrafish that successfully hatched during the exposure to the Ag^+ . Newly hatched embryos were observed every 5 hours during incubation and recorded at (a) 56 hpf in black; (b) 66 hpf in pink; (c) 76 hpf in cyan; (d) 86 hpf in purple; and (e) 96 hpf in orange. The means and standard deviations (error bars) of the percentage of total number of embryos that hatched at given time points shown for each given concentration are from triplicate measurements.

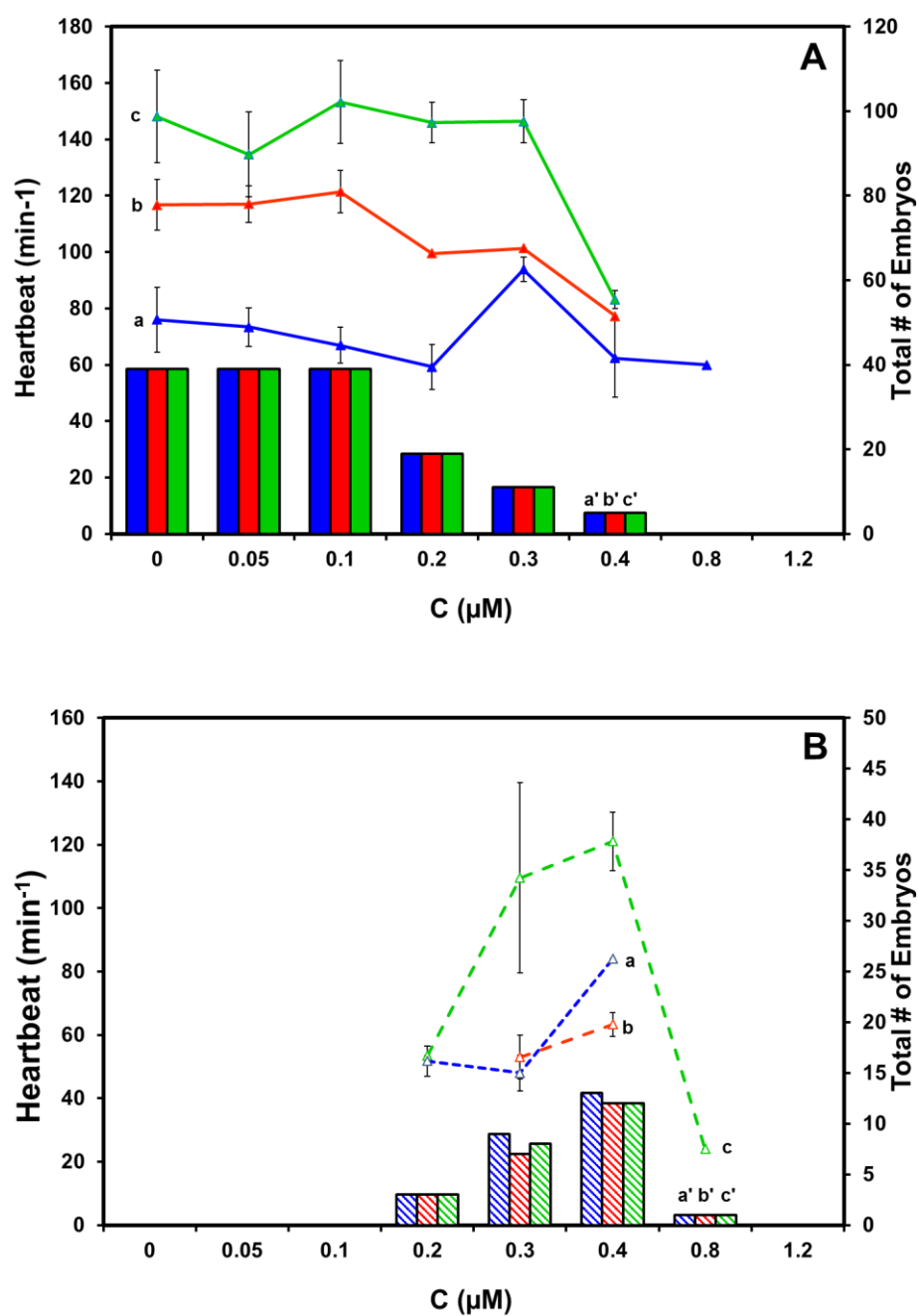


Figure 9: Study of heart rates of zebrafish treated chronically by AgNO_3 .

(A) Plotted graph of the average heart rate and standard deviation (error bars) of normally developed Zebrafish exposed to the Ag^+ . Heart Rates were recorded at (a) 24 hpf in blue; (b) 48 hpf in orange; and (c) 120 hpf in green. Total number of zebrafish counted during

the study represented at each time point as (d) 24 hpf as blue bar; (e) 48 hpf as orange bar; and (f) 120 hpf as green bar. (B) Plotted graph of the average heart rate and standard deviation (error bars) abnormally developed Zebrafish exposed to the Ag^+ . Heart Rates were recorded at (a) 24 hpf in blue; (b) 48 hpf in orange; and (c) 120 hpf in green. Total number of zebrafish counted during the study represented at each time point as (d) 24 hpf as blue bar; (e) 48 hpf as orange bar; and (f) 120 hpf as green bar.

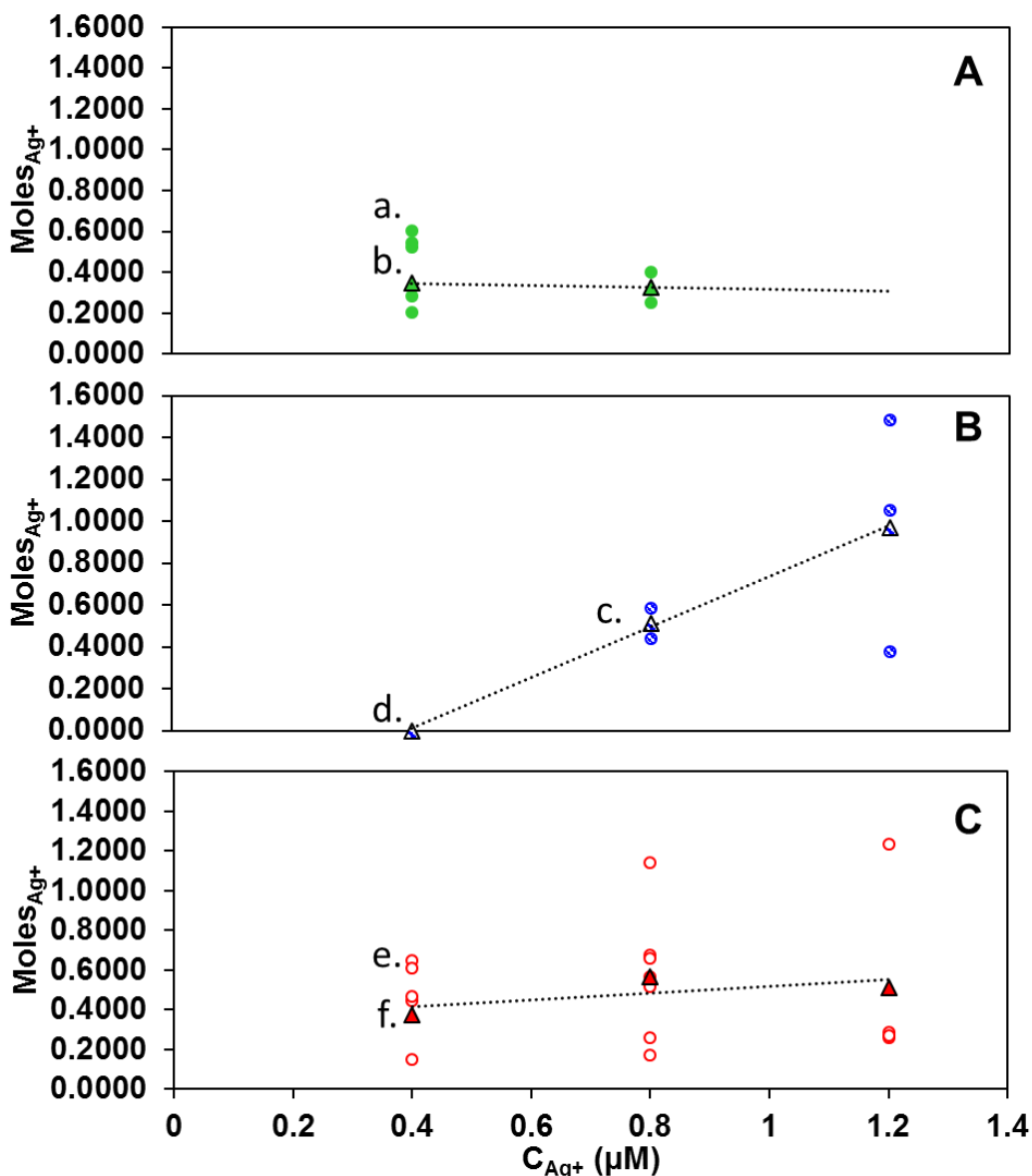


Figure 10: Study of Ag^+ ion uptake in zebrafish treated chronically by AgNO_3 since their cleavage stage shows concentration dependency.

Histogram of the number of micromoles (μmole) of Ag^+ that was uptake by the embryo during treatment. Treatment solution was collected before and after ion exposure and analyzed using GFAAS. The recovered ionic moles was plotted against the concentration of the treatment solution for each (A) Normal developed larvae with (a) green circle being

individual normal larvae and (b) green triangle being the average of the individual normal larvae; (B) Abnormally developed larvae with (c) blue circle being individual deformed larvae and (d) blue triangle being the average of the individual deform larvae; or (C) dead embryos with (e) red circle being individual dead embryos and (f) red triangle being the average of the individual dead embryos, to represent the zebrafish embryo at 120 hpf after treatment.

MATERIALS AND METHODS

Reagents and supplies

Deionized (Di) water (18 M Ω , Barnstead) was used to prepare all solutions. AgNO₃ was purchased from Sigma and stored in small premeasured aliquots in small amber bottles until treatment solution preparation.

Breeding and monitoring of zebrafish embryos

Wild type adult zebrafish (Aquatic Habitats) were raised and maintained as previously described.⁴¹⁻⁴⁴ A 4:3 (female: male) ratio of breedable adult zebrafish were set up the night before the experiment in a 10.0 L clear housing tank (Pentair Aquatic Habitats) for mating using fresh circulated system water maintained at 28.5°C. Once the light was on the next morning (14 h light: 9 h dark circadian cycle), adults were allowed to chase and breed until a sufficient amount of embryos were present. Healthy fertilized embryos were collected into fresh system water using a siphoning collection hose. Once collected, healthy embryos were transferred into a petri dish containing egg water (1.0 mM NaCl) and washed three times with egg water to remove the surrounding debris. All experiments involving embryos and zebrafish were conducted in compliance with IACUC guidelines (protocol # 15-012).

Study of concentration-dependent toxicity of Ag⁺ on embryonic development

Once embryos reached cleavage stage (2 hpf), embryos were treated in egg water and incubated with a dilution series of AgNO₃ (0.00, 0.05, 0.10, 0.20, 0.30, 0.40, 0.80, and 1.20 μ M) in 24-well plates for 120 h, one embryo per well. The treated embryos were incubated in a water bath at 28.5 °C for 120 h for which no light was provided to prevent photodecomposition of the Ag⁺ ion. The developing zebrafish embryos were imaged over

time at 0, 24, 48, 72, 96, and 120 hpf by bright field optical microscopy using an inverted microscope (Zeiss Axiovert) equipped with a CCD camera (Coolsnap, Roper Scientific) and a color camcorder (Sony). Twelve embryos were studied for each concentration in one run of the experiment and three replicates of the runs were used, bringing the total number of 36 embryos studied for each concentration.

Study of hatching rate of zebrafish upon Ag^+ concentrations

When the embryos developed to the hatching stage of developed (48 hpf), we monitored the embryos every 2 hours for any newly hatched from the embryonic barrier of the chorions. Newly hatched embryos were imaged for any abnormalities. Hatching rate was then determined each concentration by counting the number of newly hatched embryos at each given time point and graphed over time.

Quantitative study of heart-beat of developing zebrafish upon Ag^+ concentrations

Both treated and control embryos were analyzed for heart rates. Embryos were recorded using the Sony camcorder and Coolsnap Ez (Roper Scientific) using 100 frames with a 50 ms interval delay. The recordings were taken at 24, 48, and 120 hpf. The movies were then converted and analyzed for manual counting of the hearts contractions. The heartbeat per minute was then compared graphically to both the normal and abnormal developed fish at each concentration.

Study of the accumulation of Ag^+ in zebrafish embryos using GF-AAS

A series of dilutions of standard solutions of Ag^+ was prepared using Silver spectrometric standards (100 ppm) for calibration purposes. Treatment solution from each individual zebrafish embryo was pipetted out at the beginning and end of the treatment into 2 mL centrifuge tube. Samples were briefly centrifuged to remove any

embryo debris. Each solution was analyzed using GF-AAS (Shimadzu Atomic Absorption Spectrophotometer AA-7000 Series). Calculations were made to determine the uptake of the ion by the embryo by subtracting the initial silver ion concentrations from the final silver ion concentrations. The final delta concentration, ΔC , was then plotted over the treated concentrations.

Data analysis and statistics

Each experiment related to this study was performed at least four times and a total of 70-75 embryos for each experiment were studied to gain sufficient data for statistical analysis, permitting the study of the effect of AgNO_3 on a bulk amount of embryos at the single embryo level. We presented averaged the number of normally developed, dead and deformed zebrafish vs. Ag^+ concentration with standard deviations. We used conventional statistical analysis methods (t-test, ANOVA, Tukey's, SigmaStat 3.5 with $P = 0.05$) to determine the significance of the different observations between all concentrations for development, hatching, heartrate and uptake results. A Pairwise T-test comparison was performed of Deformities Histogram.

CHAPTER III

***IN VIVO* STUDY OF THE ACUTE TOXICITY OF SILVER IONS ON EARLY DEVELOPMENT OF ZEBRAFISH EMBRYOS**

INTRODUCTION

Nanomaterials exhibit distinctive physicochemical properties leading to their unique functions and a wide range of potential applications in engineering, medicine, and electronics. For example, their surface areas allow effective surface modification for more effective and more specific in order to increase drug efficacy. Silver nanoparticles (Ag NPs) have also been increasingly used in consumer products such as socks, home appliances, and disinfectants.⁴⁵⁻⁵³ The potential release of NPs into aquatic environments could have an adverse impact on human health.⁵⁴ Thus many studies have indicated toxicity of nanomaterials including Ag NPs in living organisms. For example, trace concentrations of Ag NPs result in death and deformities in zebrafish. In the environment, some types of nano-metals will gradually dissolve by dissolution of metal ions from the surface of the particle. In addition to nanomaterial toxicity, Ag⁺ ions could possibly lead to adverse environmental impacts as Ag⁺ ions have been utilized as salt precursors in Ag NP synthesis. Ag⁺ ions have been reported to interact with thiol groups which are found in antioxidant resulting in oxidative stress.³² Moreover, metal ions including Ag⁺ ions can also inhibit the bronchial Na⁺/K⁺-ATPase. Ag⁺ ions causing osmoregulatory failure in fish. For example, low concentrations of Ag⁺ ion as low as 1.7 ng mL⁻¹ resulted in a reduction in the Na⁺, K⁺-ATPase activity in rainbow trout (*Oncorhynchus mykiss*) gill. ⁵⁵

Zebrafish (*Danio rerio*) embryos can serve as an important model organism to study aquatic environmental toxicity because of numerous advantages, including (i) the

rapid embryonic development (within 120 h) with well-defined developmental stages *ex utero*, which facilitates experimental manipulation and allows the direct observation organogenesis *in vivo*; (ii) massive amounts of zebrafish embryos can generate at once providing high throughput screening animals to analyze; (iii) the organization of the genome and the genetic pathways controlling signal transduction and development are highly conserved between zebrafish and human.

Zebrafish are time efficient for care and maintenance and they effortlessly spawn in large numbers from week to week producing macroscopic fertilized eggs, which are ideal for observing different developmental stages.⁵⁶⁻⁶⁰ The embryonic development is so rapid that the first stages of development are completed in the first 24 hours post fertilization (hpf) and the normal embryo will hatch and swim by 72 hpf. The majority of developmental mutations identified in zebrafish have close counterparts in other vertebrates, suggesting that this system can be effectively used as a model for understanding the developmental processes of higher organisms, including humans.^{40, 61-}

63

Despite superior intrinsic properties of zebrafish embryos, they have not yet been widely used as a standard *in vivo* assays for screening of biocompatibility and toxicity of nanomaterials and metal ions at specific developmental stages. Our lab was one of the first groups to utilize this model to study size-dependent and stage-dependent biocompatibility on smaller size Ag NPs using this animal model. ⁶⁴

RESULTS AND DISCUSSION

Study of effects of Ag⁺ on different developing stage of embryos

The normal course of embryonic development in zebrafish in the absence of Ag⁺ ions for each acute treatment stage is depicted in Figure 11. Acute treatment occurred at five different stages of development for a 2 hour incubation time with silver ions: stage I, cleavage stage (2-4 hpf) (Figure 11 A (a)), stage II, gastrula stage (6-8 hpf) (Figure 11 A (b)), stage III, early segmentation stage (12-14 hpf) (Figure 11 A (c)), stage IV, late segmentation stage (21-23 hpf) (Figure 11 A (d)) and stage V, hatching period (48-50 hpf) (Figure 11 A (e)). During stage I, the embryo will undergo dramatic changes like rapid cellular division and meticulous embryonic pattern formation.^{51, 65, 66} During stage II, embryos will undergo cell migration, early gastrulation for the establishment of organ and organ system development.⁶⁶⁻⁶⁹ Stage III and stage IV is the segmentation stages. In stage III, embryos will begin somitogenesis and notochord formation, which is important for proper development of the axial skeleton, the vertebrate spinal column, and skeletal muscle.⁶⁹⁻⁷² During stage IV, embryos will undergo cardiovascular and circulatory development where the first embryonic heartbeat and pumping can be observed.^{62, 69} Stage V is the hatching stage, where the primary organs of the embryo would have underwent development, and the embryo will hatch out of its protected chorion to finish its development. Their developmental stages were selected because of their importance during embryogenesis. Changing the embryonic environment and exposure of toxins and chemicals during these stages have been known to influence embryos phenotypical development and survivability. These development stages are proven to be the most sensitive to exposure.^{62, 63}

Embryos at each stage were observed throughout development after acute treatment with Ag^+ ions. Stage I-IV embryos were observed after acute treatment at 24 hpf (Figure 11 B (a)), 48 hpf (Figure 11 B (b)), 72 hpf (Figure 11 B (c)), 96 hpf (Figure 11 B (d)), and 120 hpf (Figure 11 B (e)). Stage V embryos were only observed after acute treatment at 72 hpf through 120 hpf, (Figure 11 B (c-e)).

Concentration and development stage dependent toxicity study

Danio rerio embryos exposed to sublethal concentrations of Ag^+ ions acutely at selected stages revealed that Ag^+ ions induced death, as well as variations in the severity of morphological defects, increasing with increasing concentrations of the Ag^+ ion. Figure 12 shows the overall status of controls and treated embryos at 120 hpf for each Acute Stage. Stage I is shown in Figure 12A, stage II is shown in Figure 12B, stage III is shown in Figure 12C, stage IV is shown in Figure 12D, and stage V is shown in Figure 12E. The critical concentrations for each stage are shown in Table 1. Here, we define the critical concentration of the Ag^+ ions at which only 50% of embryos develop normally.

Stage I resulted in an increasing number of deformities in Ag^+ treated embryos as the concentration increased (Figure 12A), with a critical concentration of least than 0.1 μM . Even after exposure to the lower concentration of silver ions, stage one treatment resulted in abnormalities. With increasing concentration, there was also an increasing number of embryonic deaths. At the two highest tested concentrations, a majority of embryonic death was observed. Because this stage is prominent for rapid cellular division, exposure of Ag^+ ions at this stage can significantly influence the development of embryos long term. Thus we see a significantly lower critical concentration at 0.1 μM , which is the lowest for all five treatment stages.

Embryos treated in stage II had an increasing rate of embryonic death observed in higher concentrations. Formation of deformities were also observed amongst the lowest treated Ag^+ ion concentration. Critical concentration for stage II was observed at $0.2 \mu\text{M}$. Stage II appeared to display an ample amount of abnormal development amongst all treatment groups when compared to all other stages. The highest number of deformed embryos were observed in stage II. As the concentration of Ag^+ ion also increased, there was a decrease in normally developed embryos, and correspondingly, an increased in embryonic death. The highest concentration treated resulted in complete elimination of normally developed embryos, with only abnormal or death displaying. The early gastrulation stage is significant because at this stage, cellular movement is observed, where cells start to migrate into positions that will determine their cellular fate.

Stage III shows that embryo treated at this time point did not have drastic embryonic death until the two highest treated concentration (Figure 11 a). At those concentrations, there was a majority of embryonic death amongst treated embryos. This stage presented the lowest amount of abnormally developed embryos from all treatment groups. The critical concentration was determined to be between $0.40 - 0.80 \mu\text{M}$. Stage III is the early segmentation stage where the notochord and spinal cord are heavily influenced.

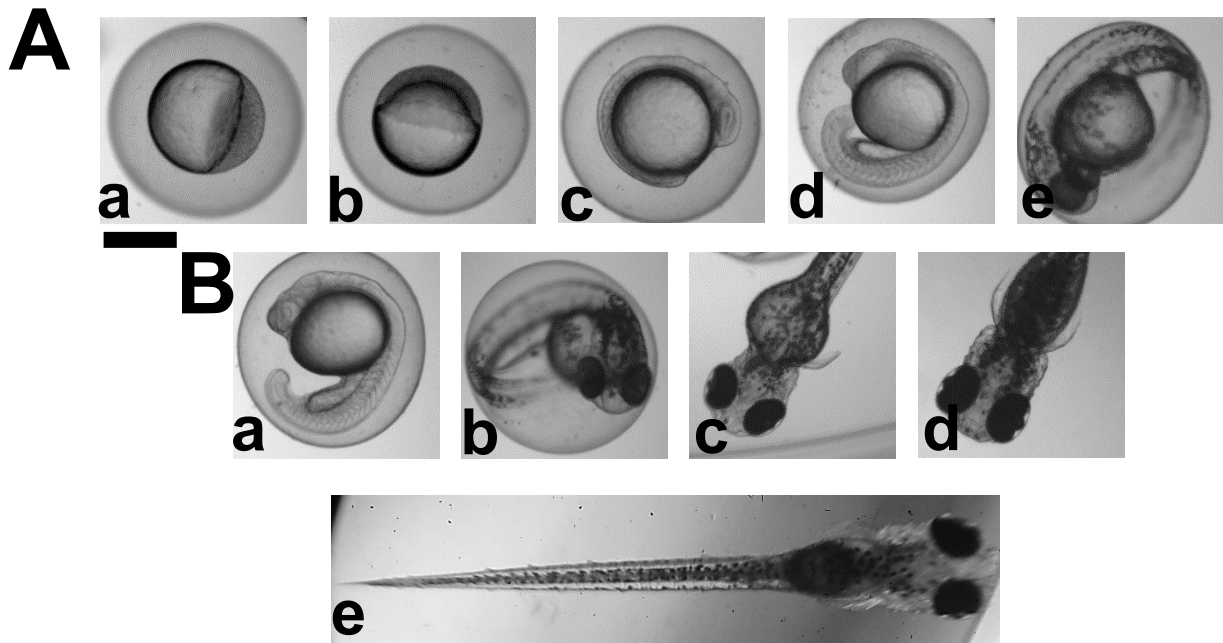


Figure 11: Normally developed zebrafish at stages I – V at the time of acute treatment and observations after acute treatment.

(A) Representative optical images of normally developed zebrafish at the time of acute treatment for stage I – V, (a) 2 hpf (cleavage stage); (b) 6 hpf (early gastrula stage); (c) 12 hpf (early segmentation stage); (d) 21 hpf (late segmentation stage) and (e) 48 hpf (hatching stage). (B) Representative optical images of normally developed zebrafish observations after acute treatment for stages I – IV, (a) 24 hpf (late segmentation stage); (b) 48 hpf (hatching stage); (c) 72 hpf (pharyngula stage); (d) 96 hpf larvae and (e) 120 hpf fully developed larvae. Note that observations for stage V began at (c-e). Scale bar = 250 μm.

Stage V was the least sensitive to toxic treatment stage out of all acute stages. At this stage, there were a significant number of embryos which were not affected by the Ag^+ ion treatment. There was abnormal development in each treatment group, but the toxic effects of the ion were slightly less than the other concentrations. The most embryonic death was at the highest treatment concentration, where at least 50% of the embryos did not survive. The critical concentration was $0.80 \mu\text{M}$. This stage also showed the most amount of embryonic survivalist between all stages. At this stage, the embryo will start hatching out of their chorions, because of the primary organ development. These results show the embryo is less affected by the exposure of the silver ion at this stage.

From our previous studies, we were able to compare the toxicity effects of Ag^+ to our Ag NPs studies. These results show that the toxicity of single Ag NPs, at different sizes, have a more toxic effect acutely than their bulk counterparts.

We treated stage I through V embryos acutely with increasing concentrations of Ag^+ ions ($0.00 - 1.20 \mu\text{M}$). Embryos were carefully monitored post-treatment at 24, 48, 72, 96, and 120 hpf (Figure 11). We examined the abnormalities in developing embryos at each treated stage. Many morphological defects were observed in the developing embryo, which included abnormal finfold and tail development, cardiac malformation, yolk sac edema, and head and eye abnormalities, as recorded in Figure 13.

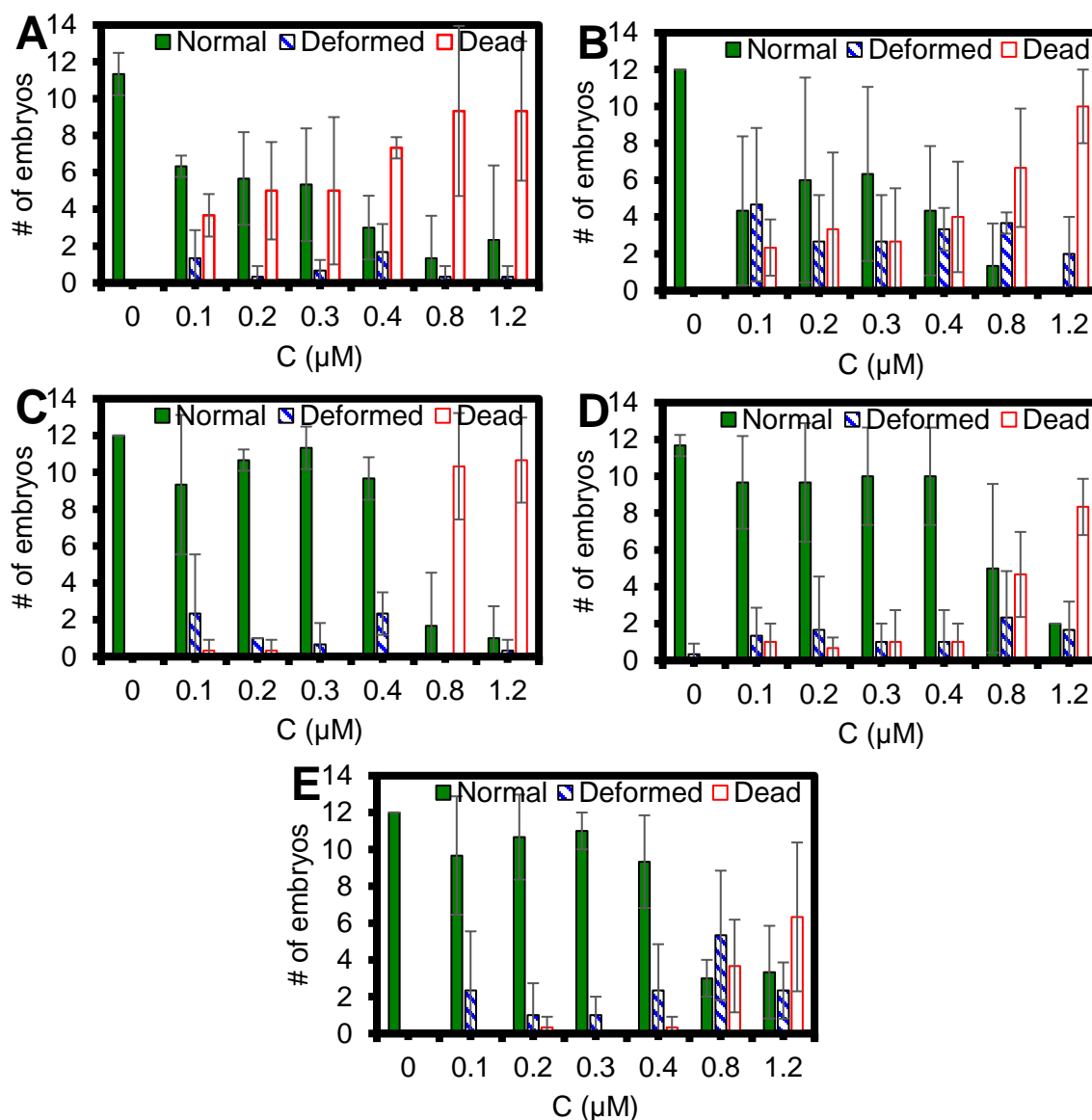


Figure 12: Study of concentration and stage dependent toxic effects of AgNO_3 on embryonic developments.

Histograms show the average number of staged embryos (A-E; stages I – V), incubated with given concentrations of AgNO_3 for 2 h, that developed into normal or deformed zebrafish or died in egg water over 120 hpf. The means and standard deviations (error bars) of the number of embryos shown for each given concentration are from triplicate measurements.

Table 2: Critical Ag⁺ ion Concentration for Specific Developmental Stages of Zebrafish.

Stage	I	II	III	IV	V
Critical Concentrations (μM)	$>0.1 \mu\text{M}$	$0.2 \mu\text{M}$	$0.4\text{-}0.8 \mu\text{M}$	$0.8 \mu\text{M}$	$0.8 \mu\text{M}$

All stages presented some abnormal developing embryos. The shared common type of abnormality amongst all stages was finfold abnormalities, which typically affects the median finfold region (Figure 13A (a)). In a normally developing embryo, the median of the finfold is clear and organized thin membrane around the trunk region which contains unsegmented fin rays. However, in the abnormal finfold region, we observed that the tissue is disorganized and the structure is altered. In the more severe deformed embryos, the fin rays are severely misshaped and the shambolic. We also observed tail and spinal cord flexures in most of the deformed embryos from all stages (Figure 13A (a)). In normally developed embryos, the tail and spinal cord will develop straight to the posterior-most tip of the tail. However, in those embryos treated with Ag⁺ ions, the tail was often curved or flexed. In some more severe cases, the tail was extremely truncated compared to normally developed embryos. These severities in the tail flexure usually resulted from increased Ag⁺ ion concentrations.

Severity and other forms of observed deformities usually depended on the treated developmental stage. Embryos treated with higher Ag⁺ ion concentrations in all stages usually resulted in edema in the pericardial sac, the double-layered conical sac of fibrous

tissue which surrounds the developing heart muscles. In normal embryos, the pericardial sac is a thin membrane serving as a protective barrier to the developing heart. However, observed swelling of this region resulted in enlargement of the heart muscles. Additionally, enlargement of the yolk sac region was also observed. The yolk sac region is a bulbous area containing nutrients needed for the developing embryo, which will usually shrink during the development, as the embryo becomes less depended on those nutrients. We, however, observed this region to be swollen after 120 h of treatment with the Ag^+ ions.

In the most severe cases, we observed head and eye abnormalities in those embryos treated with Ag^+ ions. In these cases, we observed smaller or irregularly we observed either one or both lenses were altered. These cases were rarely observed, but when present, was usually together with the other observed abnormalities previously mentioned.

Figure 13 shows the represented deformities shown in all treated stages. In embryos treated in all stages, we observed all of the described abnormalities (Figure 13 (a-d)) with the finfold and tail flexures being common for the treated concentrations, where most were found in the 0.10 and 0.20 μM treatment groups. For stages, I, II, and III, yolk sac and pericardial sac edemas were commonly found in the 0.20 – 0.40 μM treatment groups. In stage IV we observed pericardial sac edemas and yolk sac edemas in all treated groups. In stage V, although rarely observed, we only saw the presence of all categorized abnormalities in the higher concentrations.

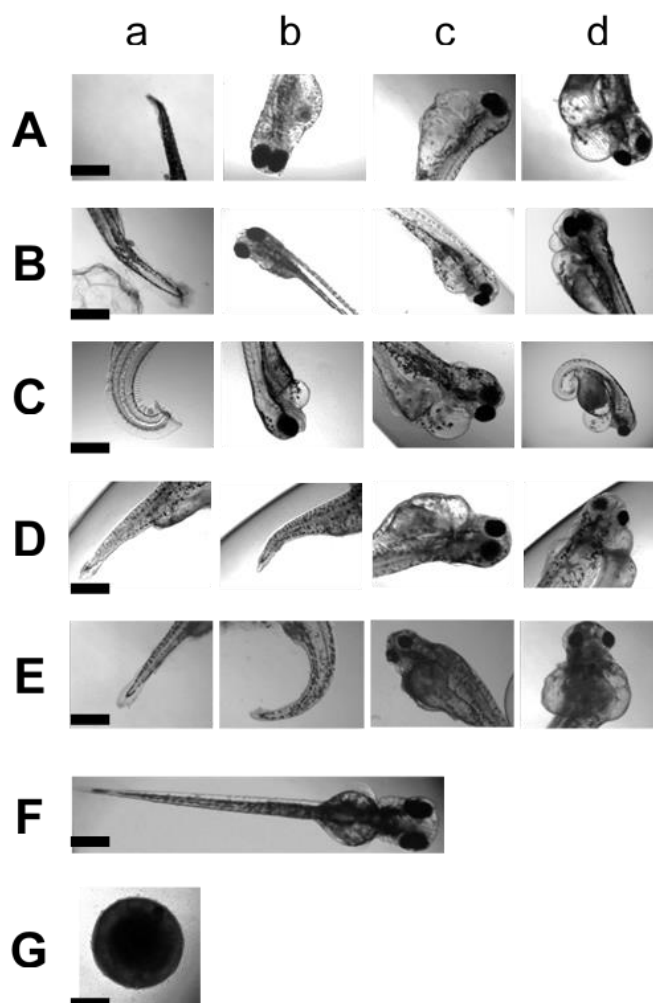


Figure 13: Representative optical images of deformities observed in stages I – V after acute treatment with AgNO_3 .

(A) Stage I, (B) Stage II, (C) Stage III, (D) Stage IV, (E) Stage V represents deformed zebrafish displaying (a) finfold abnormality; (b) tail/spinal cord flexures; (c) pericardia malformation and yolk sac edema; (d) head and eye abnormality. (F) Represents normally developed Zebrafish larvae at 120 hpf. (G) Represents dead embryo after treatment. Scale bar: 250 μm .

shaped of tissues where defined craniofacial anatomy was clearly observed. The eyes would become smaller in size compared to a normally developed embryo. In minor cases,

In stage III, we did observe more severe cases of tail curvatures and spinal cord inflections in those higher concentrations of the Ag^+ ions. This is significant in that stage III is the early segmentation stage where the notochord and spinal cord are forming. The phenotypes observed suggest that exposure to the Ag^+ ions at this developmental stage is highly influenced to result in tail malformation. Likewise, in stage IV, pericardial sac edemas were prominent in all treated concentrations. These observed results suggest a phenotypical depended occurrence in developing embryos when Ag^+ ions are present. Possible reasons for the high dependence of type and severity of defects on the stage of development and concentration of Ag^+ ions could be due to the following: (i) Ag^+ ions enter inside the chorion space of the embryo during the specific stage of development and affect the specific proteins, signaling, and developmental pathways during that period of development. (ii) An increase in the number of Ag^+ ions inside the chorion space of the embryo during the specific stage of development increases the altering effects of the protein, signaling, and developmental pathways during development increasing severity of the deformity observed or death.

Our results describe a range of developmental defects and absolute death following exposure of developing zebrafish embryos to micromolar concentrations of Ag^+ ions at particular embryonic stages of development. Specific developmental pathways of embryonic development are still unknown, such as, differentiation into specialized tissues and organs, specifically how cells communicate with each other, how they become committed to a certain fate, and how they formulate a pattern to become a structure. ^{18,}

^{73, 74} Stage-dependent developmental responses to Ag⁺ ions, shown here, in a concentration-dependent manner, demonstrates the possibility of being able to pick specific developmental pathways to create particular phenotypes and as potential developmental therapeutic agents to treat specific disorders and generate specific developmental mutation in zebrafish, by alteration of the time of application of the Ag⁺ ions.

Study of stage-dependent effects of Ag⁺ on embryonic cardiac development

As we observed pericardial sac edema and cardiac malfunctions in zebrafish treated with silver ions, we further studied the effects of these ions on the cardiac function of zebrafish after their exposure to the Ag⁺ ion compared with the controls at different time points. Basically, individual myocardial cells begin to contract irregularly around the 22-somite stage (21 hpf) giving heart rate at about 25 beats per minute. Heart rates dramatically increase to about 90 beats per minute by 24 hpf when shortly thereafter blood circulation begins. As the heart developed, morphological differentiation progresses in an arterial to venous direction. The heart tube has looped and beat at higher rates to provide a strong circulation to the trunk and head. ^{75, 76}

In all stages, we found that the number of embryos with normal developed heart decreased as the Ag⁺ ion concentration increased since some embryos exposed to Ag ions were either dead or deformed. In normally developed zebrafish, heart rates increased as the heart developed. Heart rates of normally developed zebrafish at 48 hpf and 120 hpf were significantly greater than those at 24 hpf when the heart was at the early developmental stage (Figure 14). However, Ag⁺ ions insignificantly reduced embryo heart rates at 24, 48, and 120 hpf in a dose-dependent manner (Figure 14). In contrast,

those cardiac deformed zebrafish at all concentrations surprisingly showed no significant difference in heart rates over developmental periods. Their heart rates at 48 hpf and 120 hpf were at the same or lower than those at 24 hpf (Figure 14). This suggests that the heart became increasingly deformed over time which could lead to lower heart rates, less blood flow, and oxygen supply, and thus possibly contributing to mortality. Ag NPs have previously shown to interfere with regular cardiac functions.^{44, 64, 77-79} Improper blood flow could starve the cells of gases and essential nutrients, resulting in cell death.^{74, 80, 81}

It is worth noting that the heart rates of cardiac deformed zebrafish were much lower than zebrafish with normal cardiac development but not in a concentration-dependent manner. Although the mechanisms are still not well understood, Ag⁺ ions could disrupt heart development contributing to heart deformities and then leading to the depressed heart rates.

Specifically, we did not observe a significant difference between treated stages, as all stages displayed similar heart rates, despite the differences in overall development and toxicity, which showed a stage-dependent trend. Stage I – V (Figure 14 A-E) all resulted in similar trends, where, the higher the Ag⁺ ion, the lower the heart rate recorded. One notable difference we did observe was for stage IV (Figure 14 D) when it came to those deformed zebrafish in the 1.20 μ M treatment group. The heart rate for the deformed embryos was noted to be significantly higher at 120 hpf. This could be influenced by treatment at this particular developmental stage, where cardiogenesis is majorly affected during the development of the heart muscles. More studies would need to be conducted to further examine this phenomenon.

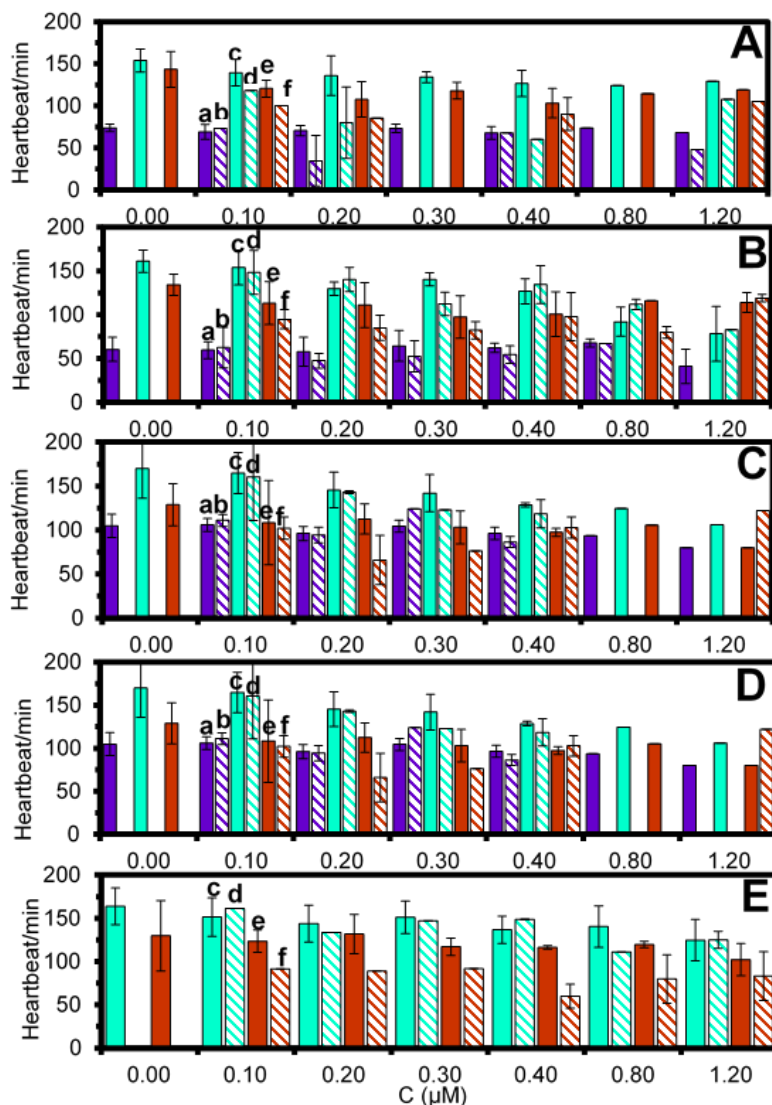


Figure 14: Quantitative Heartbeat Analysis for specific developmental stages of embryos.

Heartbeats were taken at 24, 48, and 120 hpf for all embryos. Based on development, heartbeats per minute was graphed by concentration for (a) 24 hpf Normal, (b) 24 hpf Deformed, (c) 48 hpf Normal, (d) 48 hpf Deformed, (e) 120 hpf Normal, and (f) 120 hpf Deformed Analysis for (A) Stage I embryos, (B) Stage II, (C) Stage III, (D) Stage IV, (E) Stage V.

Study of stage-dependent hatched time of zebrafish upon Ag⁺ concentration

Zebrafish hatching is a vital step for survival. Longer hatching duration could leave organisms more susceptible to predators and if hatching is inhibited, embryos could die in their chorions.^{14, 82} In fact, zebrafish hatching is associated with two processes.^{16, 20, 22} Initially, the hatching enzyme from the hatching gland is released to break down the inner vitelline envelope of the cellular chorion, and then the movement of the embryo breaks the weakened chorion³⁹. Delayed hatching in response to Ag NP exposure has been reported. For example, zebrafish had delayed hatching after exposure to 1 μM Ag NPs. However, the occurrence of delayed hatching due to Ag⁺ ion exposure in zebrafish has not yet been widely studied.

We studied the concentration-dependent effects of Ag⁺ ions on the hatching time of zebrafish embryos (Figure 14) for each developmental stage. Embryos were exposed to Ag⁺ ions with various concentrations (0-1.2 μM) in egg waters for 120 hr. The developing zebrafish embryos were imaged and we monitored newly hatched embryos over time at 4, 24, 48, 72, 96, and 120 hpf. The numbers of newly hatched embryos are shown in Figure 9 for stages I - V. Embryos started to hatch at 48 hpf and the majority of them hatched at 72 and 96 hpf. In all stages, the hatching of embryos was significantly delayed by Ag⁺ ion exposure in a concentration-dependent manner. The embryos that were exposed to higher concentrations of Ag⁺ ions had hatched later than the control and those exposed to the lower Ag⁺ ion concentrations. For example, as shown in Figure 14A, in stage I, at 72 hpf, the majority of control embryos hatched and the numbers of hatched embryos decreased as the concentration increased while at 96 hpf, majority of the

embryos exposed to low Ag ion concentrations (0.05 and 0.10 μM) hatched and at 120 hpf, most of the embryos exposed to high Ag^+ ion concentrations (0.20-1.2 μM) hatched.

In stage III - V treated embryos, we observed a significant number of embryos started to hatch at 60 hpf, which differs from stage I and II. This suggests that this developmental time point results in treated embryos being less sensitive to the Ag^+ ions upon hatching. This difference may suggest that when treated at earlier developmental stages, hatching is reasonably delayed to later time points when Ag^+ ions are present, exhibiting a stage dependent effect on hatching.

Mechanisms of Ag ions causing delayed hatch is still unclear. The delay possibly associates with slowing maturation of the hatching gland, inhibition of hatching enzyme and stunted growth and movement. Notably, zebrafish contains two zinc-based matrix metalloproteinase enzyme genes (ZHE1 and ZHE2) and gene duplication events and subsequent mutations lead to extremely low expression of ZHE2 and non-functioning of hatching. Interestingly, a study showed that Ag^+ ions did not interfere with ZHE1 activity suggesting that the hatching delay could result from another injury mechanism.^{39, 68}

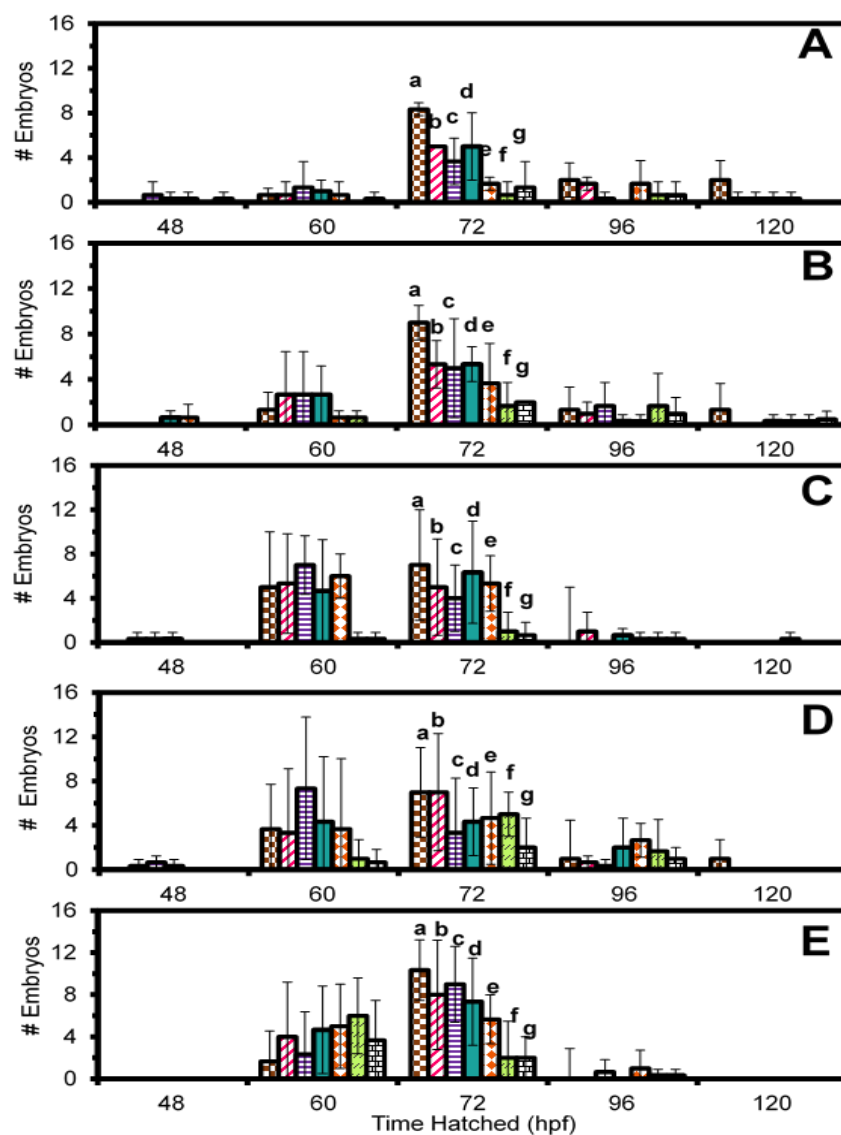


Figure 15: Rate of Hatched Zebrafish Exposed to Ag^+ ions at specific developmental stages.

The overall hatching rate of embryos were taken at 48, 60, 72, 96, and 120 hpf. Hatching was reported by dilution of treated (a) 0.00 μM , (b) 0.10 μM , (c) 0.20 μM , (d) 0.3 μM , (e) 0.40 μM , (f) 0.80 μM , and (g) 1.2 μM AgNO_3 for (A) Stage I embryos, (B) Stage II, (C) Stage III, (D) Stage IV, (E) Stage V.

SUMMARY

In summary, we have studied the toxicity of Ag^+ ions on zebrafish embryos *in vivo* at specific stages of development, aiming to assess nanotoxicity on embryonic development, heart functions, and hatch time. Concentration-dependent, as well as stage-dependent, toxic effects of the Ag^+ ions on embryonic development, were observed, showing that the number of zebrafish developed normally decreased while the number of dead zebrafish increased as Ag^+ ion concentrations increased. We observed a phenotypical dependence of abnormal development upon developmental stage when exposed to Ag^+ ions. Many morphological defects were observed in the developing embryo, including yolk sac edema, abnormal finfold and tail development, and cardiac malformations at each stage of development, corresponding to the stage of treatment. In general, the number of different types of defects and the severity of each varied with the stage of treatment and increased with increasing concentration of Ag^+ ions demonstrating the possibility of selectively targeting specific embryonic developmental pathways by altering the stage of development and dose of NPs for developmental therapeutic studies. The Ag^+ ions not only interfere with embryonic development but also heart development and functions. We observed heart deformities and lower heart rates in zebrafish exposed to Ag^+ ions. Additional studies are necessary for elucidating the mechanism of Ag^+ ion induced heart deformities. Moreover, delays hatching in zebrafish were observed in a dose-dependent manner. Zebrafish embryos exposed to high concentrations of Ag^+ ions hatched later. The investigation of biocompatibility of silver ions, in comparison to the study of metal and metal oxide nanomaterials in specific stages of development of embryos can offer new knowledge about the developmental processes and environment,

and provide new insights into the mechanics of the developing embryo as well as aid in the finding for functional nano-developmental treatments for various disorders in early development. The study of nanomaterials, as well as their bulk counterparts, can lead to understanding their mechanism of toxicity, which is needed since they are increasingly used in many areas of biomedical research.

MATERIAL AND METHODS

Breeding of zebrafish embryos

Wild-type adult zebrafish were housed in a stand-alone system (Aquatic Habitat). They were maintained and bred as described previously. Briefly, we placed two pair adults zebrafish in a clean 10-gallon breeding tank and used a light (14 h)-dark (10h) cycle to trigger breeding and fertilization of embryos. We collected embryos at 2 hpf, transferred them to a Petri dish, and well-rinsed them with egg water to remove surrounding debris. The washed embryos were then used for the study of dose-dependent toxicity of Ag^+ on embryonic development. All experiments involving embryos and zebrafish were conducted in compliance with IACUC guidelines (protocol # 15-012).

Treatment and monitoring of zebrafish embryos

Embryos were collected and transferred into a petri dish containing egg water (1.2 mM NaCl), washed twice with egg water to remove the surrounding debris, and placed into 48-well plates with each well containing one embryo in egg water. Sixteen embryos were tested per concentration, per stage of development; each experiment was repeated 3 times, totaling 48 embryos analyzed per concentration, per stage of development. Treatment for each developmental stage is for 2 h, followed by a wash with egg water, then placed in new wells for remaining of development. Embryos were directly

imaged by bright-field optical microscopy using an inverted Zeiss Axiovert microscope equipped with a 4x objective, CCD (Coolsnap, Roper Scientific) and a digital color camera (Sony).

Study and characterization of toxicity of Ag⁺ on embryonic development

To study the concentration-dependent effects of Ag⁺ ion on embryonic development, a dilution series of Ag⁺ ion treatment solutions (0, 0.10, 0.20, 0.30, 0.40, 0.80 and 1.20 μ M) were incubated acutely with 5 stages of embryos in egg water for 2h. Each experiment was carried out at least 3 times and a total number of embryos at 48 was studied for each individual concentration to gain representative statistics. Ag⁺ ion concentrations were calculated to correspond to previous studied Ag NPs studies. Embryos in egg water in the absence of Ag⁺ ion and in the presence of supernatant were placed in 48-well plates as control experiments to probe the effects of possible trace chemicals from NP synthesis. The embryos in the 48-well plates were incubated at 28.5°C, and directly observed at room temperature using an inverted Zeiss Axiovert microscope equipped with a digital color camera at 24, 48, 72, 96, and 120 hpf.

Data analysis and statistics

For the study of dose-dependent effects of NPs on embryonic development, a total number of 48 embryos were studied for each NP concentration and each control experiment over 120 hpf with a minimum of 12 embryos studied in each measurement. We presented averaged the number of normally developed, dead and deformed zebrafish vs. Ag⁺ concentration with standard deviations. We used conventional statistical analysis methods (t-test, ANOVA, Tukey's, SPSS Statistics with P = 0.05) to determine the significance of the different observations between all concentrations for development,

hatching, and heartrate results. A Pairwise T-test comparison was performed of Deformities Histogram.

CHAPTER IV

STUDY OF STAGE DEPENDENT BIOCOMPATIBILITY AND TOXICITY OF SINGLE 42 NM SILVER NANOPARTICLES USING EARLY DEVELOPMENT OF ZEBRAFISH EMBRYOS

INTRODUCTION

Nanoparticles (NPs), per their small size and unique physical properties, are ideal for use in probing the nanoscale environments of living organisms, which enables the study of a developing living organism at specific developmental stages of embryonic development.^{72, 83-86} Single nanoparticles and their unique optical properties make imaging *in vivo* more sensitive, allowing the transport of the NP in living vertebrates to be monitored and offers new information on the developing mechanisms of the embryonic organism. NP probes can be used in a variety of applications for new insight into developmental processes, such as the improvement of screening tools in developmental biology to investigate the embryonic innermost environment, to potentially control and regulate certain processes in development, and to target specific system regulators for biomedical biological uses. Nanomaterials could demonstrate developmental stage-dependent requirement of phenotypical morphology induced, suggesting that the nanomaterials, at higher concentration, may interact with target developmental pathways of interest.^{43, 64, 77, 87-89} In this study, we used our previously described nanomaterials,⁴⁴ Ag NPs, and our effective embryo developmental model system, zebrafish embryos, to focus on acute developmental stage-dependent biocompatibility and understand the impact of nanomaterial exposure during embryogenesis and their mechanisms to induce toxicity at specific development periods.

Commonly, fluorescent probes have been used for probing and imaging *in vivo* cellular pathways during embryonic development.⁹⁰ However, using fluorescent probes have their limitations because they will undergo photodecomposition, which limits the time for intrusive analysis of the embryonic environment for specific stages of interest in real-time. Nanomaterials, such as quantum dots (QDs) and noble metal NPs (Ag, Au and their alloys), are being used more as sensors for *in vivo* assays because they offer unique properties that make them ideal for imaging.^{45, 47, 91-94} Though QDs have unique optical properties compared to their fluorescent counterparts, they still experience a certain extent of photodecomposition which still introduces a sense of variance from real-time analysis.

Ag NP probes have unique optical properties over many fluorescent imaging approaches because they have localized surface plasmon resonance (LSPR), enabling characterization of their size and shape, and they offer high quantum yield (QY) of Rayleigh scattering making them bright and easy to see using dark-field optical microscopy and spectroscopy (DFOMS).^{60, 95-97} Ag NPs can be used as a probe for real-time study over an unlimited period of time because they do not experience photodecomposition as fluorescent beads can. In addition, the LSPR spectra, or color of the Ag NPs, can be used to show size-dependence.^{60, 95, 96} Using the LSPR spectra of the multicolor Ag nanoparticles it is possible to be able to directly characterize the uptake and diffusion of the same color nanoparticle at the nanometer scale in real-time, in different biological environments based on using the same sized Ag NPs.^{93, 98, 99}

Zebrafish (*Danio rerio*) have been extensively employed as a well-studied vertebrate model for embryological development because of its small size, its short

breeding cycle, and the wealth of information available for manipulation.^{63, 70, 100-102} Its transparency throughout development allows observation of all internal organ development from outside the chorion without disturbing the living embryo. Zebrafish are time efficient for care and maintenance and they effortlessly spawn in large numbers from week to week producing macroscopic fertilized eggs, which are ideal for observing different developmental stages. The embryonic development is so rapid that the first stages of development are completed in the first 24 hours post fertilization (hpf) and the normal embryo will hatch and swim by 72 hpf. The majority of developmental mutations identified in zebrafish have close counterparts in other vertebrates, suggesting that this system can be effectively used as a model for understanding the developmental processes of higher organisms, including humans.^{66, 103} Therefore, zebrafish embryos offer a unique opportunity to investigate developmental processes upon treatment with NPs to investigate stage dependence NP effects on embryonic development.

Zebrafish have been used as a model organism for many chemical-screening and drug studies, however, the acute biocompatibility on different zebrafish developmental stages is not well studied.^{101, 104} The acute biocompatibility of Ag NPs on specific sensitive stages of embryonic development has, to our knowledge, only been attempted by our previous studies with smaller sized nanoparticles. It is important to explore the biocompatibility of Ag NPs acutely at specific stages of embryonic development to assess the ability of Ag NPs to be used for *in vivo* imaging at any embryonic stage of development as well as probes in real-time to explore the changing embryonic environment during development, including cardiac influences and neurological changes.

In this study, we have designed *in vivo* assays to study the biocompatibility of Ag NPs in embryonic development to probe developmental changes that could help aid in the investigation of molecular mechanism altered during nanoparticle exposure. We used imaging assays and quantitative cardiac studies to probe the effects on zebrafish embryos.

RESULTS AND DISCUSSION

Synthesis and characterization of Ag nanoparticles (NPs)

We used our previously developed sphere-shaped silver-based nanoparticles that were washed and purified to study their interactions and biocompatibility with key stages in developmental biology. Thus, we can determine Ag NPs role in developmental processes, including stage dependent and dose-dependent morphological responses, for their potential use as developmental targeting probes for biomedical applications.⁴⁴ We characterized the stability, size and optical properties of the purified Ag NPs in egg water embryo media (1.2 mM NaCl) for 120 h using UV-vis absorption spectroscopy, dark field optical microscopy and spectroscopy (DFOMS) and high resolution transmission electron microscopy (HRTEM).

We characterized the size of the Ag NPs using HRTEM and the size was with an average diameter of 41.5 ± 7.6 nm (Figure 16). A representative optical image of Ag NPs in Figure C illustrates that the majority of NPs appear to be blueish green to green, with a few reds. These results suggest that Ag NPs are uniform in size and shape based on their color (LSPR). The representative LSPR spectra of single blue, green and red Ag NPs with peak wavelengths (λ_{max}) at 498 nm (blue) (FWHM = 38 nm), 554 nm (green) (FWHM = 47 nm), and 659 nm (red) (FWHM = 47) nm, respectively (Figure 16). Thus,

the color of Ag NPs can be used as size index to directly distinguish and determine the size of NPs using DFOMS, even though the size of NPs cannot be directly measured due to the optical diffraction limit. We characterized the stability of Ag NPs in egg water for 120 hours, which is the length of embryonic studies. The results are given in Figure 17. The absorbance spectra of freshly prepared and purified Ag NPs before and after the incubation time with egg water demonstrated a peak wavelength (λ_{\max}) at 401nm (FWHM = 56 nm) and remained unchanged for 120 hours (Figure 17 A). We found that the number of NPs remained relatively unchanged when incubated in egg water for 120 h, where the average of total number of NPs from triplicate runs at 0 h and 120 h is $2,044 \pm 28$, and $1,979 \pm 12$, respectively. The unchanged number of NPs and stable absorbance spectra indicates that the Ag NPs are very stable in egg water media and remain non-aggregated.

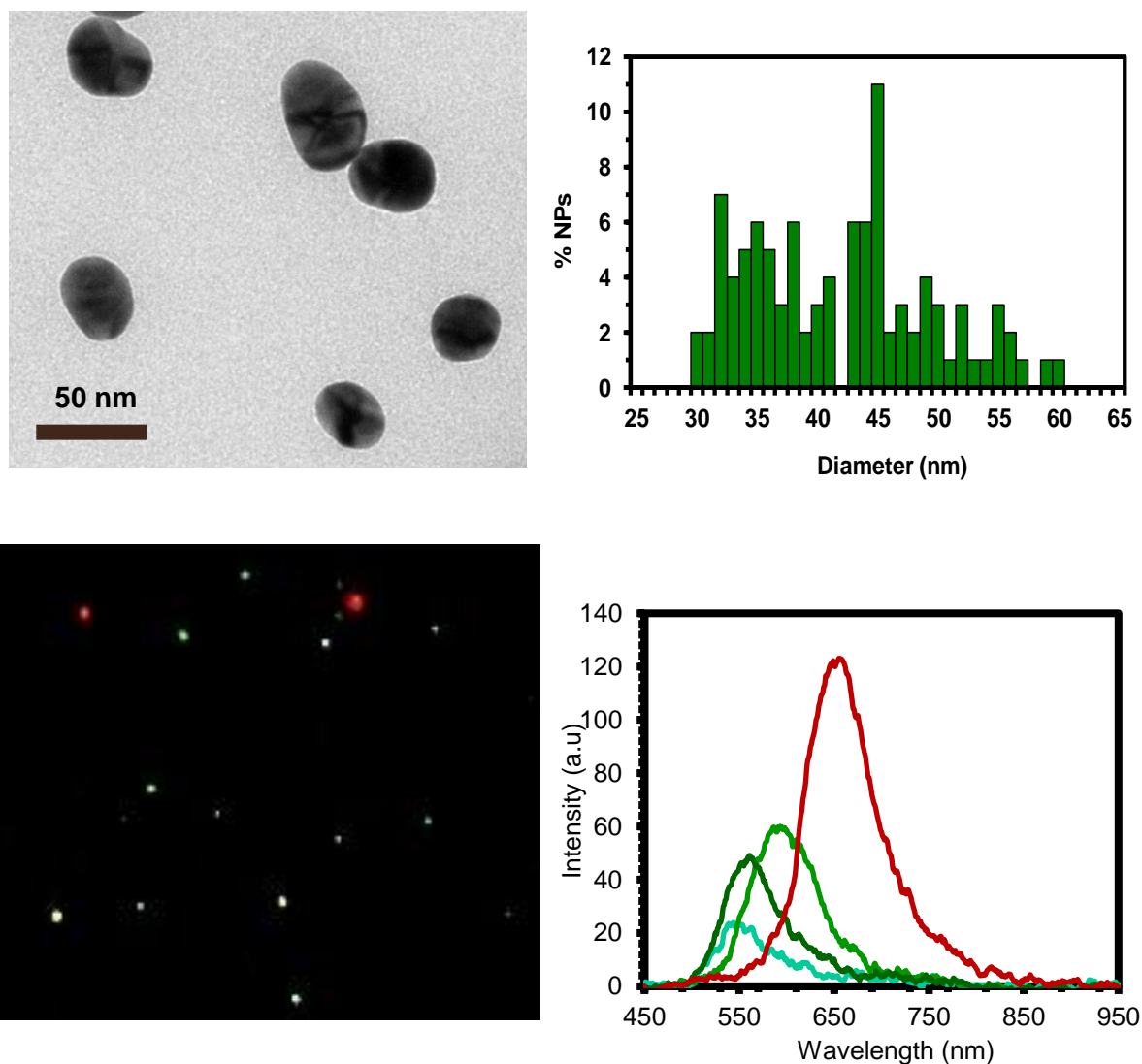


Figure 16: Characterization of sizes, shapes, and plasmonic optical properties of single Ag NPs.

(A) HRTEM image shows the spherical shape of single NPs. (B) Histogram of size distribution of single NPs determined by HRTEM shows average diameters of 41.5 ± 7.6 nm. (C) Dark-field optical image of single NPs shows that a majority of NPs are plasmonic green with some blue-green and red. (D) LSPR spectra of representative single NPs.

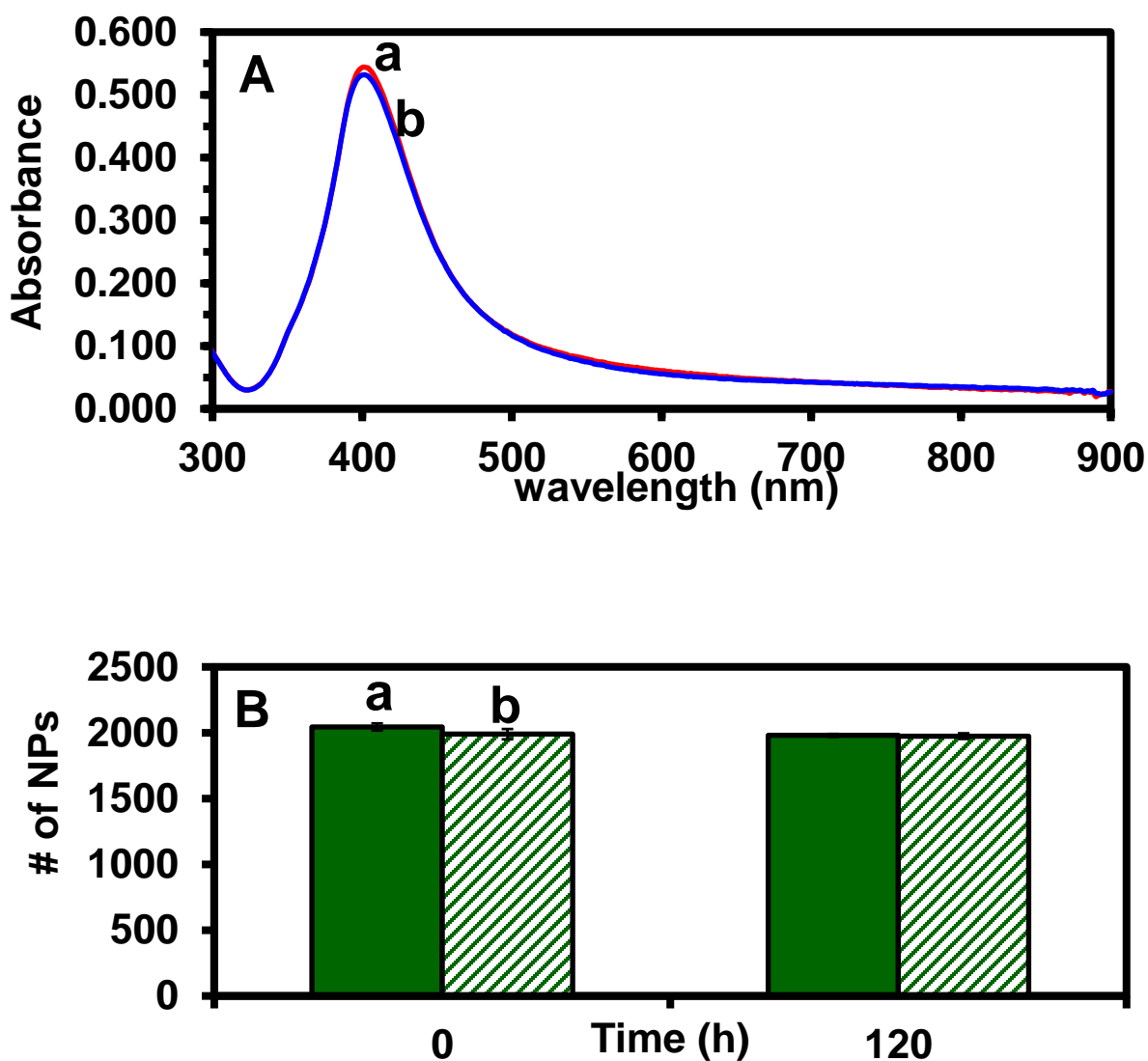


Figure 17: Characterization of stability of Ag NPs in egg water ($C_{\text{NPs}} = 0.5 \text{ nM}$) for 120 h.

(A) UV-Vis absorption spectra of the NPs dispersed in egg water at 28.5 °C for (a) 0 and (b) 120 h show that its peak absorbance of 401 nm (FWHM = 56 nm) remains unchanged for 120 h. (B) The average of total number of NPs from triplicate runs at 0 and 120 h is $2,044 \pm 28$, and $1,979 \pm 12$, respectively. The 10 images are acquired at each given time point using DFOMS.

Exposure of Ag NPs to specific developmental stages of zebrafish embryos

Imaging and monitoring live animals throughout development provides a more informative view of these biological events. That is why we selected zebrafish embryos to serve as our animal model. *Danio rerio* embryos are prominent animal models for real-time analysis during embryogenesis.^{15, 21, 105} In fact, zebrafish have several noteworthy advantages for live animal imaging in real time. Foremost, both adult and young zebrafish can be easily maintained for imaging applications. Secondly, zebrafish are optically transparent during early development and, as a result, optical imaging techniques can be easily applied. Thirdly, zebrafish fertilization is external, which enables live animal imaging during all stages of embryonic development. Finally, zebrafish have a high homology with mammals. Having these genetic similarities allows for complex investigation to study those can be used to model biological defects that occur in higher animals.

The normal course of embryonic development in zebrafish in the absence of NPs for each acute treatment stage is depicted in Figure 18. Acute treatment occurred at five different stages of development for a 2 h incubation time with NPs: stage I, cleavage stage (2-4 hpf) (Figure 18 A), stage II, gastrula stage (6-8 hpf) (Figure 18 B), stage III, early segmentation stage (12-14 hpf) (Figure 18 C), stage IV, late segmentation stage (21-23 hpf) (Figure 18 D) and stage V, hatching period (48-50 hpf) (Figure 18 E). The stages were determined by choosing critical events in embryonic development for studying molecular mechanisms from exposure with NPs. During stage I, embryos undergo dramatic changes like rapid cellular division and embryonic pattern formation.^{61,}
¹⁰⁶ During stage II, embryos undergo cell movements and migration and establishment

of the early organ systems. In stage III, embryos begin somitogenesis and notochord formation, which is important for proper development of the axial skeleton, the vertebrate spinal column, and the skeletal muscle.^{39, 68, 69} During stage IV, embryos undergo development of the circulatory system and the heart is being formed.^{39, 68, 104} During stage V, the embryo is in the hatching stage and finishing its development.

Danio rerio embryos exposed to a series concentrations of Ag NPs acutely at select stages revealed that NPs induced death, as well as a variety of morphological defects and the number of different types of defects and the severity of each increased with increasing concentration of NPs. Results of overall morphology are presented in Figure 19. Stage I resulted in an increasing percentage of deformities in Ag NP treated embryos as the concentration was increased (Figure 18 A) with a critical concentration at 0.10 nM. This stage appeared sensitive to the treatment with NPs causing death of the embryos. In stage I, exposure to the lowest concentration even produced a small percentage of abnormalities and death. At higher concentrations, an increasing percentage of Ag NP treated embryos died; correspondingly, recovery of viable abnormalities also declined. At the highest tested concentration, a majority of embryonic death was observed (Figure 19 A).

Embryos treated in stage II had a high rate of death but showed a low number of deformities (Figure 19 B), correlating with increasing NP concentration and having a critical concentration at 0.20 nM. This stage also appeared sensitive to the treatment with NPs causing death of the embryos. This was specific for this stage of development and most likely due to the fact that during this stage of development the embryos are undergoing vast cellular movements and formation of the early organ systems.^{107, 108}

During this period the germ layers of the embryos are also being established.^{107, 108} Stage II of development is a time when the onset of gene expression is starting and cell migration is prominent. Exposure of the Ag NPs could affect the pathways during development causing an increase in death at this stage, which is directly related to the increase in the NP concentration.

Stage III resulted in an increasing number of embryonic death as the concentration was increased (Figure 19 C) with a critical concentration is between 0.20 and 0.50 nM. Exposure to the lowest concentration in stage III produced small quantities of abnormalities. At the highest tested concentration, a total embryonic death was observed (Figure 19 C).

Stage IV treated embryos resulted in increased deformities with the lowest concentration and remained consistently constant throughout Ag NP concentration rises (Figure 19 D). The critical concentration was determined to be 0.20 nM. In stage IV even exposure to the lowest concentration produced abnormalities. At higher concentrations, a small increasing percentage of Ag NP treated embryos died. At the higher tested concentrations in stage IV, a majority of embryonic death was observed (Figure 19 D).

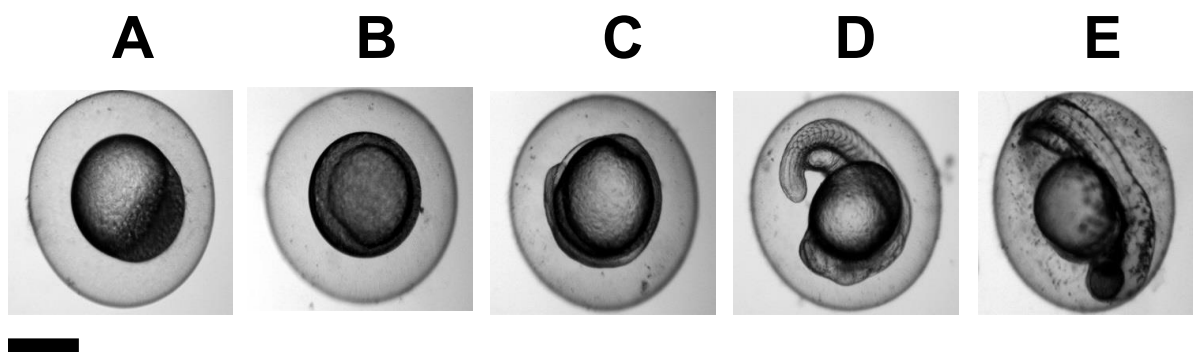


Figure 18: Normally developed zebrafish at stages I – V at the time of acute treatment and observations after acute treatment.

Representative optical images of normally developed zebrafish at the time of acute treatment for stage I – V, (a) 2 hpf (cleavage stage); (b) 6 hpf (early gastrula stage); (c) 12 hpf (early segmentation stage); (d) 21 hpf (late segmentation stage) and (e) 48 hpf (hatching stage). Scale bar = 500 μm .

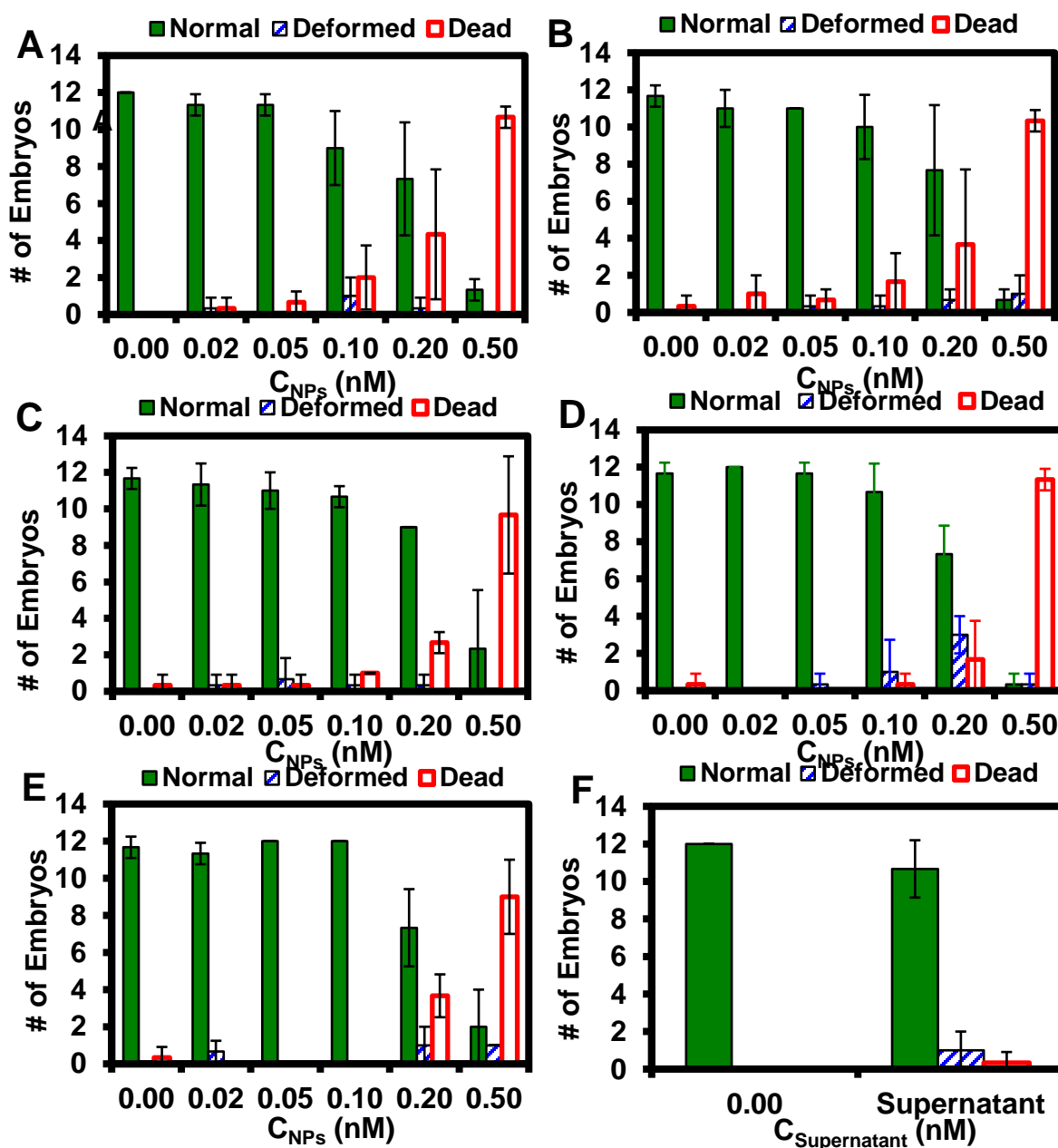


Figure 19: Histograms displaying the distribution of effects resulting from treatment with Ag NPs and the supernatant on zebrafish.

(A) Normally developed, deformed, and dead zebrafish vs. concentration of Ag NPs in stage I. (B) Normally developed, deformed, and dead zebrafish vs. concentration of Ag

NPs in stage II. (C) Normally developed, deformed, and dead zebrafish vs. concentration of Ag NPs in stage III. (D) Normally developed, deformed, and dead zebrafish vs. concentration of Ag NPs in stage IV. (E) Normally developed, deformed, and dead zebrafish vs. concentration of Ag NPs for stage V. (F) Normally developed and dead zebrafish vs. concentration of supernatant removed from Ag NP washing.

Stage V resulted in no morphological defects and only a slight increase in the death rate (Figure 19 E) with a critical concentration between 0.20 nM and 0.50 nM. This is possibly due to that during stage V, the embryo is in the hatching stage and finishing its development.¹⁰⁸ Untreated control embryos for stages I through V (0.00 nM) produced no abnormal embryos and embryo viability was within normal limits (Figure 19 A-F). Control embryos exposed to (nanoparticle-free) supernatant from the NP washing process showed minimal levels of toxicity at all tested concentrations (Figure 19 F).

The effective dose for our acute studies was determined from our previous chronic studies.^{42, 44, 64, 77, 78, 88, 109} We treated stage I through V embryos acutely with various concentrations of Ag NPs (0.00 – 0.50 nM). Embryos were carefully monitored post-treatment at 24, 48, 72, 96, and 120 hpf. We examined the defects associated with the treatment of developing embryos with Ag NPs at each treated developmental stage. Many morphological defects were observed in the developing embryo, including abnormal finfold and tail development, cardiac malformation (pericardial sac edema), yolk sac edema, and head and eye abnormalities as shown in Figure 20. Every treated stage presented some abnormalities. The shared abnormality among stages I, II, IV, and V treated embryos was finfold abnormalities, typically affecting the median finfold region (Figure 20 A, B, D, E (a)). In normally developing embryos, the median finfold area is a clear, thin membrane around the entire trunk region containing unsegmented fin rays.^{65, 69} In treated embryos at these stages, the tissue structure of the finfold was disorganized and in the more severe cases, the shapes of the finfold and the developing fin rays were altered.

Treated embryos from stages I, II, III, and V displayed as another common defect, an abnormal tail (spinal cord) flexure phenotype (Figure 20 A-C, E (b)). This defect was often accompanied by tissue abnormalities of the finfold. In normal developing embryos, the notochord and spinal cord develop straight to the posterior-most tip of the tail. In the treated embryos for these stages, however, the tail region was flexed to some extent. In the more severely flexed embryos, the flexure was extreme and the overall length of the tail was reduced (Figure 20 C (b)). The tail flexure defect also increased in severity with increasing NP concentration.

Another commonly shared defect, which was presented in all stages, was presented as a cardiac malformation. More specifically, we observed swelling of the housing membrane where the ventral and artery bulbs develop and starts pumping, resulting in pericardial sac edema. In contrast to normal embryos, in the stage I treated embryos; the pericardial sac region was swollen and enlarged (Figure 20 A-E (c)). In severe cases, the pericardial sac was extremely large and the cardiac ventricle was decreased in size.

Yolk sac edemas were readily observed in stages II, IV, and V (Figure 20 B, D-E (d)). In normally developing embryos, the yolk sac region is a bulbous area containing yolk that provides nutrients to the developing embryo and during the later developmental process, the yolk sac shrinks. In the affected treated embryos of these stages, however, the yolk sac region was swollen and enlarged. This type of edema is a common defect in treated embryos. It is thought that the dependence of the nutrients during treatment blocks those enzymes responsible for decreasing this area.^{61, 63, 104, 110} Similar to our previous studies and treatment with both Ag NPs and Ag⁺ ions, we see this type of defect

combined with another type of deformities, normally, finfold abnormalities and pericardial sac edemas. This leads us to believe that this lack of shrinkage in an area important for embryo survivability is highly influenced by the development of other major organs in the zebrafish. If certain areas are not properly developed and outside nutrients cannot be sought by on the embryo's own, then the yolk sac will continue to serve as the embryos main source of nutrients during development.

In stages III – V, we observed head and eye abnormalities (Figure 20 C-E (e)). The heads of these abnormal zebrafish were smaller than, and not as round as, a normal embryo would appear (Figure 20 F).

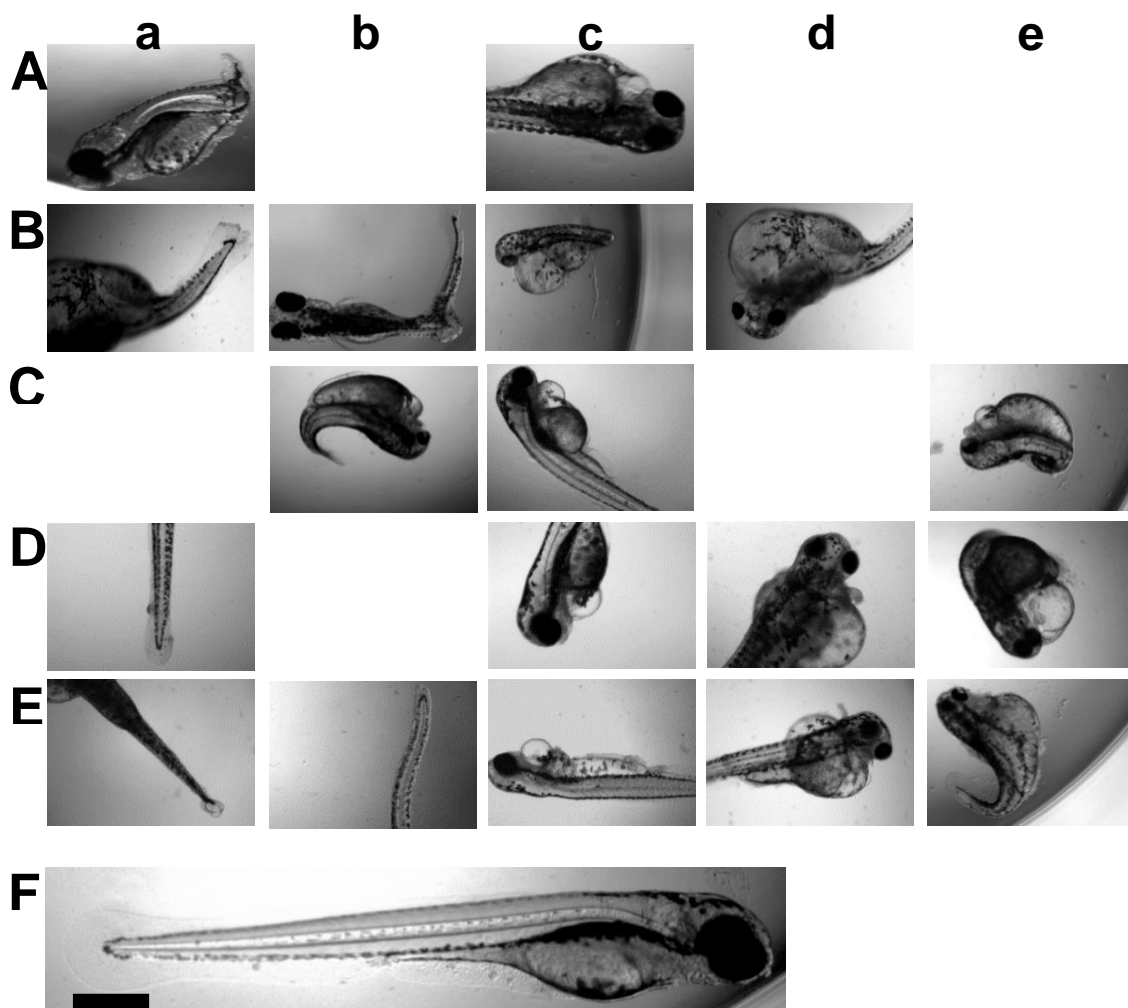


Figure 20: Representative optical images of deformities observed at 120 hpf in stages I – V after acute treatment with Ag NPs.

Optical images of deforms observed : (a) finfold abnormality; (b) tail/spinal cord flexure; (c) pericardial sac edema; (d) yolk sac edema and (e) head and eye abnormalities. Stage I (A), Stage II (B), Stage III (C), Stage IV (D), and stage V (E) images represent common deformed found in each stage. (F) Normally Developed zebrafish. Scale bar = 500 μ m.

A histogram of the average number of embryos observed with different types of deformities at each stage for treated Ag NPs concentrations is presented in Figure 21. Here, we see that in stage I, the lowest Ag NP concentration, 0.02 nM, presented only pericardial sac edemas, whereas 0.10 and 0.20 nM treatment groups presented tail flexures and yolk sac edemas (Figure 21 A). For stage II, the lowest treated concentration of Ag NPs where deformed zebrafish were observed was 0.05 nM. At this concentration, only finfold abnormality was recorded. The higher concentrations all resulted in tail flexures, pericardial sac edema, and/or head abnormality (Figure 21 B). For stage III, we observed the most abnormal zebrafish from lower concentration groups, where multiple defects were recorded for 0.02 and 0.05 nM (Figure 21 V). This, as a result, was the most sensitive stage for this particular size of NPs. Stage IV presented few defects only observed in the 0.10 and 0.20 nM treatment groups (Figure 21 D). Stage V, the hatching stage, interestingly enough, presented many different types of deformities in the higher treated concentrations (Figure 21 E). This is significant because, in other stages, these type of deformed zebrafish did not survive in the higher treated group (0.20 and 0.50 nM). The fact that these deformed zebrafish were able to survive after exposure is a manner that needs to be further explored.

Possible reasons for the high dependence of type and severity of defects on the stage of development and concentration of NPs could be due to the following: (i) The NPs enter inside the chorion space of the embryo during the specific stage of development and affect the specific proteins, signaling, and developmental pathways during that period of development. (ii) An increase in the number of NPs inside the chorion space of the embryo during the specific stage of development increases the altering effects of the

protein, signaling, and developmental pathways during development increasing severity of the deformity observed or death. Our results describe a range of developmental defects and absolute death following exposure of developing zebrafish embryos to nanomolar concentrations of Ag NPs at particular embryonic stages of development. Specific developmental pathways of embryonic development are still unknown, such as differentiation into specialized tissues and organs, specifically how cells communicate with each other, how they become committed to a certain fate, and how they formulate a pattern to become a structure.^{107, 110} Stage-dependent developmental responses to Ag NPs, shown here, in a dose-dependent manner, demonstrates the possibility of being able to pick specific developmental pathways to create particular phenotypes and as potential developmental therapeutic agents to treat specific disorders and generate specific developmental mutation in zebrafish, by alteration of the time of application of the NPs.

Quantitative heartbeat study of zebrafish upon Ag NPs concentration

As we observed pericardial sac edema and cardiac malfunctions in zebrafish treated with Ag NPs during all stages of treatment, we further studied effects of Ag NPs on cardiac functions of zebrafish after their exposure to NPs compared with the controls at three different time points: 24 hpf (early heart formation period); 48 hpf (embryo hatching period); and 120 hpf (full development period). We plotted the average heart rate per minute for all treatment groups at each stage (line plots), along with the total number of zebrafish analyzed (bar plots) (Figure 22 A-E). Essentially, individual myocardial cells begin to contract irregularly around the 22-somite stage (21 hpf) giving heart rate at about

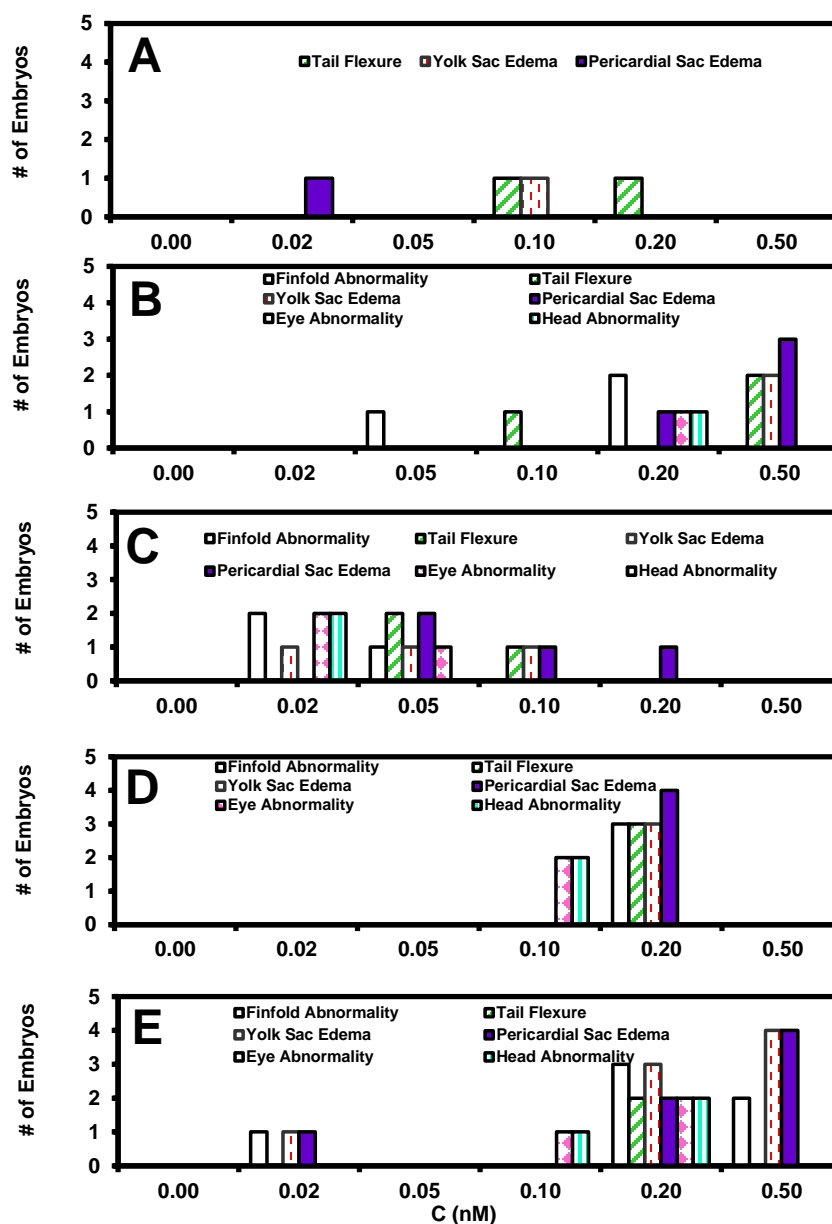


Figure 21: Histograms of the types of deformities concentration of Ag NPs treatment in zebrafish.

Deformities type was plotted for each developmental stage; Stage I (A), Stage II (B), Stage III (C), Stage IV (D), and stage V (E) images represent common deformed found in each stage.

40-45 beats per minute. Heart rates dramatically increase to about 70-80 beats per minute by 24 hpf when shortly thereafter blood circulation begins.¹¹¹ As the heart develops, morphological differentiation progresses in an arterial to venous direction. The heart tube has looped and beats at higher rates to provide a strong circulation to the trunk and head.¹¹¹ Around 48 hpf, the observed normal beating heart of a zebrafish will roughly be around 120 beats per minute. At 120 hpf, the will slightly increase in normal zebrafish to roughly 150 beats per minute and will remain around this average until adulthood.

We found that the number of embryos with normally developed heart decreased as the Ag NP concentration increased, resulting in a dose-dependent manner. In normally developed zebrafish, heart rates increased as the heart developed. Heart rates of normally developed zebrafish at 48 hpf and 120 hpf were significantly greater than those at 24 hpf when the heart was early developed (Figure 22 A-E). However, Ag NPs insignificantly reduced embryo heart rates at 24, 48, and 120 hpf in a dose-dependent manner at every stage (Figure 22 A-E). In contrast, cardiac malformed zebrafish found after NPs exposure at all concentrations showed insignificant differences in heart rates over the examined developmental periods. Their heart rates at 48 hpf and 120 hpf were at the same or lower than those at 24 hpf. This suggests that the heart became more deformed over time which could lead to lower heart rates, less blood and oxygen supply, which possibly attributes to mortality. Ag NPs have previously shown to interfere with regular cardiac functions^{24,112}. Improper blood flow could starve the cells of gases and essential nutrients resulting in cell death. It is worth noting that the heart rates of heart deformed zebrafish were much lower than normal heart-developed zebrafish (Figure 22 A-E) but not in a dose-dependent manner. Although the mechanisms are still not well

understood, Ag NPs could disrupt heart development contributing to heart deformities and then leading to the depressed heart rates.

In stages I, II, and IV, we observed a huge decrease in the highest treatment group (0.50 nM) at 48 hpf. This decrease shows that at this particular concentration, the effects on the cardiac function was significantly influenced by the NPs presence. This is definitely interesting to note, considering that these particular stages are highly significant for proper development of the cardiovascular system, and cardiac function, as we can observe, is particularly sensitive to any outside toxins. This can also coordinate with the fact that pericardial sac edemas being the most common type of deformity resulting from Ag NPs treatment.

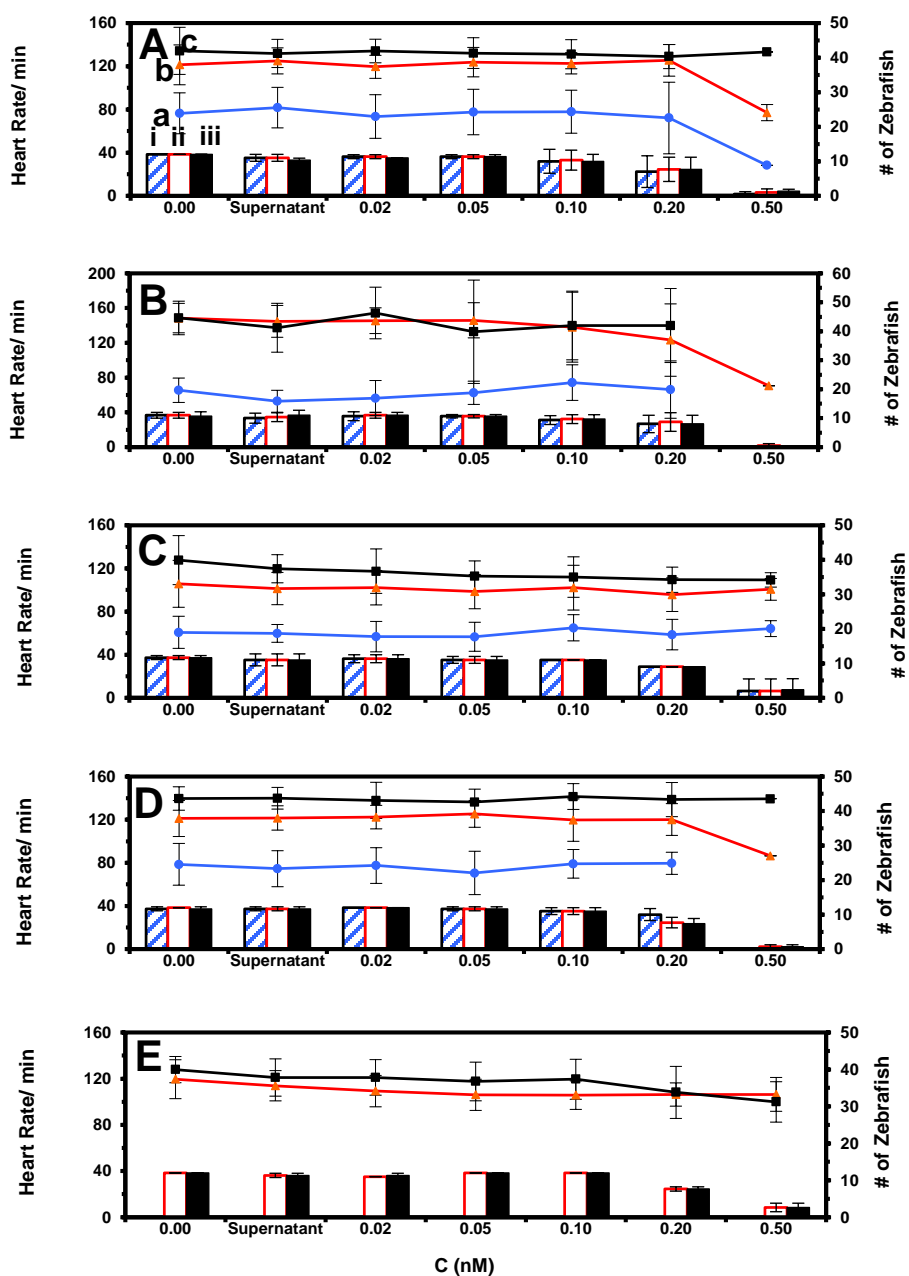


Figure 22: Quantitative Study of Heart Rates of Treated embryos per stage of development.

Heart rates were measured for each treated embryo at 24 (a), 48 (b), and 120 (c) hpf and represented by the lines. The average number of embryos for 24 (i), 48 (ii), and 120 (iii) hpf are plotted in the bar graph. Stages I – V are shown here (A – E).

SUMMARY

In summary, we examined the biocompatibility and toxicity of single Ag NPs in vivo at specific stages of development and the defects associated with treatment at specific developmental stages. Increasing Ag NPs concentration resulted in all stages of development resulted in a significant increase in embryonic death, and a correlated decrease in survivability of normal and deformed zebrafish. Many morphological defects were observed in the developing embryo, including yolk sac edema, abnormal finfold and tail development, head and eye abnormalities, and cardiac malformations at each stage of development, corresponding to the stage of treatment. In general, the number of different types of defects and the severity of each varied with the stage of treatment and increased with increasing dose of NPs demonstrating the possibility of selectively targeting specific embryonic developmental pathways by altering the stage of development and dose of NPs for developmental therapeutic studies. Moreover, it was noted that at this particular size of single Ag NPs, cardiac malformation was significant no matter the developmental stage. Pericardial sac edemas were one of the most common types of deformity observed throughout the experiment. In that matter, quantitative analysis of cardiac function was found to be significantly influenced with increasing Ag NPs concentrations. In particular, we saw a stage-dependent effect on cardiac malformation, where stages I, II, and IV were highly influenced by exposure to a higher dose of the Ag NPs. The investigation of biocompatibility of nanomaterials in specific stages of development of embryos at single NP level can offer new knowledge about the developmental processes and environment, and provide new insights into the mechanics of the developing embryo as well as aid in the finding for function

MATERIALS AND METHODS

Reagents and supplies

Sodium citrate (99%), AgClO_4 (99%), NaBH_4 (98%), and NaCl were purchased from Sigma-Aldrich. All reagents were used as received. The nanopure water (18 M Ω water, Barnstead) was used to prepare all solutions and rinse glassware.

Synthesis and characterization of stable and purified Ag NPs

Ag NPs (41.5 ± 7.6 nm in diameter) were synthesized as we described previously. Briefly, sodium citrate (10 mL, 34 mM) was quickly added into a refluxing (100°C) AgNO_3 aqueous solution (500 mL, 1.1 mM) under stirring. The mixture was refluxed and stirred for 45 min, as the solution color turned from colorless to straw yellow, then opaque and finally muddy yellow. The heating was stopped and the solution was cooled gradually to room temperature under stirring. The NP solution was filtered using 0.22- μm filters. All chemicals, except those indicated, were purchased from Sigma and used as received.

The NPs were immediately washed three times with nanopure DI water (18 M Ω , Barnstead) using centrifugation (Beckman, JA-14) to remove any residual chemicals involved in NP synthesis. The washed NPs were resuspended in DI water and then egg water. The washed NPs were very stable (non-aggregated) in DI water for months and remained stable in egg water (1.0 mM NaCl , 99.95% Sigma, in DI water) throughout the duration of the entire experiment (120 h, period of full embryonic development) (Figure 1). Concentrations of NPs were calculated, as we described previously.

Sizes of NPs were characterized using high-resolution transmission electron microscopy (HR-TEM) (FEI Tecnai G2 F30 FEG) and dynamic light scattering (DLS) (Nicomp 380ZLS particle sizing system). LSPR spectra and images of single NPs in

solution, embryos and embedded in zebrafish tissues were acquired using dark field optical microscopy and spectroscopy (DFOMS), which we described previously. In this study, we used a charge coupled device (CCD) camera (Micromax, Roper Scientific) and Multispectral Imaging System (Nuance, CRI) was used to acquire LSPR spectra of single NPs.

Stability of NPs in solution and egg water was followed over time for 120 h using UV-vis spectroscopy, DLS and DFOMS. The purified and stable NPs were used for probing their diffusion into embryos and their effects on embryonic development.

Breeding of zebrafish embryos

Wild-type adult zebrafish (Aquatic Ecosystems) were housed in a stand-alone system (Aquatic Habitats), and they were maintained and bred, as we described previously. Briefly, two pairs of mature zebrafish were placed into a clean 10-gallon breeding tank. A light (14 h)–dark (10 h) cycle was used to trigger breed and fertilization of embryos. The embryos at the cleavage stage were collected and transferred into a Petri dish containing egg water. They were well rinsed with egg water to remove any possible debris prior to imaging and characterization. All experiments involving embryos and zebrafish were conducted in compliance with IACUC guidelines (protocol # 15-012).

Treatment and monitoring of zebrafish embryos

Wild type adult zebrafish (Aquatic Ecosystems) were maintained, bred, and collected, as described previously.^{44, 113} Embryos were collected and transferred into a petri dish containing egg water (1.2 mM NaCl), washed twice with egg water to remove the surrounding debris, and placed into 48-well plates with each well containing one embryo in egg water. 16 embryos were tested per concentration, per stage of

development; each experiment was repeated 3 times, totaling 48 embryos analyzed per concentration, per stage of development. Each developmental stage of embryos in the wells was directly imaged by bright-field optical microscopy using an inverted Zeiss Axiovert microscope equipped with a 4x objective and a digital color camera.

Study and characterization of transport and biocompatibility of NPs

To study the dose-dependent effects of NPs on embryonic development, a dilution series of washed Ag NP solutions (0, 0.02, 0.05, 0.10, 0.20 and 0.50 nM) were incubated acutely with 5 stages of embryos in egg water for 2h. Each experiment was carried out at least 3 times and a total number of 48 embryos were studied for each individual concentration to gain representative statistics. NP concentrations were calculated as described previously.⁴⁴ Embryos in egg water in the absence of NPs and in the presence of supernatant were placed in two rows of the 48-well plates as control experiments to probe the effects of possible trace chemicals from NP synthesis. The embryos in the 48-well plates were incubated at 28.5°C, and directly observed at room temperature using an inverted Zeiss Axiovert microscope equipped with a digital color camera at 24, 48, 72, 96, and 120 hpf.

Quantitative heartbeat study of zebrafish upon Ag NPs concentration

Both treated and control embryos for stages I - V were analyzed for heart rates. Embryos were recorded using the Sony camcorder and Coolsnap Ez (Roper Scientific) using 100 frames with a 50 ms interval delay. The recordings were taken at 24, 48, and 120 hpf. The movies were then converted and analyzed for manual counting of the hearts contractions. The heartbeat per minute was then compared graphically to both the normal and abnormal developed fish at each concentration.

Data analysis and statistics

A minimum of 100 Ag NPs was imaged and characterized for each measurement of their sizes and stability in egg water using HRTEM and DFOMS. A minimum of 300 NPs in total was studied for each sample via three repeated measurements. For the study of dose-dependent effects and qualitative heart rate analysis of NPs on embryonic development, a total number of 48 embryos were studied for each NP concentration and each control experiment over 120 hpf with a minimum of 12 embryos studied in each measurement. We presented averaged the number of normally developed, dead and deformed zebrafish vs. Ag+ concentration with standard deviations. We used conventional statistical analysis methods (t-test, ANOVA, Tukey's, SPSS Statistics with $P = 0.05$) to determine the significance of the different observations between all concentrations for development, hatching, heartrate and uptake results. A Pairwise T-test comparison was performed of Deformities Histogram.

CHAPTER V

STUDY OF EFFECTS OF SILVER NANOPARTICLES ON EARLY NEUROLOGICAL DEVELOPMENT OF ZEBRAFISH EMBRYOS

INTRODUCTION

Our lab has previously demonstrated that stable purified silver nanoparticles can induce unique and rare abnormalities in developing embryos.¹¹⁴⁻¹¹⁸ The abnormal phenotypes in development included cardiac malformations, abnormal tail and spinal cord formation, and head and severe eye abnormalities. We wanted to understand more about how and why these unique phenotypes occur from exposure to silver nanoparticles, understanding the molecular mechanisms that are involved and identify primary biological biomarkers that are highly influenced during embryogenesis from this induced nanotoxicity.

The development of the brain and all of its mysteries is still an area that needs to be explored. Neurological development is a well-regulated and regionalized operation that is highly complex during embryogenesis.¹¹⁹ Studies show that the formation of the embryonic brain requires interaction from many essential biomarkers and inductive interactions between different regions of the developing embryo. In recent genetic studies, some of these key biomarkers that play important roles within the developmental process have been recognized, but exact mechanisms are still being explored. Some of these biomarkers include the signaling molecules like *noggin* and *follistatin*, and the regulating transcription factors *otx*, *emx*, *pax*, and *engrailed* genes. Although the genetic assay approach allows for detailed genetic information to be discovered, this approach still limits the understanding of mechanisms and the dynamics of these biomarkers in real

time. They limit the view of understanding in cases where the molecular process is trying to be correlated. We aim to approach this with a different strategy that allows us to study, in real time, how these key biomarkers are influenced during development by nanotoxicity.

To approach this, we chose to identify a key neurological protein biomarker that has shown to have fundamental responsibility during neurological development. *Pax2a* gene is a prominent protein that plays important roles in central and peripheral nervous system development.

Paired box gene 2a (*pax2a*) is highly expressed during the segmentation stage of development, largely involved in the formation of the midbrain-hindbrain boundary. This region of the developing embryonic brain is essential to pattern formation and organization of neural networks in both adjacent midbrain and hindbrain zones. *Pax2a* is also uniquely expressed during eye and ear morphogenesis and has been shown to be involved in multicellular organism development, like kidney, locus cerebellum formation, otic placode formation, peripheral and central nervous system development, and pronephros development.^{120, 121} Transgenic zebrafish models expressing the *pax2a* gene have been used to study the developmental migration of neuronal cells as well as targeted for toxicological studies.¹²²⁻¹²⁷ This biomarker is important in this study because mutations in the *pax2a* gene results in abnormal phenotypes in developing embryos that showed similarities to those induced in our nanotoxicity studies.^{120-122, 128}

Nanoparticles (NPs) are ideal for biomedical research in developmental biology because of their unique capability in probing the nanoscale environments of living organisms, enabling the study of a developing organism at different developmental

stages.^{72, 83-86} Their unique optical properties makes imaging *in vivo* more convenient, allowing the transport and diffusion of the NP to be monitored and offers new information on the developing fluid mechanics of the embryonic organism. NP probes can be used in a variety of applications for new insight into developmental processes, such as development screening tools in developmental biology to investigate the embryonic internal environment, to potentially control and regulate certain processes in development, and to target specific system regulators for biomedical biological uses. Nanomaterials could possibly demonstrate developmental stage-dependent regulation of deformity type induced, suggesting that the nanomaterials, at higher concentration, may interact with target developmental pathways of interest. In this study, we used our previously described nanomaterials,⁴⁴ Ag NPs, and an effective embryo developmental model system, zebrafish embryos, and focused on biocompatibility targeting important transgenic developmental *in vivo* models for analysis and independent NP entry into each embryonic stage, hoping to identify possible developmental stage applications and the ability for NPs to enter the developing embryo independent of the time of development.

Ag NP probes have unique optical properties over many fluorescent imaging approaches because they have localized surface plasmon resonance (LSPR), enabling characterization of their size and shape, and they offer high quantum yield (QY) of Rayleigh scattering making them bright and easy to see using dark-field optical microscopy and spectroscopy (DFOMS).^{60, 95-97} Ag NPs can be used as a probe for real-time study over an unlimited period of time because they do not experience photodecomposition as fluorescent beads can. In addition, the LSPR spectra, or color of the Ag NPs, can be used to show size-dependence.^{60, 95, 96} Using the LSPR spectra of

the multicolor Ag nanoparticles it is possible to be able to directly characterize the diffusion of the same color nanoparticle at the nanometer scale in real-time, in different biological environments based on using the same sized Ag NPs.^{93, 98, 99}

Zebrafish (*Danio rerio*) have been extensively employed as a well-studied vertebrate model for embryological development because of its small size, its short breeding cycle, and the wealth of information available for manipulation.^{63, 70, 100-102} Their transparency throughout development allows observation of all internal organ development from outside the chorion without disturbing the living embryo. Zebrafish are time efficient for care and maintenance and they effortlessly spawn in large numbers from week to week producing macroscopic fertilized eggs, which are ideal for observing different developmental stages. The embryonic development is so rapid that the first stages of development are completed in the first 24 hours post fertilization (hpf) and the normal embryo will hatch and swim by 72 hpf. The majority of developmental mutations identified in zebrafish have close counterparts in other vertebrates, suggesting that this system can be effectively used as a model for understanding the developmental processes of higher organisms, including humans.^{66, 103} Therefore, zebrafish embryos offer a unique opportunity to investigate developmental processes upon treatment with NPs to investigate stage dependence NP effects on embryonic development.

It is important to explore the biocompatibility of Ag NPs during embryonic development to assess the ability of Ag NPs to be used for *in vivo* imaging at any embryonic stage of development as well as probes in real-time to explore the changing embryonic environment during development, including neurological changes and understanding mechanism in brain development.

This study aimed to understand in real time how a key neurological developmental biomarker is influenced in the presence of Ag NPs, thus allowing us to explore their mechanisms and roles during embryogenesis. We designed an ultrasensitive *in vivo* bioanalytical imaging tool to study molecular changes at the single cell resolution of cells expressing Pax2a protein biomarkers. Using transgenic zebrafish models, we were able to determine the effects of Ag NPs and understand how nanotoxicity can influence the molecular mechanism of these protein biomarkers in expressing cells at various stages of embryogenesis.

To that end, we selected a vital protein biomarkers that play important roles in neurological development, used transgenic embryos that express the protein biomarkers fused with fluorescence proteins as model organisms, and studied the effects of NPs on their functions using fluorescence microscopy and plasmonic spectroscopy.

RESULTS AND DISCUSSION

Synthesis and characterization of Ag nanoparticles (NPs)

Ag NPs were synthesized, purified and characterized, as described in Methods. Notably, highly purified Ag NPs were produced by thoroughly washing Ag NPs with deionized (DI) water to remove potential residual chemicals involved in NP synthesis via centrifugation. A representative optical image of Ag NPs in Figure 23 C illustrates that the majority of NPs appear to be blueish green to green, with a few reds. These results suggest that Ag NPs are uniform in size and shape based on their color (LSPR). The representative LSPR spectra of single blue, green and red Ag NPs with peak wavelengths (λ_{\max}) at 468 nm (blue) (FWHM = 38 nm), 554 nm (green) (FWHM = 47 nm), and 659 nm (red) (FWHM = 47) nm, respectively (Figure 23). Thus, the color of Ag NPs can be used

as size index to directly distinguish and determine the size of NPs using DFOMS, even though the size of NPs cannot be directly measured due to the optical diffraction limit. The NPs were then suspended in egg water (1.0 mM NaCl, embryonic medium) for the study of their stability and their effects on embryonic development. We characterized the stability, size and optical properties of the purified Ag NPs in egg water embryo media (1.0 mM NaCl) for 120 h using UV-vis absorption spectroscopy, dark field optical microscopy and spectroscopy (DFOMS) and high-resolution transmission electron microscopy (HRTEM). The size was with an average diameter of 41.5 ± 7.6 nm (Figure 23). We found that the number of NPs remained relatively unchanged when incubated in egg water for 120 h. The absorbance spectra of freshly prepared and purified Ag NPs before and after the incubation time with egg water demonstrated a peak wavelength (λ_{max}) at 401 nm (FWHM = 52 nm) and only showed a slight decrease in absorbance for 120 hours (Figure 23). The unchanged number of NPs and stable absorbance spectra indicates that the Ag NPs are very stable in egg water media and remain non-aggregated throughout the entire experiment.

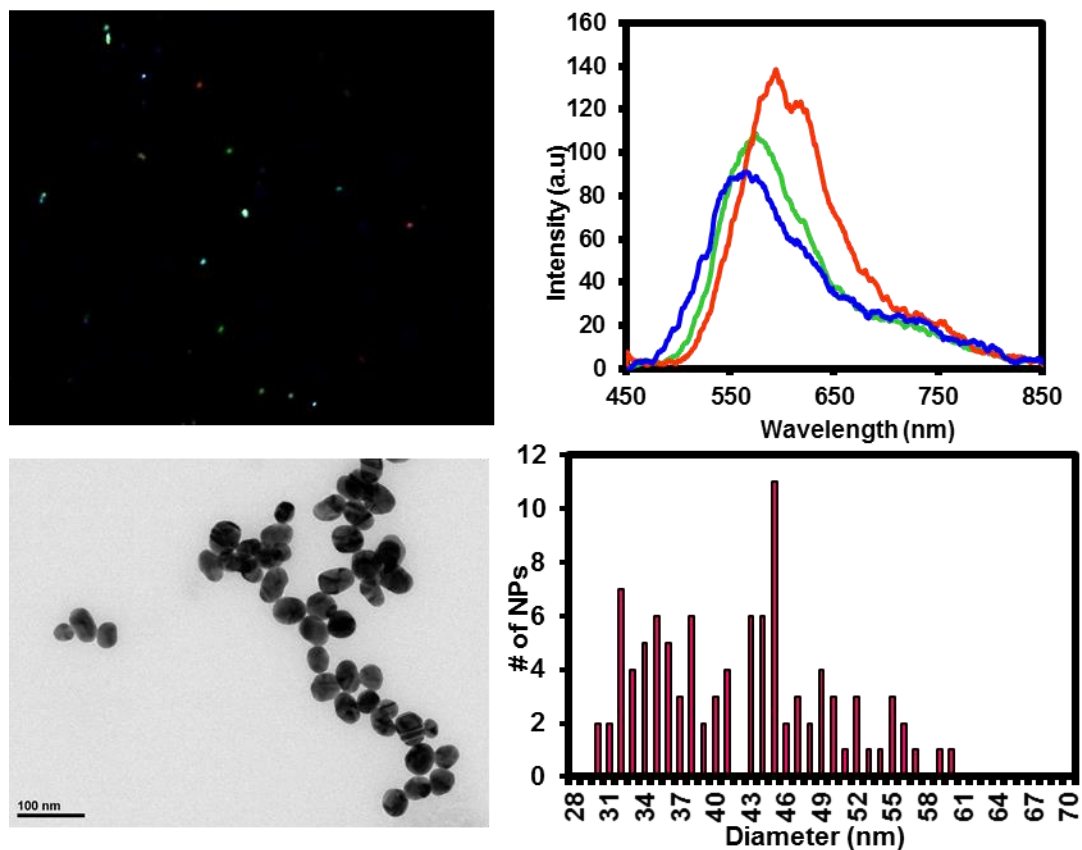


Figure 23: Characterization of sizes, shapes, and plasmonic optical properties of single Ag NPs.

(A) Dark-field optical image of single NPs shows that a majority of NPs are plasmonic green with some blue-green and red. (B) LSPR spectra of representative single NPs (C) HRTEM image shows the spherical shape of single NPs. (D) Histogram of size distribution of single NPs determined by HRTEM shows average diameters of 41.5 ± 7.6 nm.

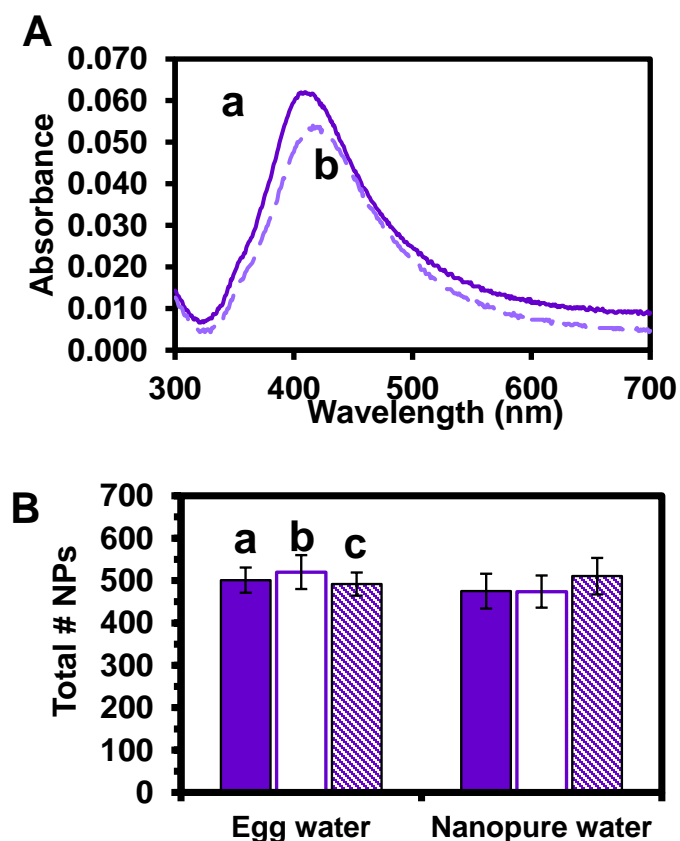


Figure 24: Characterization of stability of Ag NPs in egg water ($C_{NPs} = 0.5 \text{ nM}$) for 120 h.

(A) UV-Vis absorption spectra of the NPs dispersed in egg water at 28.5 °C for (a) 0 and (b) 120 h show that its peak absorbance of 401 nm shows only a slight decrease after incubation for 120 h. (B) The average of total number of NPs from triplicate runs at (a) 2 h, (b) 48 h, and (c) 120 h in both egg water and deionized nanopure water. The average total number of NPs is 501, 520, and 492, respectively in egg water, and 475, 474, and 510 respectively in nanopure water. The 10 images are acquired at each given time point using DFOMS.

Early-development transgenic embryos as ultrasensitive *in vivo* assays

Optical images in Figure 25 A shows normal developmental stages of zebrafish embryos, which includes cleavage (0.75-2.25 hours-post-fertilization, hpf), early segmentation (12 hpf), late segmentation (24 hpf), hatching stages (48 hpf and 72 hpf and a fully developed zebrafish (120 hpf). All embryonic developmental stages of zebrafish are well defined.^{40, 66, 68, 103} The earlier developmental stage, such as cleavage stage, is likely more prone and sensitive to the effects of external substances (e.g., drugs, NPs) than later stages. Notably, during the cleavage-stage embryos undergo drastic changes to lay down the foundation for developing different organs. Their related and important developmental mechanisms remain not yet fully understood.^{59, 100, 101} Thus, we select cleavage-stage embryos for the study of biocompatibility and toxicity of NPs, aiming to develop ultrasensitive *in vivo* assays for effectively screening of NPs and to rationally design biocompatible NP probes for *in vivo* imaging.

Study of dose-dependent biocompatibility and toxicity of NPs and control experiments

We studied dose-dependent toxic effects of NPs on embryonic development by incubating cleavage-stage embryos with various concentrations (0- 5.00 pM) of Ag NPs suspended in egg waters for 120 h. Representative embryonic developmental stages were imaged and assayed over time until the embryos were fully developed. The number of embryos that developed to normal zebrafish (Figure 25 A), became dead (Figure 25 B), and deformed zebrafish (Figure 26 B) were recorded.

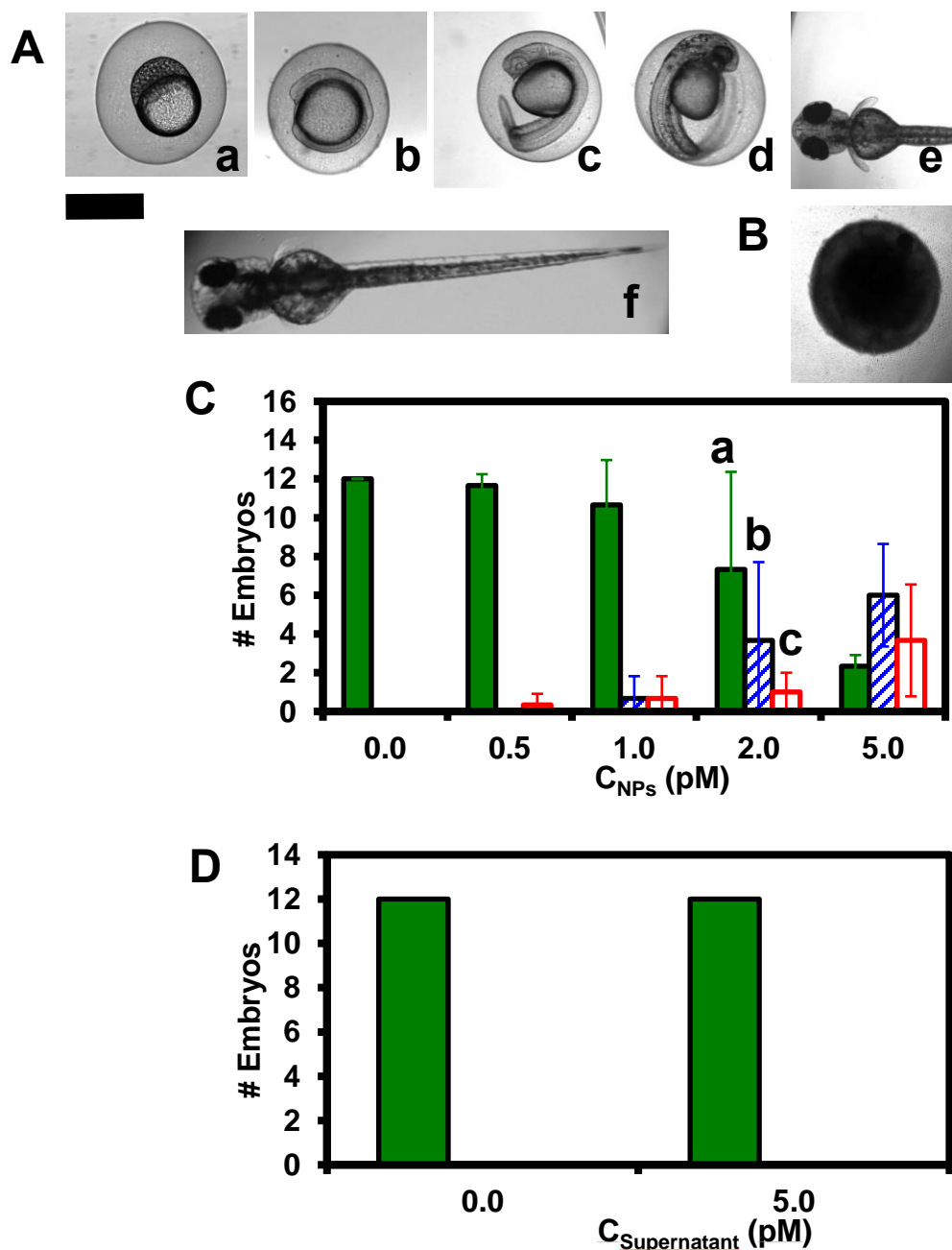


Figure 25: Study of dose-dependent effects of Ag NPs on embryonic development using embryos as ultrasensitive *in vivo* assays.

(A) Optical images of normally developing embryos at (a) cleavage-stage (0.75-2.25 hpf); (b) late gastrula stage (10 hpf); (c) late segmentation stage (24 hpf); (d) hatching stage (48 hpf); (e) 72 hpf hatched embryo; (f) fully developed larvae (120 hpf). (B) Dead

embryo. (C) Histograms of distributions of embryos that developed to normal and deformed zebrafish or became dead versus NP concentration. (D) Control experiments: histograms of the distributions of embryos that developed to normal zebrafish or became dead either in egg water alone or versus concentration of supernatant, which was collected from the last washing of NPs with DI water. A total of 48 embryos were studied for each NP concentration and control in

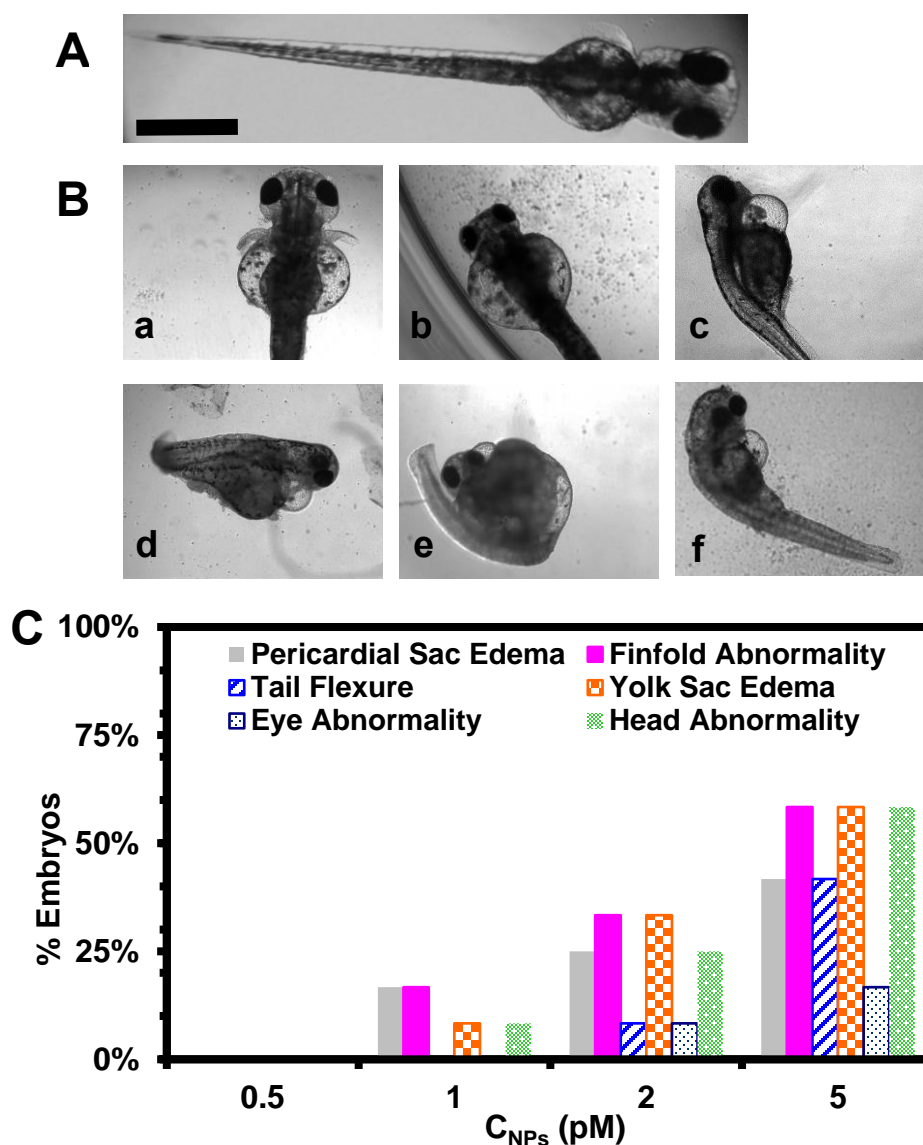


Figure 26: Dependence of types of deformed zebrafish on NP concentration.

(A) Optical image of a normally developed Zebrafish Larvae at 120 hpf. (B) Optical images of deformed zebrafish show: (a-b) head and eye abnormalities; (c-d) pericardial sac and yolk sac edema; (e) tail/spinal cord flexure; and (f) finfold abnormalities. (B) Histograms of distributions of embryos that developed to deformed zebrafish with six distinctive types of deformities at NP concentration of 0.5, 1.0, 2.0 and 5.0 pM. Scale bar is 500 μm for all images in (A) and (B).

Similar to our chronic study using similar sizes on wild type zebrafish embryos, the effects of 43 nm Ag NPs on *pax2a* transgenic embryos resulted in dose-dependent toxicity, as well as phenotypical dependent effect upon exposure to Ag NPs. This, again, shows that the larger NPs are more toxic than smaller NPs.

Expression of *pax2a*:GFP in Ag NPs treated embryos

Treated transgenic embryos that were positive for the GFP protein was imaged for their protein expression at key developmental time points during brain development, shown in Figure 27. In the normally developed zebrafish, we observed the expression of *pax2a*:GFP to decrease during brain development. This correlates with the function of the *pax2a* gene. In fact, the analysis of the *pax2.1* gene in zebrafish shows embryonic expression pattern and requirement is regulated after brain development.¹²⁰
¹²⁶ The *pax2a*:GFP expression is most significant during early brain development, during the midbrain-hindbrain boundary constriction.¹²⁹ Figure 28 shows examples of the GFP expression during 15 hpf (A), 24 hpf (B), and 48 hpf (C). Figure 29 shows the intensity of the GFP embryonic expression at 24 hpf. Here, we observed that in expression intensity decreased slightly as the Ag NPs concentration increase in normally developed zebrafish. However, we did not observe this decrease to be significantly different from our control embryos. These results may show that the *pax2a* gene is not greatly affected by exposure of Ag NPs, however, other upregulated genes might still be hugely affected, considering the phenotypical morphologies we see from treated embryos. This *in vivo* assay may be used to explore those genes in more details

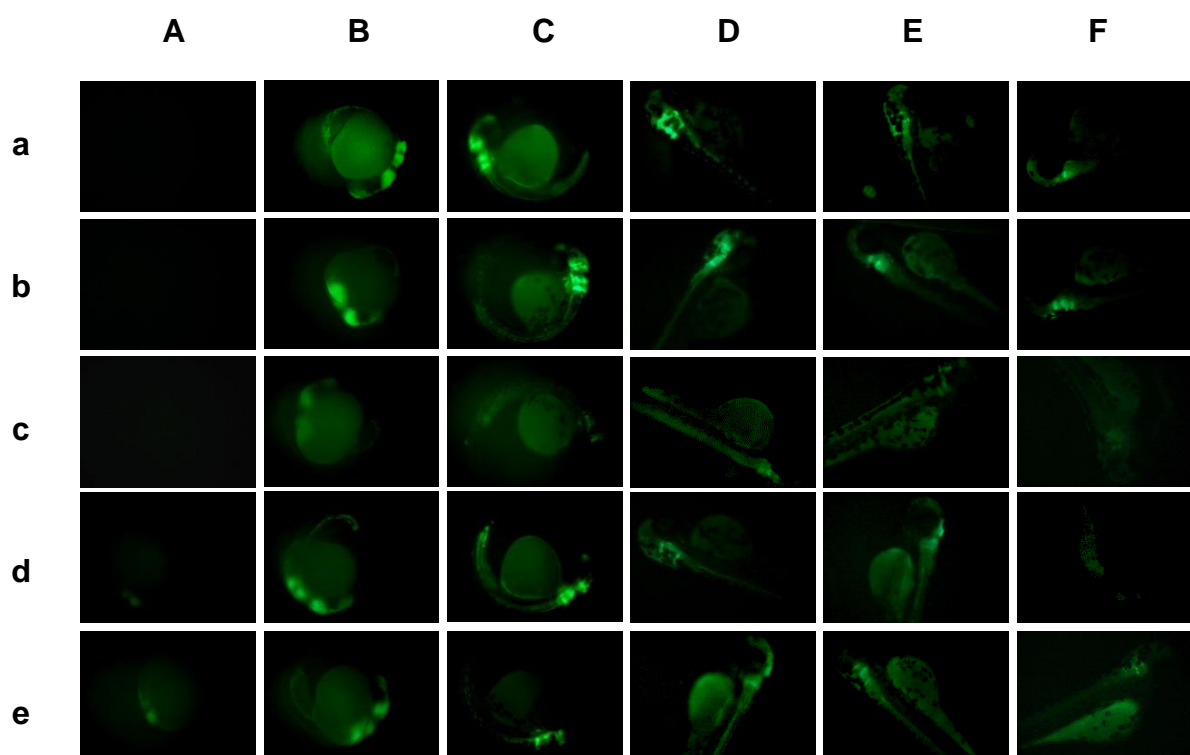


Figure 27: Representative images of Expression of Tg(*pax2a*:GFP) in developing embryos exposed to Ag NPs.

Fluorescence imaging of the expression patterns of the zebrafish embryos captured at (A) 15 hpf, (B) 24 hpf, (C) 48 hpf, (D) 72 hpf, (E) 96 hpf, and (F) 120 hpf for all NPs treated concentrations of (a) 0.00 pM, (b) 0.50 pM, (c) 1.00 pM, (d) 2.00 pM, and (e) 5.00 pM. Expression is shown in the midbrain, hindbrain regions, and along the spinal cord of the growing zebrafish. Expression does decrease over time. Imaging was captured using a Coolsnap HQ (Photometrics) CCD using 4x objective and GFP (455 ex /505 dclp/525 em) custom cube.

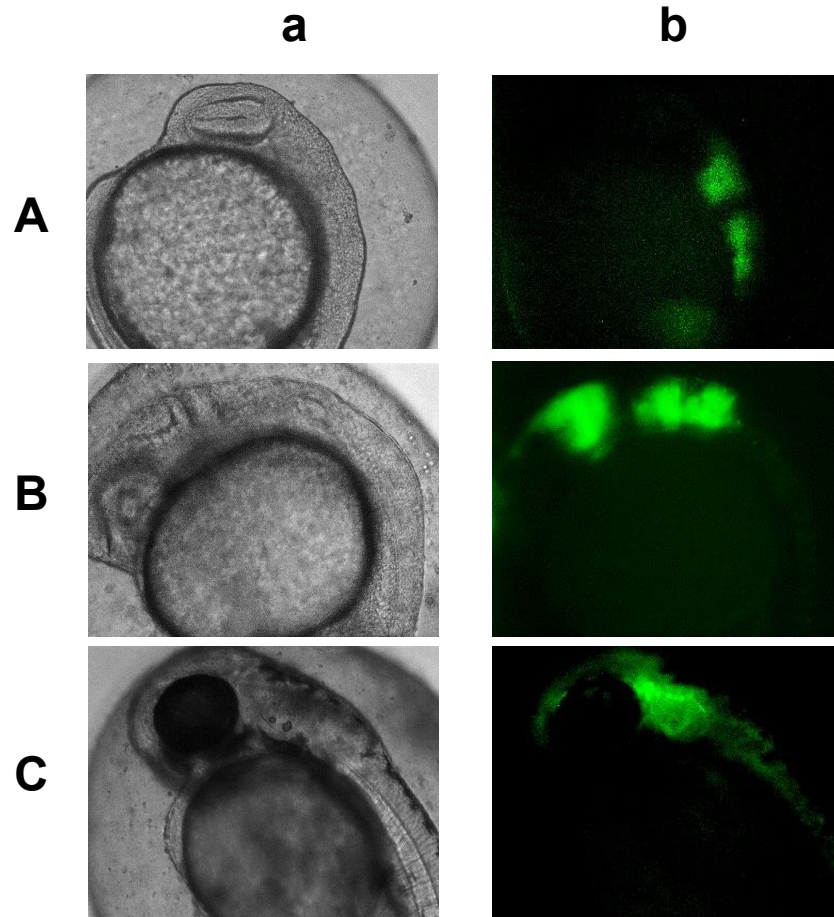


Figure 28: Development of *Tg(pax2a:GFP)* embryos at 1 key developmental stages of brain development.

Optical (a) and Fluorescence (f) imaging of embryos at different developmental time points; (A) 15 hpf, (B) 24 hpf, and (C) 48 hpf. Expression patterns are found along the midbrain and hindbrain areas during brain development. The midbrain-hindbrain segmentation can clearly be observed from the expression of GFP. Imaging was captured using a Coolsnap HQ (Photometrics) CCD using 10x objective.

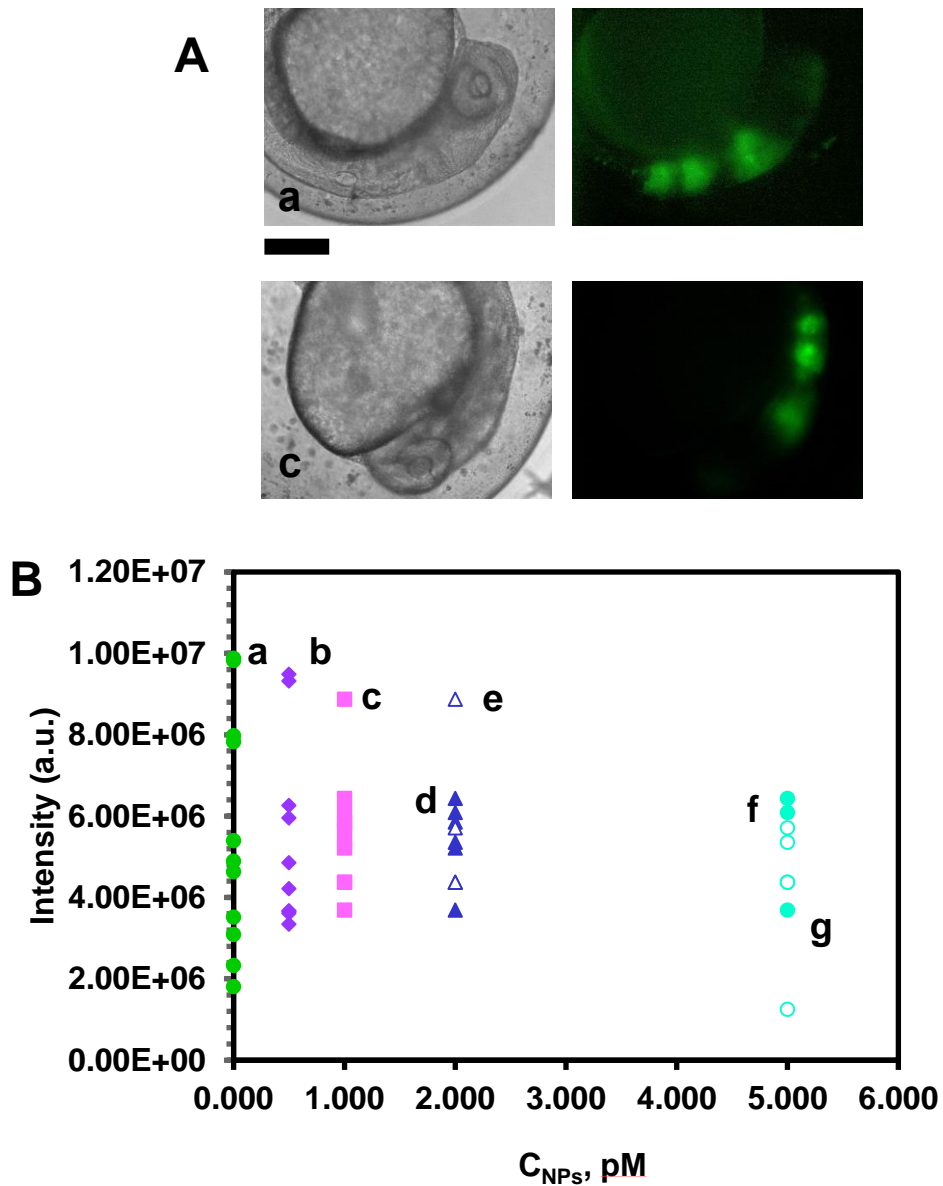


Figure 29: Expression of *pax2a*:GFP protein in zebrafish embryos at 24 hpf.

(A) Representative 10x images of 24 hpf embryos. (a) Optical image of a 24 hpf 0.00 pM control embryo (b) Fluorescence image of a 24 hpf 0.00 pM control embryo (c) Optical image of a 24 hpf 5.00 pM control embryo (f) Fluorescence image of a 24 hpf 5.00 pM control embryo. Imaging of the expression patterns was captured in the hindbrain area beside the optic placode. Imaging was captured using a Coolsnap HQ (Photometrics) CCD using 10x objective. (B) Histogram of GFP intensity plotted in over different

treatments at 24 hpf in treated embryos; (a) Individual normally developed 0.00 pM embryos fluorescent intensity, (b) Individual normally developed 0.50 pM embryos fluorescent intensity, (c) Individual normally developed 1.00 pM embryos fluorescent intensity, (d) Individual normally developed 2.00 pM embryos fluorescent intensity, (e) Individual abnormally developed 2.00 pM embryos fluorescent intensity, (f) Individual normally developed 5.00 pM embryos fluorescent intensity, (g) Individual abnormally developed 5.00 pM embryos fluorescent intensity. Scale bar for images in (A) was 350 μm .

Quantitative heartbeat study of zebrafish upon Ag NPs concentrations.

With many of the Ag NPs treated zebrafish resulting in pericardial sac edemas, along with other cardiac malfunctions, we further monitored the effects of Ag NPs on heart function of developing zebrafish. We compared those treated with Ag NPs with control zebrafish at three major developmental time points: 24 hpf (early heart formation period); 48 hpf (embryo hatching period); and 120 hpf (full development period). We found that the number of embryos with normal developed heart decreased as the Ag NPs concentration increased since some embryos exposed to Ag NPs became either dead or deformed. In normally developed zebrafish, heart rates increased as the heart developed. Heart rates of normally developed zebrafish at 48 hpf and 120 hpf were significantly greater than those at 24 hpf when the heart was in early cardiogenesis development (Figure 30 A). However, Ag NPs significantly reduced embryo heart rates at 24, 48, and 120 hpf in a dose-dependent manner (Figure 30 A). In contrast, deformed zebrafish found after Ag NPs exposure at 1.00 – 5.00 pM concentrations showed a significant difference in heart rates over developmental periods. Their heart rates at 48 hpf and 120 hpf were at the similar to those at 24 hpf (Figure 30 B) in normal embryos. Ag NPs have previously shown to interfere with regular cardiac functions.^{24,112} Significantly enough, we noted that the heart rates of heart deformed zebrafish were much lower than normal heart-developed zebrafish (Figure 30 B) but not in a dose-dependent manner.

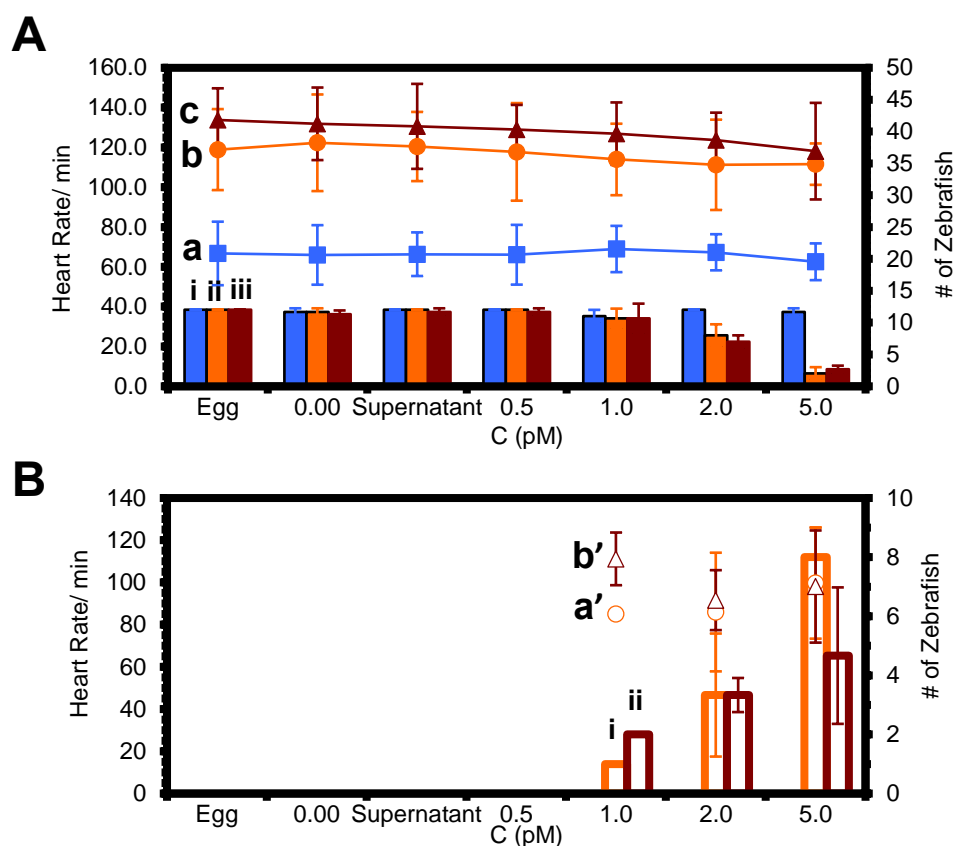


Figure 30: Quantitative analysis of heartbeat of normally developed and heart deformed zebrafish.

Plots of heartbeat per minute of normally developed zebrafish (A) and of deformed zebrafish (B) at (a) 24 hpf which is an early stage of heart development, (b) 48 hpf which is a hatching stage, and (c) 120 hpf when zebrafish fully developed versus Ag NPs concentrations. Histogram (secondary axis) presents the total numbers of zebrafish from three replicates used for heartbeat analysis at 24 hpf (i), 48 hpf (ii), and 120 hpf (iii). Comparison of heartbeats between normal and deformed zebrafish (C) demonstrates that heartbeat of the normal zebrafish at (a) 24 hpf, (b) 48 hpf, and (c) 120 hpf are higher than deformed zebrafish (a') 48 hpf and (b') 120 hpf. Note that there were no deformed zebrafish present at 24 hpf.

Dose-dependent exposure to Ag NPs on optical development

Because head and eye abnormalities are readily recorded from exposure of single Ag NPs from different sizes, an assay designed to analyze the craniofacial development in zebrafish was explored. Analysis of the fully developed zebrafish optic area was observed at 120 hpf. Eye measurements were plotted for all normally and abnormally developed zebrafish. Figure 31 A shows the optical examples of how these measurements were taken, as further described in the Methods section. We observed that as the concentration of the Ag NPs increased, the average size of the eye area of both normal and deformed zebrafish larvae decreased, where 5.00 pM showed the smallest size. Notably, those zebrafish that were deformed showed a significantly smaller size of the eye area. Microphthalmia, the condition of reduced eye sizes in developing embryos, can occur as a consequence of several developmental mechanism including increased cell death or reduced cell proliferation in the developing eye.¹³⁰ This condition in zebrafish has also affected behavioral response to light stimulation during behavioral studies.¹³¹ In fact, microphthalmia is associated with contralateral brains structural abnormalities, resulting in unresponsive optical development.

Our results show that Ag NPs exposure highly influences the development of the eye and other craniofacial areas, which can have permanent effects in the adult zebrafish. Further research will need to be applied to investigate the mechanism that is responsible for this developmental delay.

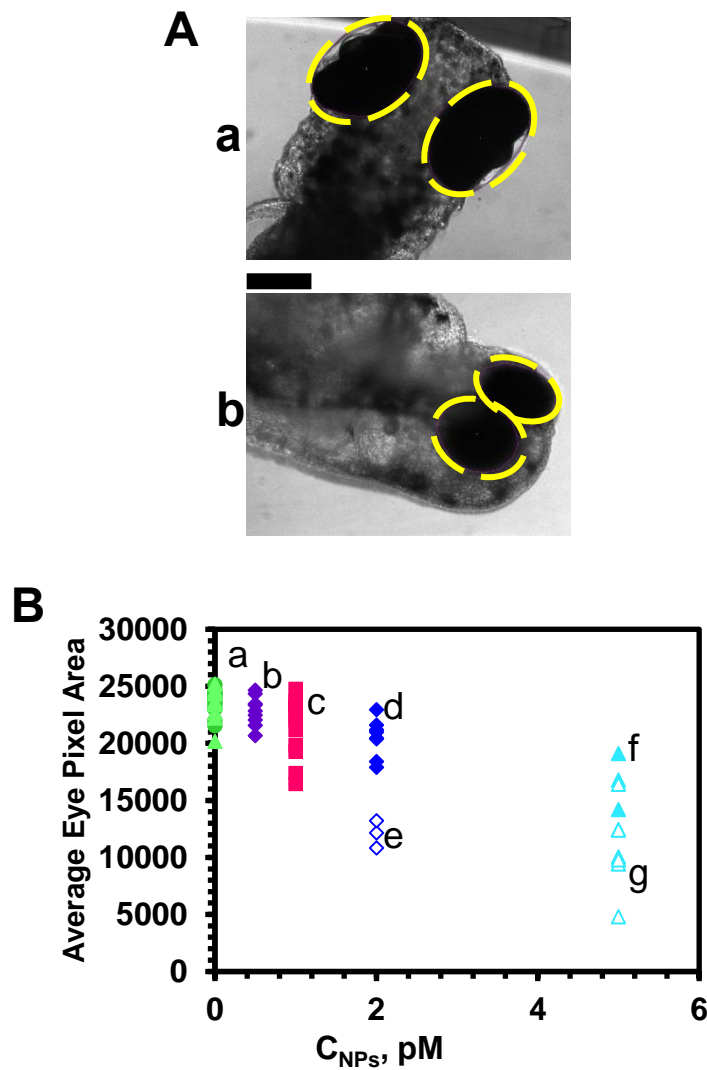


Figure 31: Zebrafish embryos exposed to Ag NPs result in microphthalmia after 120 h incubation.

Analysis of eye measurements of Zebrafish at 120 hpf. The yellow dashed outlines highlights measured areas taken for each embryo. (A) Representative 10x images of 120 hpf zebrafish. (a) 0.00 pM normally developed embryo (b) 5.00 pM abnormally developed embryo. Imaging was captured using a Coolsnap HQ (Photometrics) CCD using 10x objective. (B) Histogram of GFP intensity plotted in over different treatments at 24 hpf in treated embryos; (a) Individual normally developed 0.00 pM embryos fluorescent

intensity, (b) Individual normally developed 0.50 pM embryos fluorescent intensity, (c) Individual normally developed 1.00 pM embryos fluorescent intensity, (d) Individual normally developed 2.00 pM embryos fluorescent intensity, (e) Individual abnormally developed 2.00 pM embryos fluorescent intensity, (f) Individual normally developed 5.00 pM embryos fluorescent intensity, (g) Individual abnormally developed 5.00 pM embryos fluorescent intensity. Scale bar for images in (A) was 350 μm .

Quantitative study of accumulation of Ag NPs in developing zebrafish embryos

Our previous studies have shown how different sizes of Ag NPs can diffuse into different locations of a developing zebrafish after chronic and acute exposure. Here, we quantitatively plotted the uptake of Ag NPs during chronic exposure to Ag NPs. Figure 32 shows the amount of Ag NPs in pmoles that was removed by normal, deformed, and dead embryos. As noted, we observed a dose-dependent trend of uptake of Ag NPs in treated embryos as the concentration of the NPs increased. In those embryos that were deformed or dead during treatment, the amount of Ag NPs was significantly higher than those that developed normally. These normally developed embryos also were more apparent in normal embryo behavior like hatching from the embryos protective barrier, the chorion, and swimming reflexes. We observed those embryos who were developed abnormally had delayed hatched response, hatching at time points later than normal range of 48 – 72 hpf. It is also notable that those embryos who did not survive during treatment still resulted in higher NPs uptake. This increased uptake significantly corresponds to the mortality rate displayed in Figure 25.

This might be because those normally developed embryos were more resistant to the diffusion of the NPs. These results are similar to uptake studies of commercial metal and metal oxide nanoparticles when acutely exposed at much higher rates.¹³² This proves the need to observe and study the uptake of nanomaterials during toxicity studies, and to further study the molecular mechanisms that could potentially be responsible for this uptake.

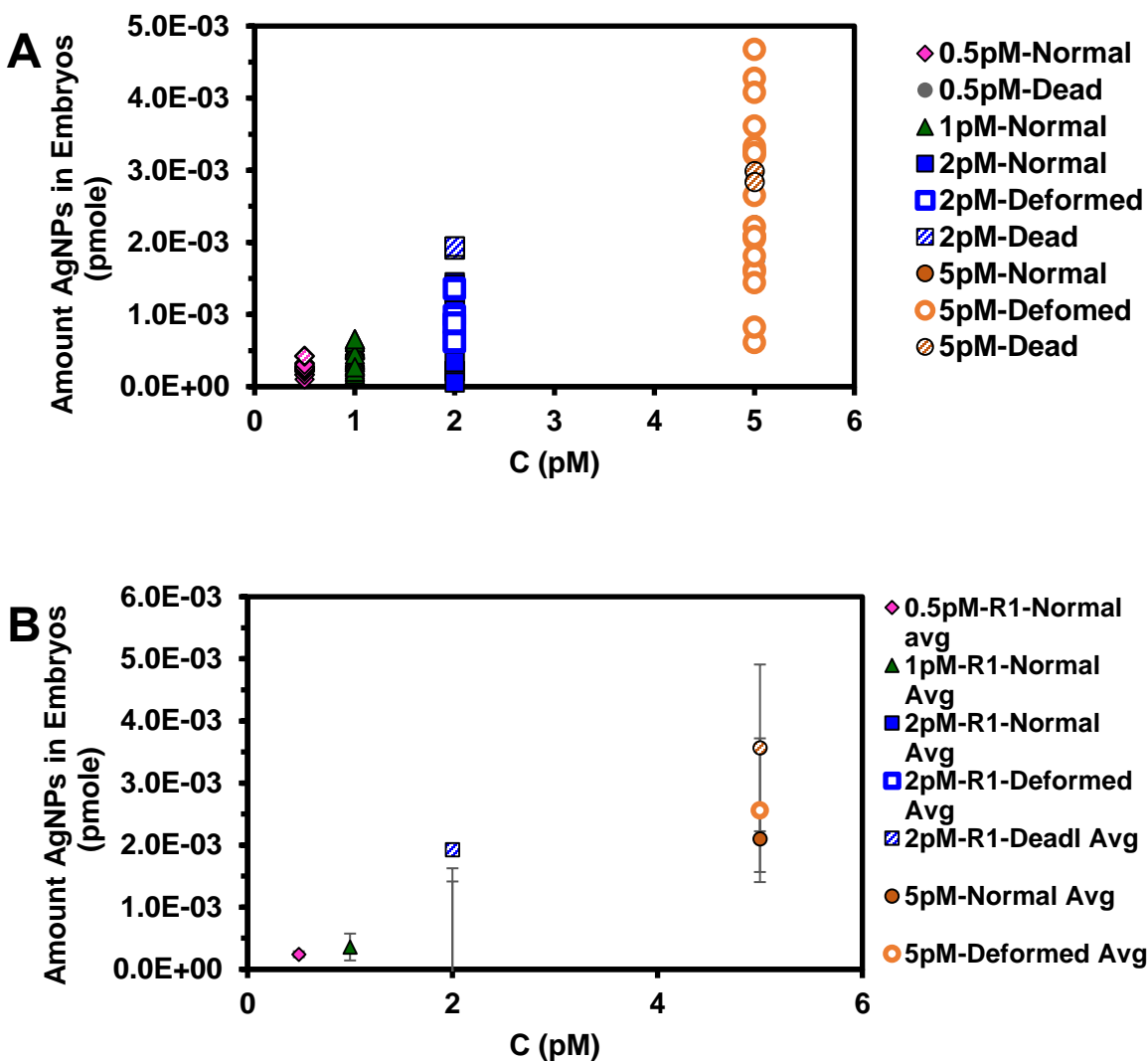


Figure 32: Quantitative study of accumulation of Ag NPs in normally developed and deformed zebrafish after treatment.

Plot of the amount of Ag NPs in embryos of single larvae (A) and of average accumulation for each treatment group (B) after 120 hpf. Solution from each individual well was collected at the start and end of treatment and the absorption, measured using UV-Vis spectroscopy, was used to calculate the number of nanoparticles that accumulated in the embryos during treatment. Plot shows the results for the normal, deformed, and dead zebrafish.

SUMMARY

Embryonic neurological development composes of many different components that all work in unison to develop a functional pathway of neurological function. This study objectively aimed to solidify a more cohesive understanding of how the *pax2a* functional pathway operates, while at the same time explores how nanotoxicity can inhibit or influence the behavior of these pathways. We found that exposure of Ag NPs (41.5 ± 7.6 nm in diameter) have a dose-dependent effect on Tg(*pax2a*:GFP) embryos during embryogenesis. Sublethal concentrations of the Ag NPs also showed a phenotypical dependent morphological effect during development. However, we did not observe a significant decrease in expression of GFP when exposed to Ag NPs. We observed that a higher dose of the Ag NPs leads to severe deformities. We also demonstrated the effects of Ag NPs on cardiac response during exposure. We observed that Ag NPs can decrease the heart rate of both normal and deformed zebrafish. This study also demonstrated dose-dependent effects of Ag NPs on eye development, where higher concentrations of the Ag NP lead to microphthalmia. We also designed an *in vivo* assay to study the uptake of Ag NPs in developing embryos. Here, we observed a significant difference in uptake of those embryos that developed abnormally or who did not survive during treatment.

This study emphasized different *in vivo* assays that can be explored to gain more knowledge on neurological development in zebrafish, which can lead to better design or more biocompatible biosensors to explore therapeutic and molecular assays of embryogenesis and neurological diseases.

METHODS

Reagents and supplies

Sodium citrate (99%), AgClO₄ (99%), NaBH₄ (98%), and NaCl were purchased from Sigma-Aldrich. All reagents were used as received. The nanopure water (18 M Ω water, Barnstead) was used to prepare all solutions and rinse glassware.

Synthesis and characterization of Ag nanoparticles (NPs)

We used our previous developed sphere-shaped silver-based nanoparticles that were washed and purified to remove any chemicals that remained from the synthesis to study their interactions and biocompatibility to determine Ag NPs role in developmental processes, including concentration-dependent morphological responses, for the potential of use as developmental intermediates for biomedical applications.⁴⁴ We characterized the stability, size and optical properties of the purified Ag NPs in egg water embryo media (1.2 mM NaCl) for 120 h using UV-vis absorption spectroscopy, dark field optical microscopy and spectroscopy (DFOMS) and high resolution transmission electron microscopy (HRTEM). The size was with an average diameter of 41.5 ± 7.6 nm (Figure 21). A representative optical image of Ag NPs in Figure 21C illustrates that the majority of NPs appear to be blueish green to green, with a few reds. These results suggest that Ag NPs are uniform in size and shape based on their color (LSPR). The representative LSPR spectra of single blue, green and red Ag NPs with peak wavelengths (λ_{max}) at 468 nm (blue) (FWHM = 38 nm), 554 nm (green) (FWHM = 47 nm), and 659 nm (red) (FWHM = 47) nm, respectively (Figure 21). Thus, the color of Ag NPs can be used as size index to directly distinguish and determine the size of NPs using DFOMS, even though the size of NPs cannot be directly measured due to the optical diffraction limit. We found that the

number of NPs remained relatively unchanged when incubated in egg water for 120 h. The absorbance spectra of freshly prepared and purified Ag NPs before and after the incubation time with egg water demonstrated a peak wavelength (λ_{max}) at 401 nm (FWHM = 52 nm) and only showed a slight decrease in absorbance for 120 hours (Figure 22). The unchanged number of NPs and stable absorbance spectra indicates that the Ag NPs are very stable in egg water media and remain non-aggregated throughout the entire experiment.

Synthesis and characterization of stable and purified Ag NPs

Ag NPs (41.5 ± 7.6 nm in diameter) were synthesized as we described previously. Briefly, sodium citrate (10 mL, 34 mM) was quickly added into a refluxing (100°C) AgNO_3 aqueous solution (500 mL, 1.1 mM) under stirring. The mixture was refluxed and stirred for 45 min, as the solution color turned from colorless to straw yellow, then opaque and finally muddy yellow. The heating was stopped and the solution was cooled gradually to room temperature under stirring. The NP solution was filtered using 0.22- μm filters. All chemicals, except those indicated, were purchased from Sigma and used as received.

The NPs were immediately washed three times with nanopure DI water (18 M Ω , Barnstead) using centrifugation (Beckman, JA-14) to remove any residual chemicals involved in NP synthesis. The washed NPs were resuspended in DI water and then egg water. The washed NPs were very stable (non-aggregated) in DI water for months and remained stable in egg water (1.0 mM NaCl, 99.95% Sigma, in DI water) throughout the duration of the entire experiment (120 h, period of complete embryonic development) (Figure 22). Concentrations of NPs were calculated, as we described previously.

Sizes of NPs were characterized using high-resolution transmission electron microscopy (HR-TEM) (JEOL, JEM-2100F) and dynamic light scattering (DLS) (Nicomp 380ZLS particle sizing system). In this study, the DFOMS is equipped with a dark-field optical microscope with a dark-field condenser (oil 1.43–1.20, Nikon) and a 100× objective (Nikon Plan fluor 100× oil, iris, SL. N.A. 0.5–1.3, W.D. 0.20 mm), a CCD camera (Micromax, Roper Scientific) and a Multispectral Imaging System (Nuance, CRI) was used to acquire LSPR spectra of single NPs. Stability of NPs in solution and egg water was followed over time for 120 h using UV-vis spectroscopy, DLS and DFOMS.

Breeding of zebrafish embryos

Wild-type adult zebrafish (Aquatic Ecosystems) and Tg(*pax2a*:GFP) adult zebrafish were housed in a stand-alone system (Aquatic Habitats), and they were maintained and cross-bred, as described previously.^{44, 113} Briefly, two pairs of mature female transgenic zebrafish and with one wild type male were placed into a clean 10-gallon breeding tank. A light (14 h)–dark (10 h) cycle was used to trigger breed and fertilization of embryos. The embryos at the cleavage stage were collected and transferred into a Petri dish containing egg water. They were well rinsed with egg water to remove any possible debris prior to imaging and characterization. All experiments involving embryos and zebrafish were conducted in compliance with IACUC guidelines (protocol # 15-012).

Treatment and monitoring of zebrafish embryos

Embryos were collected and transferred into a petri dish containing egg water (1.2 mM NaCl), washed twice with egg water to remove the surrounding debris, and placed into 48-well plates with each well containing one embryo in egg water. 16 embryos were

tested per concentration, per stage of development; each experiment was repeated 3 times, totaling 48 embryos analyzed per concentration, per stage of development. Each developmental stage of embryos in the wells was directly imaged by bright-field optical microscopy using an inverted Zeiss Axiovert microscope equipped with a 4x objective and a digital color camera.

Study and characterization of biocompatibility and toxicity of NPs

The cleavage-stage embryos in egg water were incubated with a dilution series of NPs (0, 0.50, 1.00, 2.00 and 5.00 pM). Each experiment was carried out at least 3 times and the total number of embryos, 48, were studied for each individual concentration to gain representative statistics. NP concentrations were calculated as described previously.⁴⁴ Embryos in egg water in the absence of NPs and in the presence of supernatant were placed in two rows of the 48-well plates as control experiments to probe the effects of possible trace chemicals from NP synthesis. The embryos in the 48-well plates were incubated at 28.5°C, and directly observed at room temperature using an inverted Zeiss Axiovert microscope equipped with a digital color camera at 24, 48, 72, 96, and 120 hpf. Using fluorescent microscopy equipped with filters specific for GFP (455 ex /505 dclp/525 em), expression of *pax2a*:GFP will be captured using CCD. Positive embryos were imaged in real time at key developmental time points that are important to Brain development (i.e. around the somites and otic placode regions at 17 hpf, and areas designated for midbrain and hindbrain at 21 hpf) using 10x objective and at each additional imaged time point using 4x objective. Embryos were monitored in real time to note any significant changes in the expression of the protein biomarkers in the presence of Ag NPs as well as any abnormal developmental phenotypes that occur from exposure.

Quantitative heartbeat study of zebrafish upon Ag NPs concentrations

Both treated and control embryos were analyzed for heart rates. Embryos were recorded using the Sony camcorder and Coolsnap Ez (Roper Scientific) using 100 frames with a 50 ms interval delay. The recordings were taken at 24, 48, and 120 hpf. The movies were then converted and analyzed for manual counting of the hearts contractions. The heartbeat per minute was then compared graphically to both the normal and abnormal developed fish at each concentration.

Dose-dependent accumulation of Ag NPs in developing zebrafish embryos

Treatment solution was sampled out at the start of treatment and at the end of treatment. The solution was then analyzed using UV-Vis Spectroscopy and spectral analysis was used to calculate the amount (pmole) of Ag NPs remaining in the solution. This was then used to calculate the uptake amount (pmole) of Ag NPs that was delivered to the embryo.

Data analysis and statistics

A minimum of 100 Ag NPs was imaged and characterized for each measurement of their sizes and stability in egg water using HRTEM and DFOMS. For the study of dose-dependent effects and qualitative heart rate analysis of NPs on embryonic development, a total number of 48 embryos were studied for each NP concentration and each control experiment over 120 hpf with a minimum of 12 embryos studied in each measurement. Expression data analysis was taken for all positive embryos from each experiment, totaling a number of 24 embryos per concentration for expression analysis.

CHAPTER VI

CONCLUSION

In conclusion, as described in **chapter II**, we utilized zebrafish embryos as our *in vivo* model organism to study the toxicity of Ag^+ ions. By statistically comparing the distributions of normal, deformed, and dead embryos upon their exposure to various concentrations of Ag^+ ion, we found that the Ag^+ ion caused deformities and death of the developing embryos in a concentration-dependent manner, where the critical concentration of the Ag^+ ion was $0.20 \mu\text{M}$. Exposure of Ag^+ ions led to specific types of defects in development. However, it is far less drastic than the developing embryos were exposed to Ag NPs. Thus, we can conclude that toxicity of Ag NPs is not due to the release of its ions, but rather their own unique physicochemical properties. To this notion, further investigation into mechanisms of toxicity of Ag NPs is needed to truly understand them. We found that the Ag^+ ion highly affected embryonic development of cardiac formation and function. We found that heart rate highly depends upon Ag^+ concentration. Likewise, we found a large decrease in embryonic heart-rate of those zebrafish that developed abnormally, which were significantly lower than the controls at every development stage. We also found that hatching was significantly delayed for embryos treated at higher concentrations of the Ag^+ .

In **chapter III**, we utilized the developing embryos as *in vivo* model organisms used in chapter I, and the same dilution series of Ag^+ concentrations to study the stage-dependent biocompatibility and toxicity effects of Ag^+ . Specific developmental stages during embryogenesis were selected. We observed that the Ag^+ resulted in concentration-dependent toxicity similar to chapter I in all developmental stages. Our

results describe a range of developmental defects and absolute death following exposure of developing zebrafish embryos to micromolar concentrations of Ag^+ at particular embryonic development stages. We also observed cardiac malfunction in all treated stages, where the Ag^+ resulted in a significant decrease in heart rate with increasing concentration. We did also observe a significant decreased in deformed embryos. Similar to results described in chapter I, when comparing the sensitivity of these specific developmental stages to exposure of the Ag^+ to those same specific developmental stages exposed to our Ag NPs, we found the Ag^+ did not cause toxicity as severely as NPs. This finding further suggests that the toxicity of Ag NPs are not caused by its ions, but its own unique properties. This study offers new insight into the need to further study the effects of nanomaterials on developmental biology.

In **chapters IV and V**, the stability of purified Ag NPs (42 nm) in egg media was comprehensively characterized before using them to study the biocompatibility and toxicity of Ag NPs on embryonic development. We found that the NPs remained stable in egg water up to 120 h, the duration of entire embryonic development.

In **chapter IV**, we examined the effects of Ag NPs upon the development of specific stages of development and the defects associated with treatment at those specific developmental stages. The design of this study was used in this dissertation to compare stage-specific toxicities of Ag^+ ion from chapter II to the toxicity of Ag NPs. In this study, we observed that increasing NPs concentration at all stages of development resulted in a significant increase in embryonic death and a correlated decrease in survivability of normal and deformed zebrafish. Many morphological defects were observed in the developing embryo, including yolk sac edema, abnormal finfold and tail development,

head and eye abnormalities, and cardiac malformations at each stage of development. In general, the number of different types of defects and the severity of each varied with the stage of treatment and increased with increasing dose of NPs demonstrating the possibility of selectively targeting specific embryonic developmental pathways by altering the stage of development and dose of NPs for developmental medicinal studies. Moreover, it was noted that at this particular size of single Ag NPs, cardiac malformation was significant despite exposure at different developmental time points. Pericardial sac edemas were one of the most common types of deformity observed throughout all stages. In that matter, quantitative analysis of cardiac function was found to be significantly influenced with increasing Ag NPs concentrations. In particular, we saw a stage-dependent effect on cardiac malformation, where stages I, II, and IV were highly influenced by exposure to a higher dose of the Ag NPs (0.20 and 0.50 nM). The investigation of biocompatibility of nanomaterials in specific stages of development of embryos at single NP level can offer new knowledge about the developmental processes and environment, and provide new insights into the mechanics of the developing embryo as well as aid in the finding for functional nano-developmental treatments for various disorders in early development.

In **chapter V**, we used our purified Ag NPs from **chapter IV** to study the effects of Ag NPs on embryonic neurological development. More specific, we exposed Tg(*pax2a*:GFP) zebrafish embryos to diluted concentrations of the Ag NPs, studying the expression of the *pax2a* gene during treatment using fluorescent microscopy. This design approach was more practical to study the molecular mechanism of key developmental biomarkers that regulate brain development in zebrafish. Sublethal concentrations of the

Ag NPs (0.00, 0.50, 1.00, 2.00, and 5.00 pM) also showed a phenotypical dependent morphological effect during development. However, we did not observe a significant decrease in expression of GFP when exposed to Ag NPs. We observed that a higher dose of the Ag NPs leads to severe deformities. We also demonstrated the effects of Ag NPs on cardiac response during exposure. We observed that Ag NPs can decrease the heart rate of both normal and deformed zebrafish. This study also demonstrated dose-dependent effects of Ag NPs on eye development, where higher concentrations of the Ag NP lead to microphthalmia in developing embryos. We also designed an *in vivo* assay to study the uptake of Ag NPs in developing embryos. Here, we observed a significant difference in uptake of those embryos that developed abnormally or who did not survive during treatment. This study emphasized different *in vivo* assays that can be explored to gain more knowledge on neurological development in zebrafish, which can lead to better design or more biocompatible biosensors to explore therapeutic and molecular assays of embryogenesis and neurological diseases.

The results of the research mentioned in this dissertation have demonstrated that zebrafish embryos are powerful *in vivo* model system to use to study the biocompatibility and toxicity of metal ions and nanomaterials. This opens up the possibility of using this system as a standard assay to screen many different types of multi-functional NPs, including protein-specific nanomaterials that could potentially be used for targeted therapeutic applications. There is the possibility of using NPs *in vivo* environments as effective drug delivery vehicles by attaching desired drug molecules to the surface of NPs. For this reason, it is very important to collect preliminary data on how NPs influence molecular mechanisms and function of key developmental biomarkers during developing

and if these nanomaterials will be toxic to living cells. To conclude, the chapters included in this dissertation have shown conclusively the versatile nature of using zebrafish embryos as an *in vivo* assay to study the effects of silver ions and silver nanoparticles during embryonic development.

REFERENCES

1. Xu X-HN, Brownlow WJ, Kyriacou SV, Wan Q, Viola JJ. Real-Time Probing of Membrane Transport in Living Microbial Cells Using Single Nanoparticle Optics and Living Cell Imaging†. *Biochemistry*. 2004;43: 10400-10413.
2. Nallathamby PD, Xu X-HN. Study of cytotoxic and therapeutic effects of stable and purified silver nanoparticles on tumor cells. *Nanoscale*. 2010;2: 942-952.
3. Nallathamby PD, Huang T, Xu X-HN. Design and characterization of optical nanorulers of single nanoparticles using optical microscopy and spectroscopy. *Nanoscale*. 2010;2: 1715-1722.
4. Huang T, Nancy Xu X-H. Multicolored nanometre-resolution mapping of single protein-ligand binding complexes using far-field photostable optical nanoscopy (PHOTON). *Nanoscale*. 2011;3: 3567-3572.
5. Huang T, Nallathamby PD, Xu X-HN. Photostable Single-molecule Nanoparticle Optical Biosensors for Real-time Sensing of Single Cytokine Molecules and their Binding Reactions. *Journal of the American Chemical Society*. 2008;130: 17095-17105.
6. Huang T, Nallathamby PD, Gillet D, Xu X-HN. Design and Synthesis of Single-Nanoparticle Optical Biosensors for Imaging and Characterization of Single Receptor Molecules on Single Living Cells. *Analytical Chemistry*. 2007;79: 7708-7718.
7. Cao W, Huang T, Xu X-HN, Elsayed-Ali HE. Localized surface plasmon resonance of single silver nanoparticles studied by dark-field optical microscopy and spectroscopy. *Journal of Applied Physics*. 2011;109: 034310.
8. Huang T, Xu X-HN. Synthesis and characterization of tunable rainbow colored colloidal silver nanoparticles using single-nanoparticle plasmonic microscopy and spectroscopy. *Journal of Materials Chemistry*. 2010;20: 9867-9876.
9. Ding F, Lee KJ, Vahedi-Faridi A, Yoneyama H, Osgood CJ, Nancy Xu X-H. Design and study of the efflux function of the EGFP fused MexAB-OprM membrane transporter in

Pseudomonas aeruginosa using fluorescence spectroscopy. *Analyst*. 2014;139: 3088-3096.

10. Wang X, Fang H, Huang Z, et al. Imaging ROS signaling in cells and animals. *Journal of Molecular Medicine*. 2013;91: 917-927.

11. Moravec CE, Li E, Maaswinkel H, Kritzer MF, Weng W, Sirotkin HI. Rest mutant zebrafish swim erratically and display atypical spatial preferences. *Behavioural Brain Research*. 2015;284: 238-248.

12. Morash MG, Douglas SE, Robotham A, Ridley CM, Gallant JW, Soanes KH. The zebrafish embryo as a tool for screening and characterizing pleurocidin host-defense peptides as anti-cancer agents. *Disease Models & Mechanisms*. 2011;4: 622-633.

13. Levitz J, Pantoja C, Gaub B, et al. Optical control of metabotropic glutamate receptors. *Nat Neurosci*. 2013;16.

14. de Esch C, van der Linde H, Slieker R, et al. Locomotor activity assay in zebrafish larvae: Influence of age, strain and ethanol. *Neurotoxicology and Teratology*. 2012;34: 425-433.

15. Barros TP, Alderton WK, Reynolds HM, Roach AG, Berghmans S. Zebrafish: an emerging technology for in vivo pharmacological assessment to identify potential safety liabilities in early drug discovery. *British Journal of Pharmacology*. 2008;154: 1400-1413.

16. Ackerly KL, Ward AB. How temperature-induced variation in musculoskeletal anatomy affects escape performance and survival of zebrafish (*Danio rerio*). *Journal of Experimental Zoology Part A: Ecological Genetics and Physiology*. 2016;325: 25-40.

17. Warp E, Agarwal G, Wyart C, et al. Emergence of Patterned Activity in the Developing Zebrafish Spinal Cord. *Current Biology*. 2012;22: 93-102.

18. Schmidt R, Strähle U, Scholpp S. Neurogenesis in zebrafish – from embryo to adult. *Neural Development*. 2013;8: 1-13.

19. Dunn TW, Mu Y, Narayan S, et al. Brain-wide mapping of neural activity controlling zebrafish exploratory locomotion. *eLife*. 2016;5: e12741.
20. Alsop D, Wood CM. Metal uptake and acute toxicity in zebrafish: common mechanisms across multiple metals. *Aquat Toxicol*. 2011;105: 385-393.
21. Anandhan R, Hemalatha S. Acute toxicity of aluminium to zebra fish, *Brachydanio rerio* (Ham.). *The Internet Journal of Veterinary Medicine* [serial online] 2009;7. Available from URL: <http://archive.ispub.com/journal/the-internet-journal-of-veterinary-medicine/volume-7-number-1/acute-toxicity-of-aluminium-to-zebra-fish-brachydanio-rerio-ham.html#sthash.RuHVjpvQ.dpuf> [accessed 04 Jun 2013].
22. Arai Y, Miyayama T, Hirano S. Difference in the toxicity mechanism between ion and nanoparticle forms of silver in the mouse lung and in macrophages. *Toxicology*. 2015;328: 84-92.
23. Asghari S, Johari SA, Lee JH, et al. Toxicity of various silver nanoparticles compared to silver ions in *Daphnia magna*. *J Nanobiotechnology*. 2012;10: 14.
24. Asharani PV, Yi Lian W, Zhiyuan G, Suresh V. Toxicity of silver nanoparticles in zebrafish models. *Nanotechnology*. 2008;19: 255102.
25. Atli G, Canli M. Metals (Ag⁺, Cd²⁺, Cr⁶⁺) Affect ATPase Activity in the Gill, Kidney, and Muscle of Freshwater Fish *Oreochromis niloticus* Following Acute and Chronic Exposures. *Environmental Toxicology*. 2013;28: 707-717.
26. Beer C, Foldbjerg R, Hayashi Y, Sutherland DS, Autrup H. Toxicity of silver nanoparticles—Nanoparticle or silver ion? *Toxicol Lett*. 2012;208: 286-292.
27. Bhuvaneshwari R, Babu RR, Kumar K. Induction of DNA damage and GADD45 β gene mutation in zebra fish (*Danio rerio*) due to environmentally relevant concentrations of organochlorine pesticides & heavy metals. *Int. J. Environ. Res*. 2012;7: 219-224.

28. Bilberg K, Hovgaard MB, Besenbacher F, Baatrup E. In Vivo Toxicity of Silver Nanoparticles and Silver Ions in Zebrafish (*Danio rerio*). *Journal of Toxicology*. 2012;2012: 9.
29. Brune A, Urbach W, Dietz K-J. Zinc stress induces changes in apoplasmic protein content and polypeptide composition of barley primary leaves¹. *Journal of Experimental Botany*. 1994;45: 1189-1196.
30. Chan KM, Ku LL, Chan PCY, Cheuk WK. Metallothionein gene expression in zebrafish embryo-larvae and ZFL cell-line exposed to heavy metal ions. *Marine Environmental Research*. 2006;62, Supplement 1: S83-S87.
31. Cheuk WK, Chan PC-Y, Chan KM. Cytotoxicities and induction of metallothionein (MT) and metal regulatory element (MRE)-binding transcription factor-1 (MTF-1) messenger RNA levels in the zebrafish (*Danio rerio*) ZFL and SJD cell lines after exposure to various metal ions. *Aquatic Toxicology*. 2008;89: 103-112.
32. Choi JE, Kim S, Ahn JH, et al. Induction of oxidative stress and apoptosis by silver nanoparticles in the liver of adult zebrafish. *Aquatic Toxicology*. 2010;100: 151-159.
33. Coglianese MP, Martin M. Individual and interactive effects of environmental stress on the embryonic development of the Pacific oyster, *Crassostrea gigas*. I. The toxicity of copper and silver. *Mar Environ Res*. 1981;5: 13-27.
34. De Matteis V, Malvindi MA, Galeone A, et al. Negligible particle-specific toxicity mechanism of silver nanoparticles: The role of Ag⁺ ion release in the cytosol. *Nanomedicine: Nanotechnology, Biology and Medicine*. 2015;11: 731-739.
35. Ford L. Development of chronic aquatic water quality criteria and standards for silver. *Water Environ Res*. 2001;73: 248-253.
36. Geng F, Hu N, Zheng J-F, et al. Evaluation of the toxic effect on zebrafish (*Danio rerio*) exposed to uranium mill tailings leaching solution. *J. Radioanal. Nucl. Chem*. 2012;292: 453-463.

37. Groh KJ, Dalkvist T, Piccapietra F, Behra R, Suter MJ-F, Schirmer K. Critical influence of chloride ions on silver ion-mediated acute toxicity of silver nanoparticles to zebrafish embryos. *Nanotoxicology*. 2010;4: 1-11.
38. Johnson M, Ates M, Arslan Z, Farah I, Bogatu C. Assessment of Crystal Morphology on Uptake, Particle Dissolution, and Toxicity of Nanoscale Titanium Dioxide on *Artemia salina*. *Journal of nanotoxicology and nanomedicine*. 2017;2: 11-27.
39. Yamagami K. Mechanisms of Hatching in Fish: Secretion of Hatching Enzyme and Enzymatic Choriolysis. *American Zoologist*. 1981;21: 459-471.
40. Massarsky A, Strek L, Craig PM, Eisa-Beygi S, Trudeau VL, Moon TW. Acute embryonic exposure to nanosilver or silver ion does not disrupt the stress response in zebrafish (*Danio rerio*) larvae and adults. *Science of The Total Environment*. 2014;478: 133-140.
41. Browning LM, Lee KJ, Cherukuri PK, Huang T, Warren S, Xu X-HN. Single nanoparticle plasmonic spectroscopy for study of charge-dependent efflux function of multidrug ABC transporters of single live *Bacillus subtilis* cells. *J. Phys. Chem. C*. 2016;120: 21007-21016.
42. Browning LM, Lee KJ, Cherukuri PK, et al. Single nanoparticle plasmonic spectroscopy for study of efflux function of multidrug ABC membrane transporters of single live cells. *RSC Advances*. 2016;6: 36794-36802
43. Browning LM, Lee KJ, Huang T, Nallathamby PD, Lowman J, Xu X-HN. Random walk of single gold nanoparticles in zebrafish embryos leading to stochastic toxic effects on embryonic developments. *Nanoscale*. 2009;1: 138-152.
44. Lee KJ, Nallathamby PD, Browning LM, Osgood CJ, Xu X-HN. *In vivo imaging of transport and biocompatibility of single silver nanoparticles in early development of zebrafish embryos*. *ACS Nano*. 2007;1: 133-143.

45. Agrawal A, Zhang C, Byassee T, Tripp RA, Nie S. Counting Single Native Biomolecules and Intact Viruses with Color-Coded Nanoparticles. *Anal. Chem.* 2006;78: 1061-1070.
46. Andre Nel TX, Lutz Ma"dlar, Ning Li. Toxic Potential of Materials at the Nanolevel. *Science.* 2006;311: 622-627.
47. Bruchez M, Jr., Moronne M, Gin P, Weiss S, Alivisatos AP. Semiconductor Nanocrystals as Fluorescent Biological Labels. *Science.* 1998;281: 2013-2016.
48. Kagan VE, Bayir H, Shvedova AA. Nanomedicine and nanotoxicology: two sides of the same coin. *Nanomedicine.* 2005;1: 313-316.
49. Katsuyuki Tanizawa.; Shunichi Kuroda TYYIHTHIMKCTVHFAKMUMS. Nanoparticle for the delivery of genes and drugs to human hepatocytes. *Nature Biotechnology.* 2003;21: 885-890.
50. Kyriacou SV, Brownlow WJ, Xu X-HN. Using Nanoparticle Optics Assay for Direct Observation of the Function of Antimicrobial Agents in Single Live Bacterial Cells. *Biochemistry.* 2003;43: 140-147.
51. Misra R, Acharya S, Sahoo SK. Cancer nanotechnology: application of nanotechnology in cancer therapy. *Drug Discov Today.* 2010;15: 842-850.
52. Nel A, Xia T, Madler L, Li N. Toxic potential of materials at the nanolevel. *Science.* 2006;311: 622-627.
53. Nel AE, Madler L, Velegol D, et al. Understanding biophysicochemical interactions at the nano-bio interface. *Nat Mater.* 2009;8: 543-557.
54. Johnson MS, Ates M, Arslan Z, Farah IO, Bogatu C. Assessment of Crystal Morphology on Uptake, Particle Dissolution, and Toxicity of Nanoscale Titanium Dioxide on *Artemia Salina*. *Journal of Nanotoxicology and Nanomedicine (JNN).* 2017;2: 11-27.

55. Morgan IJ, Henry RP, Wood CM. The mechanism of acute silver nitrate toxicity in freshwater rainbow trout (*Oncorhynchus mykiss*) is inhibition of gill Na⁺ and Cl⁻ transport. *Aquatic Toxicology*. 1997;38: 145-163.
56. Elwood Linney LU, Susan Donerly. Zebrafish as a neurotoxicological model. *Neurotoxicology and Teratology*. 2004;26: 709–718.
57. Gong Z, Korzh V. Fish Development and Genetics: The Zebrafish and Medaka Models. *Molecular Aspects of Fish and Marine Biology*. Singapore: World Scientific Publishing Co., 2004:87-424.
58. Hoar WS, Randall DJ. Fish Physiology: The Physiology of Developing Fish, Part A, Eggs and Larvae. New York: Academic Press, 1988.
59. Kahn P. Zebrafish hit the big time. *Science*. 1994;264: 904-905.
60. Kreibig U, Vollmer M. Optical Properties of Metal Clusters. Berlin: Springer, 1995:14-123.
61. Langheinrich U. Zebrafish: a new model on the pharmaceutical catwalk. *BioEssays*. 2003;25: 904–912.
62. Xu KJLPDNLMBJCJOX-HN. In Vivo Imaging of Transport and Biocompatibility of Single Silver Nanoparticles in Early Development of Zebrafish Embryos. *ACS Nano*. 2007;1: 133-143.
63. Zon LI, Peterson RT. *In vivo drug discovery in the zebrafish*. *Nat. Rev. Drug Discovery*. 2005;4: 35-44.
64. Lee KJ, Browning LM, Nallathamby PD, Xu X-HN. Silver nanoparticles induce developmental stage-specific embryonic phenotypes in zebrafish. *Nanoscale*. 2013;5: 11625-11636.

65. Mohideen M-APKB, L. G.; Tsao-Wu, G. S.; Moore, J. L.; Wong, A. C. C.; Chinoy, M. R.; Cheng, K. C. Histology-Based Screen for Zebrafish Mutants with Abnormal Cell Differentiation. *Developmental Dynamics*. 2003;228: 414–423.
66. Shin JT, Fishman MC. From Zebrafish to human: modular medical models. *Annu. Rev. Genomics. Hum. Genet.* 2002;3: 311-340.
67. Sandip B. Tiwari MMA. A review of nanocarrier based CNS Delivery systems. *Current Drug Delivery*. 2006;3: 219-232.
68. Stickney HL, Barresi MJF, Devoto SH. Somite development in zebrafish. *Developmental Dynamics*. 2000;219: 287–303.
69. Westerfield M. The zebrafish book: A Guide for the Laboratory Use of Zebrafish (Danio Rerio*) (http://zfin.org/zf_info/zfbook/zfbk.html) ed. Eugene, OR: University of Oregon Press 1993.
70. Teraoka H, Dong W, Hiraga T. Zebrafish as a novel experimental model for developmental toxicology. *Congenit. Anom. (Kyoto)*. 2003;43: 123-132.
71. Tinoco I, Sauer K, Wang J, Puglisi JD. Molecular Motion and Transport Properties. *Physical Chemistry-Principles and Applications in Biological Sciences*. New Jersey Prentice Hall, 2002:274-290.
72. Tiwari SB, Amiji MM. A review of nanocarrier-based CNS delivery systems. *Curr. Drug Delivery*. 2006;3: 219-232.
73. Marom S, Shahaf G. Development, learning and memory in large random networks of cortical neurons: lessons beyond anatomy. *Q Rev Biophys.* 2002;35.
74. Brownlie A, Hersey C, Oates AC, et al. Characterization of embryonic globin genes of the zebrafish. *Developmental Biology*. 2003;255: 48-61.

75. Jacob E, Drexel M, Schwerte T, Pelster B. Influence of hypoxia and of hypoxemia on the development of cardiac activity in zebrafish larvae. *American Journal of Physiology - Regulatory, Integrative and Comparative Physiology*. 2002;283: R911-R917.
76. Denvir MA, Tucker CS, Mullins JJ. Systolic and diastolic ventricular function in zebrafish embryos: Influence of norepinephrine, MS-222 and temperature. *Bmc Biotechnology*. 2008;8: 1-8.
77. Lee KJ. Design of in vivo assay for study of transport, biocompatibility and toxicity of nanoparticles. Department of Chemistry and Biochemistry. Norfolk, VA Old Dominion University, 2012.
78. Lee KJ, Browning LM, Nallathamby PD, Desai T, Cherukuri P, Xu X-HN. In vivo quantitative study of size-dependent transport and toxicity of single silver nanoparticles using zebrafish embryos. *Chem. Res. Toxicol.* 2012;25: 1029-1046.
79. Lee KJ, Browning LM, Nallathamby PD, Xu XHN. Study of charge-dependent transport and toxicity of peptide-functionalized silver nanoparticles using zebrafish embryos and single nanoparticle plasmonic spectroscopy. *Chem Res Toxicol.* 2013;26: 904-917.
80. Rees DC, Williams TN, Gladwin MT. Sickle-cell disease. *The Lancet*. 376: 2018-2031.
81. Byun H, Hillman TR, Higgins JM, et al. Optical measurement of biomechanical properties of individual erythrocytes from a sickle cell patient. *Acta Biomaterialia*. 2012;8: 4130-4138.
82. Parker T, Libourel P-A, Hetheridge MJ, et al. A multi-endpoint in vivo larval zebrafish (*Danio rerio*) model for the assessment of integrated cardiovascular function. *Journal of Pharmacological and Toxicological Methods*. 2014;69: 30-38.
83. Xu XHN, Patel RP. Imaging and Assembly of Nanoparticles in Biological Systems. In: Nalwa HS, editor. *Handbook of Nanostructured Biomaterials and Their Applications in Nanobiotechnology*: American Scientific Publishers, 2005:435-456.

84. Xu X-HN, Patel RP. Nanoparticles for Live Cell Dynamics. In: Nalwa HS, editor. Encyclopedia of Nanoscience and Nanotechnology. Stevenson Ranch, CA: American Scientific Publishers, 2004:189-192.
85. Xu X-HN, Song Y, Nallathamby PD. Probing Membrane Transport of Single Live Cells Using Single Molecule Detection and Single Nanoparticle Assay. In: Xu X-HN, editor. New Frontiers in Ultrasensitive Bioanalysis: Advanced Analytical Chemistry Applications in Nanobiotechnology, Single Molecule Detection, and Single Cell Analysis. New Jersey: Wiley, 2007:41-65.
86. Yamada T, Iwasaki Y, Tada H, et al. Nanoparticles for the Delivery of Genes and Drugs to Human Hepatocytes. *Nat. Biotechnol.* 2003;21: 885-890.
87. Browning LM, Huang T, Xu X-HN. Real-time in vivo imaging of size-dependent transport and toxicity of gold nanoparticles in zebrafish embryos using single nanoparticle plasmonic spectroscopy. *Interface Focus.* 2013;3: 20120098.
88. Browning LM, Lee KJ, Nallathamby PD, Xu X-HN. Silver nanoparticles incite size and dose-dependent developmental phenotypes and nanotoxicity in zebrafish embryos. *Chem. Res. Toxicol.* 2013;26: 1503-1513.
89. Lee JW, Na DS, Chae SK, et al. Using the chorions of fertilized zebrafish eggs as a biomaterial for the attachment and differentiation of mouse stem cells. *Langmuir.* 2005;21: 7615 - 7620.
90. Amanuma K, Takeda H, Amanuma H, Aoki Y. Transgenic Zebrafish For Detecting Mutations Caused by Compounds in Aquatic Environments. *Nat. Biotechnol.* 2000;18: 62-65.
91. Chan WC, Nie S. Quantum Dot Bioconjugates for Ultrasensitive Nonisotopic Detection. *Science.* 1998;281: 2016-2018.

92. Kyriacou SV, Nowak ME, Brownlow WJ, Xu X-HN. Single live cell imaging for real-time monitoring of resistance mechanism in *pseudomonas aeruginosa*. *J. Biomed. Opt.* 2002;7: 576-586.
93. Xu X-HN, Brownlow WJ, Kyriacou SV, Wan Q, Viola JJ. Real-time probing of membrane transport in living microbial cells using single nanoparticle optics and living cell imaging. *Biochemistry*. 2004;43: 10400-10413.
94. Xu XH, Yeung ES. Direct measurement of single-molecule diffusion and photodecomposition in free solution. *Science*. 1997;275: 1106-1109.
95. Bohren CF, Huffman DR. *Absorption and Scattering of Light by Small Particles*. New York: Wiley, 1983:287-380.
96. Mie G. Beitrag zur optik trüber medien, speziell kolloidaler metrallösungen. *Annu. Phys.* 1908;25: 377-445.
97. Mulvaney P. Surface plasmon spectroscopy of nanosized metal particles. *Langmuir*. 1996;12: 788-800.
98. Kyriacou S, Brownlow W, Xu X-HN. Nanoparticle Optics For Direct Observation Of Functions Of Antimicrobial Agents In Single Live Bacterial Cells. *Biochemistry*. 2004; 43: 140-147.
99. Xu X-HN, Chen J, Jeffers RB, Kyriacou SV. Direct measurement of sizes and dynamics of single living membrane transporters using nano-optics. *Nano Lett.* 2002;2: 175-182.
100. den Hertog J. Chemical Genetics: Drug Screens In Zebrafish. *Biosci. Rep.* 2005;25: 289-297.
101. Hill AJ, Teraoka H, Heideman W, Peterson RE. Zebrafish as a model vertebrate for investigating chemical toxicity. *Toxicol. Sci.* 2005;86: 6-19.

102. Khan JA, Pillai B, Das TK, Singh Y, Maiti S. Molecular effects of uptake of gold nanoparticles in Hela cells. *Chembiochem*. 2007;8: 1237-1240.
103. Lieschke GJ, Currie PD. Animal models of human disease: zebrafish swim into view. *Nat Rev Genet*. 2007;8: 353-367.
104. Pichler FB, Laurenson S, Williams LC, Dodd A, Copp BR, Love DR. Chemical discovery and global gene expression analysis in zebrafish. *Nat Biotechnol*. 2003;21: 879-883.
105. Beker van Woudenberg A, Snel C, Rijkmans E, et al. Zebrafish embryotoxicity test for developmental (neuro)toxicity: Demo case of an integrated screening approach system using anti-epileptic drugs. *Reproductive Toxicology*. 2014;49: 101-116.
106. Lajos Balogh SSN, Bindu M. Nair, Wojciech Lesniak, Chunxin Zhang, Lok Yun Sung, Muhammed S.T. Kariapper, Areej El-Jawahri, Mikel Llanes, Brian Bolton, Fatema Mamou, Wei Tan, MA, Alan Hutson, Leah Minc, Mohamed K. Khan. Significant effect of size on the in vivo biodistribution of gold composite nanodevices in mouse tumor models. *Nanomedicine: Nanotechnology, Biology, and Medicine*. 2007;3: 281–296.
107. Helde KA, Wilson ET, Cretekos CJ, Grunwald DJ. Contribution of early cells to the fate map of the zebrafish gastrula. *Science*. 1994;265: 517-520.
108. Kunz YW. *Developmental Biology of Teleost Fishes*. Fish and Fisheries Series. Netherlands: Springer, 2004:267-428.
109. Lee KJ, Nallathamby PD, Browning LM, Desai T, Cherukuri P, Xu X-HN. Single nanoparticle spectroscopy for real-time in vivo quantitative analysis of transport and toxicity of single nanoparticles in single embryos. *Analyst*. 2012;137: 2973-2986
110. Mathavan S, Lee SG, Mak A, et al. Transcriptome analysis of zebrafish embryogenesis using microarrays. *PLoS Genet*. 2005;1: 260-276.
111. Stainier DY, Lee RK, Fishman MC. Cardiovascular development in the zebrafish. I. Myocardial fate map and heart tube formation. *Development*. 1993;119: 31-40.

112. Massarsky A, Dupuis L, Taylor J, et al. Assessment of nanosilver toxicity during zebrafish (*Danio rerio*) development. *Chemosphere*. 2013;92: 59-66.
113. Browning LM, Lee KJ, Huang T, Nallathamby PD, Lowman JE, Xu XH. Random walk of single gold nanoparticles in zebrafish embryos leading to stochastic toxic effects on embryonic developments. *Nanoscale*. 2009;1: 138-152.
114. Lee KJ, Nallathamby PD, Browning LM, Osgood CJ, Xu XH. In vivo imaging of transport and biocompatibility of single silver nanoparticles in early development of zebrafish embryos. *ACS Nano*. 2007;1: 133-143.
115. Lee KJ, Nallathamby PD, Browning LM, Desai T, Cherukuri PK, Xu XH. Single nanoparticle spectroscopy for real-time in vivo quantitative analysis of transport and toxicity of single nanoparticles in single embryos. *Analyst*. 2012;137: 2973-2986.
116. Lee KJ, Browning LM, Nallathamby PD, Xu X-HN. Study of Charge-Dependent Transport and Toxicity of Peptide-Functionalized Silver Nanoparticles Using Zebrafish Embryos and Single Nanoparticle Plasmonic Spectroscopy. *Chemical Research in Toxicology*. 2013.
117. Lee KJ, Browning LM, Nallathamby PD, Osgood CJ, Xu XH. Silver nanoparticles induce developmental stage-specific embryonic phenotypes in zebrafish. *Nanoscale*. 2013;5: 11625-11636.
118. Lee KJ, Browning LM, Nallathamby PD, Desai T, Cherukuri PK, Xu XH. In vivo quantitative study of sized-dependent transport and toxicity of single silver nanoparticles using zebrafish embryos. *Chem Res Toxicol*. 2012;25: 1029-1046.
119. Schier AF, Neuhauss SC, Harvey M, et al. Mutations affecting the development of the embryonic zebrafish brain. *Development*. 1996;123: 165-178.
120. Picker A, Scholpp S, Böhli H, Takeda H, Brand M. A novel positive transcriptional feedback loop in midbrain-hindbrain boundary development is revealed through analysis of the zebrafish *pax2.1* promoter in transgenic lines. *Development*. 2002;129: 3227-3239.

121. Batista MF, Lewis KE. Pax2/8 act redundantly to specify glycinergic and GABAergic fates of multiple spinal interneurons. *Developmental Biology*. 2008;323: 88-97.
122. Yu H-H, Moens CB. Semaphorin signaling guides cranial neural crest cell migration in zebrafish. *Developmental Biology*. 2005;280: 373-385.
123. Yeo S-Y. Zebrafish CiA interneurons are late-born primary neurons. *Neuroscience Letters*. 2009;466: 131-134.
124. Wanner SJ, Prince VE. Axon tracts guide zebrafish facial branchiomotor neuron migration through the hindbrain. *Development*. 2013;140: 906-915.
125. Tallafuss A, Eisen J. The Met receptor tyrosine kinase prevents zebrafish primary motoneurons from expressing an incorrect neurotransmitter. *Neural Development*. 2008;3: 18.
126. Reimer Michell M, Norris A, Ohnmacht J, et al. Dopamine from the Brain Promotes Spinal Motor Neuron Generation during Development and Adult Regeneration. *Developmental Cell*. 2013;25: 478-491.
127. Mueller R, Huang C, Ho R. Spatio-temporal regulation of Wnt and retinoic acid signaling by tbx16/spadetail during zebrafish mesoderm differentiation. *BMC Genomics*. 2010;11: 492.
128. Bonkowsky J, Wang X, Fujimoto E, Lee J, Chien C-B, Dorsky R. Domain-specific regulation of foxP2 CNS expression by lef1. *BMC Developmental Biology*. 2008;8: 103.
129. Gutzman JH, Graeden EG, Lowery LA, Holley HS, Sive H. Formation of the zebrafish midbrain-hindbrain boundary constriction requires laminin-dependent basal constriction. *Mechanisms of Development*. 2008;125: 974-983.
130. Kashyap B, Frederickson LC, Stenkamp DL. Mechanisms for persistent microphthalmia following ethanol exposure during retinal neurogenesis in zebrafish embryos. *Visual neuroscience*. 2007;24: 409-421.

131. Chiandetti C, Galliussi J, Andrew RJ, Vallortigara G. Early-light embryonic stimulation suggests a second route, via gene activation, to cerebral lateralization in vertebrates. *Scientific Reports*. 2013;3: 2701.
132. Pavagadhi S, Sathishkumar M, Balasubramanian R. Uptake of Ag and TiO₂ nanoparticles by zebrafish embryos in the presence of other contaminants in the aquatic environment. *Water Research*. 2014;55: 280-291.

VITA

Martha Sharisha Johnson

Dept. of Chemistry and Biochemistry
Alfriend Chemistry Building
Old Dominion University
Norfolk, VA 23529

Education

May, 2019: Ph.D. Biomedical Sciences, Old Dominion University, Norfolk, VA 23529

May, 2013: M.S. Chemistry, Jackson State University, Jackson, MS, 39217

May, 2010: B.S. Chemistry, Jackson State University, Jackson, MS, 39217

Selected Publications

1. **M. Johnson**, P. Songkiatisak, L. Browning, X. Xu*, "Study of Acute Effects of Silver Ions on Embryonic Development", (in preparation)
2. **M. Johnson**, M. Ates, Z. Arslan, I Farah, C. Bogatu, "Assessment of Crystal Morphology on Uptake, Particle Dissolution, and Toxicity of Nanoscale Titanium Dioxide on *Artemia salina*", J. Nanotoxicol Nanomed. 2017: 2(1):11-27

Selected Presentations and Meeting Abstracts

1. **M. Johnson**, M. Hept X. Xu*, "*In Vivo* Study of Nanoparticles on Embryonic Neurological Development", ACS National Meeting, Analytical Division, Washington D.C., August 2017
2. **M. Johnson**, P. Songkiatisak, P. Cherukuri X. Xu*, "*In Vivo* Study of Nanoparticles on Embryonic Neurological Development", Pittcon'2015, New Orleans, March 2015
3. **M. Johnson**, L. Browning, P. Songkiatisak, X. Xu*, "*In Vivo* Assay for the Study of Acute Toxicity of Silver Cations on Embryonic Development", Pittcon'2014, Chicago, IL March 2014